

**A novel method to quantify gamma H2AX foci in
circulating tumour cells in patients receiving
chemotherapy for colorectal cancer**

Matilde Saggese

**A thesis submitted to the University College London (UCL) for
the degree of MD (res) in the field of Clinical Translational
Oncology**

University College London Cancer Institute

72 Huntley St

London

WC1E 6DD

November 2016

Declaration

I, Matilde Saggese, confirm that the work presented in this thesis is my own. Where information has been derived from other sources, I confirm that this has been indicated in the thesis.

A novel method to quantify gamma H2AX foci in circulating tumour cells in patients receiving chemotherapy for colorectal cancer

Abstract

Colorectal cancer (CRC) is the third most common cancer in males and females. Circulating tumour cells (CTCs) are epithelial cancer cells that mediate haematogenous metastases and can be used as predictive and prognostic markers. Gamma-H2AX (γ -H2AX) foci represent double strand DNA breaks and DNA damage. Assessing γ -H2AX foci in CTCs could be utilised as a biomarker to measure patient response to DNA-interactive anti-cancer treatments in real time, aiding treatment decisions. The aim of this study was to develop a method to quantify changes in γ -H2AX in CTCs from metastatic CRC patients undergoing treatment with FOLFOX (oxaliplatin with fluorouracil 5FU and folinic acid chemotherapy) or FOLFORI (irinotecan with 5FU and folinic acid). Human CRC cell lines (HT-29; HCT-116) treated with oxaliplatin, SN-38 and topotecan alone or spiked into healthy donor blood were evaluated to assess γ -H2AX signal using both the CellSearch® System (Janssen Diagnostics) and the DEPArray™ System (Silicon Biosystems). The fluorescent signal in cells could not be quantified using CellSearch followed by DEPArray analysis, but when DEPArray was used alone, treated cells demonstrated a significantly increased intensity of fluorescein isothiocyanate-conjugated (FITC) anti- γ -H2AX antibody staining compared with control cells. This indicated the DEPArray system was able to quantify differences in signal intensity caused by induction of γ -H2AX in CTCs. To determine if this could be applied clinically, the effect of CellSearch scanning on FITC intensity detected by DEPArray was evaluated using topotecan treated HT-29 cells that were scanned or unscanned with CellSearch followed by DEPArray analysis; scanned cells expressed a statistically significant lower FITC signal intensity compared with unscanned cells. Evaluation of γ -H2AX in CTCs from CRC patients was inconclusive due to small patient numbers. This study suggests a potential barrier for clinical application using the method of DEPArray following CellSearch analysis, therefore alternative methods should be evaluated to determine a suitable assay for use in the clinic.

Table of Contents

	Page
Declaration	2
Abstract	3
Table of Contents	4
Acknowledgements	9
List of Tables	10
List of Figures	12
Abbreviations	15
References	175
CHAPTER 1: Colorectal Cancer, its Treatment and Molecular Aberrations	
1.1. Background on CRC	20
1.1.1. Incidence	20
1.1.2. Risk Factors	20
1.1.3. Diagnosis and Symptoms	20
1.1.4. Current Classification and Prognostic Factors in CRC	21
1.1.5. Staging of CRC	22
1.1.6. Treatment of CRC	25
1.1.6.1. Management of Localised Disease	28
1.1.6.2. Management of Early Stage Rectal Cancer	28
1.1.6.3. Management of Early Stage Colon Cancer	28
1.1.6.4. Adjuvant Chemotherapy	29
1.1.6.5. Management of Metastatic Disease	31
1.1.6.6. Initial Therapy of Metastatic Disease	31
1.1.6.7. Treatment at Progression	34
1.2. Biomarkers	35
1.2.1. Signalling Pathway and Biomarkers in CRC	37
1.2.2. Transforming Growth Factor Beta (TGF- β) Pathway	38
1.2.3. EGFR/ Ras/Raf /MAPK Pathway	39
1.2.4. Phosphatidylinositol 3-kinase (PI3K) Pathway	40
1.2.5. Predictive Biomarkers for Risk Stratification and Early Detection	41
1.2.6. Predictive Biomarkers for Chemotherapy	41
1.3. The Rationale for studying Circulating Tumour Cells (CTCs) in CRC	41
1.3.1. Background	42
1.3.2. Current CTC Data in Breast and Prostate Cancer	43
1.3.3. Current CTC Data in CRC	44
1.3.4. The Role of CTCs in Clinical Trials	46
1.3.5. Molecular Characterisation of CTCs	47
1.4. Gamma H2AX as a Protein Biomarker and its use in Drug Efficacy Measurements	48
1.4.1. Gamma H2AX: Functional Role in DNA Damage Response (DDR)	48

1.4.2. Gamma H2AX as a Protein Biomarker for DNA DSBs and its Applications	51
1.4.3. Gamma H2AX as PD Biomarkers to Monitor Drug Activity in CTCs	53
1.4.4. Gamma H2AX assay types	55
1.5. Aims of This Thesis	56
CHAPTER 2: Materials and Methods	58
2.1. General materials	58
2.2. Investigational drugs	59
2.3. Cells and culture conditions	59
2.4. γ -H2AX immunofluorescence staining for adherent colon cancer cell lines treated with varying concentrations of oxaliplatin and SN-38 (Chapter 3)	61
2.4.1. Sample preparation	61
2.4.2. Treatment <i>in vitro</i> with oxaliplatin or SN-38	61
2.4.3. Immunofluorescence Staining	63
2.4.4. γ -H2AX foci detection	63
2.4.5. CellProfiler Software	64
2.4.6. Image analysis using CellProfiler Software	65
2.5. Time course experiments in colon cancer cell lines treated with oxaliplatin or SN-38 (Chapter 4)	66
2.5.1. Drug Treatment	66
2.5.2. Treatment <i>In vitro</i> with Oxaliplatin or SN-38	66
2.5.3. Immunofluorescence Staining, γ -H2AX Foci Detection and Image Analysis using CellProfiler Software	67
2.6. Development of the Protocol for quantification of γ H2AX intensity using the CellSearch System (Janssen Diagnostics) and the DEPArray™ System (Silicon Biosystems) (Chapter 5)	67
2.6.1 The CellSearch System- (Silicon Biosystems)	67
2.6.2. DEPArray™ System (Silicon Biosystems)	68
2.6.3. γ -H2AX immunofluorescence staining for adherent colon cancer cell lines treated with oxaliplatin, SN-38 or topotecan	70
2.6.4. Treatment with Oxaliplatin or SN-38	70
2.6.5. Treatment with Topotecan	70
2.7. γ -H2AX Immunofluorescence Staining Protocol for Suspension Cells (Chapter 5)	71
2.7.1. Cell Treatment	71
2.7.2. γ -H2AX Immunofluorescence Staining	71
2.8. Materials and Methods for CellSearch System (Janssen Diagnostics) (Chapter 5)	72
2.8.1. Materials for CellSearch Epithelial Cell Kit	72
2.8.2. Method for CellSearch System (Janssen Diagnostics)	74
2.8.2.1. Sample Preparation	74
2.8.2.2. CTC Analysis and Enumeration Using the CellSearch Method	75

2.8.3. Validation of the CellSearch System protocol for Detection of γ -H2AX on CTCs	76
2.8.3.1. Method Validation	77
2.9. Materials and Methods for the DEPArray™ System (Silicon Biosystems) (Chapter 5)	78
2.9.1. Materials for the DEPArray™ System (Silicon Biosystems)	78
2.9.2. Methods for the DEPArray™ System (Silicon Biosystems)	78
2.9.2.1. Sample Preparation and Buffer Compatibility	78
2.9.2.2. Cartridge Loading	79
2.9.3. Cell Browser	82
2.9.3.1 Cell Routing and Recovery	85
2.10. Materials and Methods for CellSearch Sample Pre-Processing Protocol for the DEPArray System (Silicon Biosystems) (Chapter 5)	86
2.10.1. Materials for CellSearch Sample Pre-Processing Protocol for the DEPArray System (Silicon Biosystems)	86
2.10.2. Methods for CellSearch Sample Pre-Processing Protocol for the DEPArray System (Silicon Biosystems)	87
2.10.3. DEPArray Analysis of γ -H2AX expression in treated and untreated colon cancer cells	88
2.10.4. γ -H2AX Staining for Suspension Cells and Slide Preparation for Validation with Fluorescence Microscopy	89
2.11. Methods for the Clinical Application and Characterisation of CTCs (Chapter 6)	89
2.11.1. Development of the CTC Protocol	89
2.11.2. Patient Selection and Consent	90
2.11.3. Sample and Patient Information Collection	90
2.11.4. Sample Preparation and Analysis	91
2.12. Statistical Analyses	91
CHAPTER 3: Defining the dose response in colon cancer cell lines treated with varying concentrations of oxaliplatin and SN-38	92
3.1. Introduction	92
3.2. Results	93
3.2.1. Dose Response in HT-29 Colon Cancer Cells treated with Oxaliplatin	93
3.2.2. Dose Response in HT-29 Colon Cancer Cells Treated with SN-38	95
3.3. Conclusions	97
CHAPTER 4: Time course experiments in colon cancer cell lines treated with oxaliplatin or SN-38	99
4.1. Introduction	99
4.2. Results	99

4.2.1. Time Course Experiments in HCT-116 and HT-29 Colon Cancer Cells Treated with Oxaliplatin	99
4.2.2. Time Course Experiments in HT-29 and HCT-116 Colon Cancer Cells Treated with SN-38	102
4.3. Conclusions	106
CHAPTER 5: Development of the Protocol for quantification of γ-H2AX intensity using the CellSearch System (Janssen Diagnostics) and the DEPArray™ System (Silicon Biosystems)	108
5.1 Introduction	108
5.2. Validation of the CellSearch System to detect γ -H2AX induction in treated CRC cells spiked into peripheral blood from healthy donors: Results	110
5.2.1. Validation of the CellSearch System to detect γ -H2AX induction in treated CRC cells spiked peripheral blood from healthy donors: Conclusions	113
5.3. Colon cancer cells treated with oxaliplatin and SN-38 enriched by CellSearch System and analysed by DEPArray using two exposure times	113
5.3.1. CTC Detection and Analysis on CellTracks Analyser II	113
5.3.2. DEPArray System Analysis of Colon Cancer Cells Treated with SN-38	117
5.3.3. DEPArray system analysis of untreated control colon cancer cells	118
5.3.4. Discussion and Conclusions: colon cancer cells treated with oxaliplatin and SN-38 run with the DEPArray platform after CellSearch System using two different exposure times	120
5.4. Colon cancer cells treated with SN-38 or oxaliplatin, run directly on the DEPArray platform using two different exposure times, validated with cytospin and fluorescence microscopy	125
5.4.1. DEPArray system analysis of SN-38 or oxaliplatin treated colon cancer cells	127
5.4.2. Colon cancer cells treated with oxaliplatin or SN-38, run directly on the DEPArray platform using two different exposure times, validated with cytospin and fluorescence microscopy: Discussion and Conclusions	133
5.5. Colon cancer cells treated with topotecan and run with DEPArray platform after CellSearch System using two different exposure times	133
5.5.1. Analysis with the CellSearch System	134
5.5.2. Analysis with DEPArray platform	136
5.5.3. Additional validation of CTC Analysis and Enumeration of HT-29 cells and their γ -H2AX (FITC) expression when treated with topotecan (second and third validation)	140
5.5.4. Analysis of γ -H2AX (FITC) expression with the DEPArray platform of HT-29 cells treated with topotecan that were scanned and unscanned with the CellTracks Analyzer II system	146
5.5.5. Further statistical analyses of the second and third validation runs using mean intensity only on FITCII data	151

5.5.6. Discussion and conclusions of the validation experiments for the colon cancer cells drug treated and run with the DEPArray platform after the CellSearch System	157
CHAPTER 6: Clinical Application and Characterisation of CTCs	161
6.1. Introduction	161
6.2. Patient Recruitment, demographics and baseline characteristics	162
6.3 Patient Laboratory Measurements Results	163
6.4. Discussion and Conclusions	164
CHAPTER 7: Overall Discussion and Conclusions	167

Acknowledgements

I would like to acknowledge my supervisors, Tim Meyer, John Hartley and Tobi Arkenau for their guidance.

Especially, I would like to thank those in the UCL Cancer Institute and ECMC GCLP Facility who supported me with training, assistance and data analysis required for this research. This includes Clare Vesely (Dr Meyer's lab) who helped performing the technical operations of the DEPArray system (Chapter 5); Victoria Spanswick, Leah Ensell, Helen Lowe (UCL Cancer Institute ECMC GCLP Facility) who completed the validation of the protocol for the quantification of γ -H2AX intensity on circulating tumour cells using the CellSearch System (Janssen Diagnostics) (Chapter 5, Section 5.2); and the DEPArray™ System (Silicon Biosystems S.p.A): Elena Peruzzi, Diana Cunati, Manuela Banzi, Alessandra Totaro, Barbara Baggiani, Henrik Tommerup and Massimo Scrobogna for their assistance with the validation of the DEPArray analyses (Chapter 5). Above all, I would like to thank the patients who agreed to volunteer to be a part of this research.

I would like to thank in particular my partner Salvatore, my friends and family for their patience and support during this challenging time of part-time research.

A thought goes to my father and his inspirational attitude, that has been my example and the secret behind the far steps that I took and victories I achieved.

Thanks to all those I haven't mentioned but that have been nevertheless supportive and valuable.

A big thank you to all.

List of Tables

	Page
Table 1.1. World Health Organisation classification of the carcinoma of the colon and rectum.	24
Table 1.2. Criteria for histological grading of colorectal adenocarcinoma.	24
Table 1.3. Anatomic stage/prognostic groups.	26
Table 1.4. Definitions of 'high risk' stage II colon cancer from expert groups.	30
Table 1.5. Irinotecan and oxaliplatin-based regimens for metastatic colorectal cancer.	32
Table 1.6. Molecular classification of colorectal carcinoma.	37
Table 1.7. Non-exhaustive list of clinical studies using the γ -H2AX assay to measure the effects of chemotherapeutic drugs in cancer patients.	52
Table 2.1. Cancer cell lines used.	60
Table 2.2. Downstream application and manipulation buffers.	78
Table 2.3. DEPArray Programme Parameters.	81
Table 3.1. Expression of γ -H2AX in HT-29 cell lines treated with oxaliplatin.	94
Table 3.2. Expression levels of γ -H2AX in HT-29 cell lines treated with SN-38.	97
Table 5.1. Validation run 1 results.	105
Table 5.2. Validation run 2 results.	111
Table 5.3. Validation run 3 results.	112
Table 5.4. Combined validation run results.	112
Table 5.5. DEPArray signal (FITC channel) and background gray levels of PE+/DAPI+/APC- colon cancer cells following treatment with SN-38.	112
Table 5.6. DEPArray signal and background gray levels of untreated PE+/DAPI+/APC- colon cancer cells.	118
Table 5.7. Validation of the DEPArray analysis by Silicon Biosystems.	119
Table 5.8. HT-29 cells treated with SN-38 0.01 μ M compared with the untreated control group and run into the DEPArray machine.	120
Table 5.9. HT-29 cells treated with SN-38 0.01 μ M compared with the untreated control group and run into the DEPArray machine.	128
Table 5.10. DEPArray analysis of HT-29 cells treated with topotecan from the CellSearch cartridge stained with the H2AX-FITC antibody in the fourth channel and scanned using CellTracks system or unscanned (first validation).	128
Table 5.11. Validation of the DEPArray analysis by Silicon Biosystems	137

Table 5.12. HT-29 cells treated with topotecan from the CellSearch cartridge stained with the H2AX-FITC antibody in the fourth channel and scanned using CellTracks system or unscanned (second validation).	140
Table 5.13. HT-29 cells treated with topotecan from the CellSearch cartridge stained with the H2AX-FITC antibody in the fourth channel and scanned using CellTracks system or unscanned (third validation).	147
Table 5.14. HT-29 cells treated with topotecan from the CellSearch cartridge stained with the H2AX-FITC antibody in the fourth channel and scanned using CellTracks system or unscanned (second validation).	148
Table 5.15. HT-29 cells treated with topotecan from the CellSearch cartridge stained with the H2AX-FITC antibody in the fourth channel and scanned using CellTracks system or unscanned (third validation).	152
Table 6.1. Patient demographics and baseline characteristics.	154
Table 6.2. CTC collection and γ -H2AX analysis of patient samples pre- and post-chemotherapy with FOLFOX or FOLFIRI using the CellSearch platform and Analyzer II.	162

List of Figures

	Page
Figure 1.1: The complexity of the intracellular EGFR pathway	40
Figure 1.2: Nucleosomal histones	49
Figure 1.3: Crosstalk between chromatin state and DNA damage response in cellular senescence and cancer	50
Figure 2.1: Foci identification using CellProfiler foci stain channel two (green input image)	65
Figure 2.2: Schematic of CellSearch and DEPArray system experimental workflow	69
Figure 2.3: An example of a <i>use case</i> in which the DEPArray analysis is performed using DAPI and FITC channels without the PE channel	82
Figure 2.4. Example of the Image Gallery created in the Cell Browser	85
Figure 2.5. Example of the visible attributes of the particles created in the Cell Browser	85
Figure 3.1: Expression levels of γ -H2AX measured in HT-29 cell lines in response to oxaliplatin treatment using CellProfiler Software	94
Figure 3.2: Expression levels of γ -H2AX in HT-29 cell lines treated with oxaliplatin	95
Figure 3.3: Expression levels of γ -H2AX measured in HT-29 cell lines in response to SN-38 treatment using CellProfiler Software	96
Figure 3.4: Expression levels of γ -H2AX in HT-29 cell lines treated with SN-38	97
Figure 4.1. Intra-assay variation in γ -H2AX foci induction and detection in HCT-116 cells treated with 5 μ M oxaliplatin	100
Figure 4.2. Inter-assay variation in γ -H2AX foci induction and detection in HCT-116 cells treated with 5 μ M oxaliplatin	101
Figure 4.3. Intra-assay variation in γ -H2AX foci induction and detection in HT-29 cells treated with 5 μ M oxaliplatin	101
Figure 4.4. Inter-assay variation in γ -H2AX foci induction and detection in HT-29 cells treated with 5 μ M oxaliplatin	102
Figure 4.5. Intra-assay variation in γ -H2AX foci induction and detection in HCT-116 cells treated with 0.01 μ M SN-38	103
Figure 4.6. Inter-assay variation in γ -H2AX foci induction and detection in HCT-116 cells treated with 0.01 μ M SN-38	103
Figure 4.7. Intra-assay variation in γ -H2AX foci induction and detection in HT-29 cells treated with 0.01 μ M SN-38	104
Figure 4.8. Inter-assay variation in γ -H2AX foci induction and detection in HT-29 cells treated with 0.01 μ M SN-38	104
Figure 5.1: Detection of γ -H2AX induction in whole blood samples spiked with HT-29 treated tumour cells using the CellSearch Analyzer II	111

Figure 5.2. HT -29 cells treated with (A) oxaliplatin, (B) SN-38 and (C) untreated control: CellTracks Analyser CTC candidate images demonstrating the criteria for CTC analysis	116
Figure 5.3. DEPArray images of PE+/DAPI+/APC- colon cancer cells following treatment with SN-38	117
Figure 5.4: DEPArray images of untreated PE+/DAPI+/APC- colon cancer cells	119
Figure 5.5. Overview of the experiments for colon cancer cells treated with oxaliplatin 5 μ M or SN-38 0.01 μ M and run directly on the DEPArray platform followed by validation experiments with cytopsin and fluorescence microscopy	125
Figure 5.6: DEPArray images of untreated PE+/DAPI+/APC- colon cancer cells (HT-29)	126
Figure 5.7: DEPArray images of SN-38 0.01 μ M treated PE+/DAPI+/APC- colon cancer cells (HT-29)	127
Figure 5.8: HT-29 cells treated with SN-38 0.01 μ M compared with an untreated control group using two different exposure times for FITC I (100 ms and gain 1X) and FITCII (800 ms and gain 4X)	129
Figure 5.9: Validation of the γ -H2AX signal with fluorescence microscopy using HT-29 cells exposed to SN-38 with and without antibody labelling for γ -H2AX	130
Figure 5.10: Validation of the γ -H2AX signal with fluorescence microscopy using HT-29 cells exposed to oxaliplatin with and without antibody labelling for γ -H2AX	132
Figure 5.11. HT-29 cells treated with topotecan hydrochloride run on the CellTracks Autoprep System and on the CellTracks Analyzer II	135
Figure 5.12. DEPArray analysis of HT-29 cells treated with topotecan from the CellSearch cartridge stained with the H2AX-FITC antibody in the fourth channel and scanned using CellTracks system (Sample 1) or unscanned (Sample 2) (first validation)	138
Figure 5.13: Screenshot from the Silicon Biosystems DEPArray system analysis of Sample 1 (scanned) showing three cells with FITC II signal and background level comparable	139
Figure 5.14: Screenshot from the Silicon Biosystems analysis of Sample 2 (unscanned) showing four cells with FITC II signal and background level comparable	140
Figure 5.15. A screenshot from the CellTracks Analyser demonstrating the Criteria for CTC Analysis. Topotecan treated HT-29 cells for the second validation: CTC candidate images and interpreter detection.	142
Figure 5.16. A screenshot from the CellTracks Analyser demonstrating the Criteria for CTC Analysis. Untreated HT-29 cells from second validation: CTC candidate images and interpreter detection.	143
Figure 5.17. A screenshot from the CellTracks Analyser demonstrating the Criteria for CTC Analysis. Topotecan treated HT-29 cells for the third validation: CTC candidate images and interpreter detection.	144

Figure 5.18. A screenshot from the CellTracks Analyser demonstrating the Criteria for CTC Analysis. Untreated HT-29 cells for the third validation: CTC candidate images and interpreter detection.	145
Figure 5.19. HT-29 cells treated with topotecan from the CellSearch cartridge stained with the H2AX-FITC antibody in the fourth channel and scanned using CellTracks system or unscanned (second validation).	149
Figure 5.20. HT-29 cells treated with topotecan from the CellSearch cartridge stained with the H2AX-FITC antibody in the fourth channel and scanned using CellTracks system (Sample 1) or unscanned (Sample 2) (third validation).	150
Figure 5.21. HT-29 cells treated with topotecan from the CellSearch cartridge stained with the H2AX-FITC antibody in the fourth channel and scanned using CellTracks system or unscanned (second validation).	153
Figure 5.22. HT-29 cells treated with topotecan from the CellSearch cartridge stained with the H2AX-FITC antibody in the fourth channel and scanned using CellTracks system or unscanned (third validation).	155
Figure 5.23. Distribution of the FITCII intensity observed following DEPArray analyses for the second and third validation experiments of CellTracks Analyser II scanned and unscanned cells.	156

Abbreviations

ACVR2, activin type 2 receptor

AJCC/UICC, American Joint Committee on Cancer/Union for International Cancer Control

APC, allophycocyanin

ASCO, American Society of Clinical Oncology

AT, ataxia telangiectasia

ATM, ataxia telangiectasia mutated

ATR, ataxia telangiectasia and Rad3-related

ATCC, American type culture collection

BSA, bovine serum albumin

BRAF, V-raf murine sarcoma viral oncogene homolog B1

CA125, cancer antigen 125

Cbl, casitas B-lineage lymphoma

CD45, lymphocyte/leukocyte common antigen

CEA, carcinoembryonic antigen and CA19-9

CIMP, CpG Island Methylator Phenotype

CIN, chromosomal instability

CKs, cytokeratins

CK-PE, CK-phycoerythrin

CPT, camptothecin

CRC, colorectal cancer

CT, computed tomography

CTCs, circulating tumour cells

DAG, diacyl glycerol

DAPI, diamidino-2-phenylindole

DDR, DNA damage response

DFS, disease free survival

DMSO, dimethyl sulfoxide

DNA-PK, DNA-dependent protein kinase

DSB, double-strand break

ECACC, European collection of cell cultures

ECOG, Eastern Cooperative Oncology Group

EDTA, ethylenediaminetetraacetic acid

EGFR MAPK, estimated glomerular filtration rate mitogen-activated protein kinases

EpCAM, epithelial cell adhesion molecule

ER, estrogen receptor

ERK, extracellular-signal-regulated kinase

ESMO, European Society of Medical Oncology

FACS, fluorescence-activated cell sorting

FAK, focal adhesion kinase

FAP, familial adenomatous polyposis

FBS, foetal bovine serum

FDA, Food and Drug Administration

FITC, fluorescein isothiocyanate

FOB, faecal occult blood

FOLFIRI, Irinotecan with fluorouracil (5FU) and folinic acid

FOLFOX, 5-FU, leucovorin, oxaliplatin

FOLFOXIRI, the combination of 5-FU, irinotecan and oxaliplatin

5-FU, 5-fluorouracil

G, grading

GDP, guanosine diphosphate

Grb2, growth factor receptor-bound protein 2

GSK3, glycogen synthase kinase 3

GTP, guanidine triphosphate

Gy, Gray

HCT, haematocrit

HER-2, human epidermal growth factor-2

HNPCC, hereditary nonpolyposis colorectal cancer

HR, hazard ratio

HT, human colorectal adenocarcinoma cell line

H2A, further subdivided in H2AZ and H2AX, H2B, H3 and H4, while the linker histones H1 family

IP3, inositol-1,4,5-trisphosphate

IR, ionising radiations

KRAS, V-Ki-ras2 Kirsten rat sarcoma viral oncogene homolog

LN, lymph node

LOH, loss of heterozygosity

LVI, lymphovascular invasion

MEK, methyl ethyl ketone

MGMT, O(6)-methylguanine-DNA methyltransferase

MLH1, MutL Homolog 1

MMR, DNA mismatch repair

mPFS, median PFS

MRI, magnetic resonance imaging

MSH2, MutS protein homolog 2

MSH6, MutS protein homolog 6

MSI, microsatellite instability

mTOR, mammalian target of rapamycin

mTORC, mammalian target of rapamycin complex

M0, no distant metastasis

M1, distant metastasis

M1a, metastasis confined to one organ or site

M1b, metastases in more than one organ/site or the peritoneum

mVim, VIMENTIN assay

NCCN, National Comprehensive Cancer Network

OS, overall survival

PARP, poly ADP ribose polymerase

PBMCs, peripheral blood mononuclear cell

PBS, phosphate buffer saline

PD, pharmacodynamic

PDK, phosphoinositide- dependent kinase

PE, phycoerythrin

PEAK study, panitumumab efficacy in combination with mFOLFOX6 against bevacizumab plus mFOLFOX6

PET, positron emission tomography

PFA, paraformaldehyde

PFS, progression free survival

PIGF, placental growth factor

PIK3CA, phosphatidylinositol-4,5-Bisphosphate 3-Kinase Catalytic Subunit Alpha

PK, pharmacokinetic

PLC, phospholipase C

PMS2, postmeiotic segregation increased 2

PNI, perineural invasion

PR, partial response

PSA, prostate-specific antigen

PTEN, phosphatase and tensin homologue

PTMs, histone post-translational modifications

PI3K, phosphatidylinositol 3-kinase pathway

RAF, proto-oncogene serine/threonine-protein kinase

RAS, rat sarcoma

rcf, radiochromic film

ROI, region of interest

RR, response rate

RT, radiotherapy

SMAD2, Mothers against decapentaplegic homolog 2

SMAD4, Mothers against decapentaplegic homolog 4

SN-38, 7-ethyl-10-hydroxycamptothecin

SOS, salt overly sensitive

S-phase, synthesis phase

STATs, signal transducer and activator of transcription

TME, total mesorectal excision

TD, tumour deposits

TGFBR1 and TGFBR2, Transforming Growth Factor Beta Receptor 1 and 2

TGF- β , transforming growth factor-beta

TME, mesorectal excision

TNM, tumour, node, metastases

Topo I, topoisomerase I

TS-102, trifluridine and tipiracil hydrochloride

TS-114, dUTPase inhibitor

UGT1A1, UDP-glucuronosyltransferase

VEGF-A, vascular endothelial growth factor-A

VEGF-B, vascular endothelial growth factor-B

VELOUR trial, aflibercept combined with FOLFIRI

VIM, methylated vimentin

vs, versus

V600E, amino acid substitution at position 600 in BRAF, from a valine (V) to a glutamic acid (E)

WT, wild-type

XELOX, oxaliplatin and capecitabine combination

γ-H2AX, gamma histone H2AX

CHAPTER 1: Colorectal Cancer, its Treatment and Molecular Aberrations

1.1. Background on CRC

1.1.1. Incidence

Colorectal cancer (CRC) is the third most common cancer in males and females and the fourth overall in the UK, accounting for 13% of all new cases [1]. Almost two-thirds of all CRCs originate in the colon and over one-third in the rectum [2]. Worldwide incidence rate is influenced by different environmental factors, especially poor diet, obesity and low socioeconomic status which account for 30% of increased risk [3-5]. Historically, the incidence has been 10-fold higher in Europe and the USA compared with Asia or Africa [6] but in the last 15 years this trend has changed globally, being quite stable in Western countries while increasing in several areas previously at low risk [6, 7]. More recent data from the United States SEER database and other Western cancer registries indicate that incidence rates are increasing in younger age [2, 8-10]. 5% of the normal population is potentially exposed to the risk of developing CRC, while the risk increases substantially in those patients with specific inherited conditions or inflammatory bowel disease. Overall, death rates have declined in the last 30 years with an improvement of 5-year survival rates throughout all stages due to implementation of screening programs, early diagnosis and improved treatment [2, 11, 12].

1.1.2. Risk Factors

The majority of CRCs (about 75%) are sporadic. Age is considered a major risk factor with incidence rates increasing in each following decade after the age of 50 years [2, 13]. Only 5% of CRCs are related to genetic factors; these cancers are more often localised in the right side of the colon and are characterised by early age of onset [14-21]. The most common hereditary CRC syndromes are Familial Adenomatous Polyposis (FAP) and Lynch Syndrome (hereditary non-polyposis colorectal cancer [HNPCC]). FAP is responsible for the majority of cancer in young age and is caused by germline mutations in the APC gene on chromosome 5 [22]. Lynch syndrome is an autosomal dominant

syndrome, with a germline mutation in one allele of mismatch repair genes (MMR), most commonly hMLH1, hMSH2, hMSH6, or PMS2 [23]. Along with genetic conditions, inflammatory bowel disease (ulcerative colitis and Crohn's disease) can also represent another important risk factor [24-26].

1.1.3. Diagnosis and Symptoms

The most common anatomic location of CRCs is the left side of the colon including the descending and sigmoid colon, although recently an increase in incidence of ascending colon and caecal cancers has been observed in the United States and internationally [27-30]. Improvement in screening procedures such as flexible sigmoidoscopy with removal of adenomatous polyps in the descending colon could explain fewer occurrences of left-sided tumours, while right-sided CRCs are more difficult to detect especially for their different anatomical presentation (flat adenoma). Nevertheless, biology appears to vary between left and right side, the latter appears to carry more BRAF V600E mutations with microsatellite instability [27, 28].

Despite advances in screening and early detection of CRCs, one in five patients presents with symptoms suggestive of metastatic disease [31], such as change in bowel habits, anaemia and fatigue [32]. If CRC is suspected, initial evaluation includes medical history, physical examination, FOB testing and flexible sigmoidoscopy or colonoscopy which remains the gold standard diagnostic test for detection of the majority of endoluminal adenocarcinomas of the colon and rectum [33]. All lesions detected should be biopsied for histological examination [32]. CT colonography (virtual colonoscopy) can be used in cases where direct endoscopy is precluded for medical or technical reasons, although biopsies cannot be performed during this procedure [32]. Following diagnosis of CRC, a CT scan of the chest, abdomen and pelvis should be performed to assess metastatic disease [32, 33]. There is no diagnostic role for routine laboratory blood tests in screening or staging of CRC. Elevated serum CEA and CA19-9 levels may be present in a percentage of patients with CRC, although this test is neither sensitive enough or specific enough for screening, in the preoperatively and postoperatively setting the levels are important in guiding surgical

treatment planning, assessment of prognosis and helping to detect recurrences earlier [34].

Preoperative staging of a newly diagnosed CRC includes CT scan of the chest, abdomen and pelvis while additional procedures (rigid sigmoidoscopy, transrectal endoscopic ultrasound, and/or magnetic resonance imaging [MRI]) maybe indicated for locoregional staging of patients with rectal cancer to assess the extent of local disease and assist with treatment planning such as initial radiotherapy (RT), chemo-radiotherapy or surgery. Positron emission tomography (PET) of the chest/abdomen/pelvis is usually used in cases of isolated liver metastases that can undergo surgical resection.

1.1.4. Current Classification and Prognostic Factors in CRC

Pathologic stage at diagnosis remains the best indicator of long-term prognosis for both colon and rectal cancer and the strongest predictor of postoperative outcome; this has been investigated and confirmed by multiple correlative studies between many other prognostic factors for CRCs [35]. The most robust determinants of prognosis and five-year survival rates include local involvement, regional lymph node (LN) metastasis, residual disease after definitive therapy and the presence of distant metastases.

Local involvement (pT category of TNM) independently influences survival [36-39]; regional LN metastasis (pN category of TNM staging) represents an indication for adjuvant chemotherapy for both colon and rectal cancer and is one of the strongest predictors of outcome for both stage II (node-negative) and stage III (node-positive) disease [40-48]. Following surgical resection, residual disease after definitive therapy, has also been demonstrated to be a poor prognostic factor. In a report of 152 patients with T4 colon cancers, 42 patients with incompletely resected cancers had an inferior 10-year recurrence-free survival when compared with those with fully resected T4N0 or T4 node-positive disease (19 vs 88 and 58%, respectively) [49-52].

Lymphovascular invasion is also an important prognostic determinant and an independent adverse prognostic factor for CRCs [36, 53-55]. Nevertheless, in stage IV, location and extent of distant metastatic disease are the most determinants of prognosis. The tumour

marker CEA, as previously mentioned, has prognostic significance in the preoperative setting independent of tumour stage [54, 56-58], showing an adverse impact on survival if levels are ≥ 5.0 ng/mL. CEA should be routinely measured in patients undergoing potentially curative resections for CRC and post-operatively to ensure elevated levels normalise. In contrast, there are insufficient data about the use of CEA as to determinant for adjuvant therapy [58].

The majority of CRCs are adenocarcinomas (Table 1.1) [59] which are further classified as low-grade tumours (well/moderately differentiated) and high-grade tumours (poorly/undifferentiated) (Table 1.2) [60]. Mucinous carcinoma is a subtype of CRC producing extracellular mucin, representing a small percentage of all CRCs [61, 62], often localised in the right side of the colon [63, 64] and are further characterised by late stage at diagnosis, MSI instability, BRAF mutation and poor response to treatment [65, 66]; a very aggressive variant of this subtype accounting only 1–2%, is signet ring cell carcinoma [61, 67, 68]. Small cell carcinomas with comparable poor account and neuroendocrine differentiation represent 10% of all CRCs. Adenosquamous carcinomas [69] represent only 0.05–0.2% of CRCs [70, 71] and are characterised by higher overall and colorectal-specific mortality; while the medullary carcinoma subtype is a non-gland forming cancer [72] usually associated with microsatellite instability and HNPCC syndrome.

Table 1.1: World Health Organisation classification of the carcinoma of the colon and rectum

Adenocarcinoma
Cribriform comedo-type adenocarcinoma
Medullary carcinoma
Micropapillary carcinoma
Mucinous (colloid) adenocarcinoma (>50% mucinous)
Serrated adenocarcinoma
Signet-ring cell carcinoma (>50% signet-ring cells)
Adenosquamous carcinoma
Spindle cell carcinoma
Squamous cell (epidermoid) carcinoma
Undifferentiated carcinoma

Adapted from World Health Organization Classification of Tumours of the Digestive System, 4th ed, Hamilton SR *et al.*, Criteria for histological grading of colorectal adenocarcinomas, p.138 [59].

Table 1.2: Criteria for histological grading of colorectal adenocarcinoma

Criterion	Differentiation category	Numerical grade	Descriptive grade
>95% with gland formation	Well differentiated	1	Low
50 to 90% with gland formation	Moderately differentiated	2	Low
>0 to 49% with gland formation	Poorly differentiated	3	High
High level of microsatellite instability	Variable	Variable	Low

Adapted from Colorectal carcinoma: Pathologic aspects, Fleming M *et al.*

J Gastrointestinal Oncol. 2012;3:153–173 [60]

The category 'undifferentiated carcinoma' (grade 4) is reserved for carcinomas with no gland formation, mucin production, or neuroendocrine, squamous, or sarcomatoid differentiation [59].

1.1.5 Staging of CRC

The 2010 TNM staging classification of the AJCC/UICC (Table 1.3) is the staging system for CRC currently in use [35] and has been implemented with few changes compared to the 2002 classification [35].

Stage categories

T–T4 category has been subdivided into T4a (tumour penetrates to the surface of the visceral peritoneum) and T4b (tumour directly invades or is adherent to other organs and structures).

N – Recommendation of 6th edition – to harvest at least 12 to 14 regional LN – is restated
pN1 – metastasis in one to three regional LN – has been subdivided in N1a (metastasis in one regional lymph node), N1b (metastasis in 2–3 regional lymph nodes) and N1c (*tumour deposits* in the subserosa, mesentery or non-peritonealized pericolic or perirectal tissue without regional LN metastasis).

Tumour deposits (TD, formerly named satellite nodules) defined as discrete foci of tumour found in the pericolic, perirectal or mesenteric fat, in the absence of residual LN tissue, but within the lymph drainage area of primary tumour are included both in *Site-Specific Factors* (or *Prognostic Factors*) category and also in N category.

pN2 – metastasis in four or more regional LN – has been subdivided in pN2a – metastasis in four to six regional LN – and pN2b – metastasis in seven or more nodes.

M – MX is no longer included in TNM 7. The MO category cannot be documented on pathological evaluation, but only clinical, based on history and physical exam. M1 has been subdivided into M1a (metastasis confined to one organ or site) and M1b (metastasis in more than one organ/site or the peritoneum).

Anatomic Stage/Prognostic Groups

Stage II – is now subdivided into IIA (T3N0), IIB (T4aN0) and IIC (T4bN0).

Stage III – T4bN1 (previously classified as IIIB), has been reclassified as IIIC. A number of N2 categories (formerly included in stage IIIC) have been restaged as follows:

T1N2a in stage IIIA and T1N2b, T2N2a-b and T3N2a in stage IIIB.

Table 1.3: Anatomic stage/prognostic groups [28]

Primary tumour (T)	
TX	Primary tumour cannot be assessed
T0	No evidence of primary tumour
Tis	Carcinoma in situ: intraepithelial or invasion of lamina propria
T1	Tumour invades submucosa
T2	Tumour invades muscularis propria
T3	Tumour invades through the muscularis propria into pericolorectal tissues
T4a	Tumour penetrates to the surface of the visceral peritoneum
T4b	Tumour directly invades or is adherent to other organs or structures
Regional lymph node (N)	
NX	Regional lymph nodes cannot be assessed
N0	No regional lymph node metastasis
N1	Metastasis in 1–3 regional lymph nodes
N1a	Metastasis in one regional lymph node
N1b	Metastasis in 2–3 regional lymph nodes
N1c	Tumour deposit(s) in the subserosa, mesentery, or nonperitonealized pericolic or perirectal tissues without regional nodal metastasis

N2	Metastasis in four or more regional lymph nodes				
N2a	Metastasis in 4–6 regional lymph nodes				
N2b	Metastasis in seven or more regional lymph nodes				
Distant metastasis (M)					
M0	No distant metastasis				
M1	Distant metastasis				
M1a	Metastasis confined to one organ or site (eg, liver, lung, ovary, non-regional node)				
M1b	Metastases in more than one organ/site or the peritoneum				
Stage	T	N	M	Dukes	MAC
0	Tis	N0	M0	–	–
I	T1	N0	M0	A	A
	T2	N0	M0	A	B1
IIA	T3	N0	M0	B	B2
IIB	T4a	N0	M0	B	B2
IIC	T4b	N0	M0	B	B3
IIIA	T1-2	N1/N1c	M0	C	C1
	T1	N2a	M0	C	C1
IIIB	T3-T4a	N1/N1c	M0	C	C2
	T2-T3	N2a	M0	C	C1/C2
	T1-T2	N2b	M0	C	C1
IIIC	T4a	N2a	M0	C	C2
	T3-T4a	N2b	M0	C	C2
	T4b	N1-N2	M0	C	C3
IVA	Any T	Any N	M1a	–	–
IVB	Any T	Any N	M1b	–	–

1.1.6. Treatment of CRC

1.1.6.1. Management of Localised Disease

1.1.6.2. Management of Early Stage Rectal Cancer

Treatment differs based on the initial stage of the disease. The treatment of choice for Stage I rectal cancer is radical hemicolectomy with LN dissection, and there is no indication for adjuvant therapy. For low risk tumours (T1, <3 cm and well differentiated (G1/G2) lesions), local excision can be curative, combined with TME in case of a postoperative higher T stage. For locally advanced disease (T2-4; N0-2; M0), neo-adjuvant chemo-radiotherapy with a fluoropyrimidine followed by surgery and adjuvant chemotherapy is the standard practice supported by data from randomized trials that showed a reduction in the incidence of local recurrence [73]. The dose of radiation generally used is 50.4 Gys fractionated over 5 weeks, although several studies suggest that a shorter radiation regimen is as affective [74, 75]. In the adjuvant setting capecitabine or infusional 5-fluorouracil (5-FU) can be used since no difference in survival rates were found in previous studies [76].

The German CAO/ARO/AIO-94 randomized Phase III study compared pre and post chemo-radiotherapy in locally advanced rectal cancer and showed a significant improvement in local recurrence free survival (P=0.048) in the pre-operative arm, with a 10 year relapse rate of 7.1% compared to 10.1% of the post RT arm [77], despite the occurrence of distant metastasis being similar in both arms. The addition of oxaliplatin to the standard 5-FU infusion did not show a better outcome [78, 79], while 5-FU bolus as adjuvant treatment compared with 5-FU, leucovorin, oxaliplatin (FOLFOX) resulted in a shorter disease-free survival (DFS) [77].

1.1.6.3. Management of Early Stage Colon Cancer

Surgery is the mainstay of treatment for localized colon cancer. Laparoscopic-assisted colectomy is comparable to colectomy in terms of oncologic outcomes and is associated with shorter hospital stay and a small number of moderate-to-severe postoperative

adverse events [80]. Therefore, it is a reasonable alternative to colectomy and is an acceptable option for uncomplicated patients where restoration of bowel continuity is usually feasible using a primary anastomosis. However, a temporary proximal diverting colostomy or ileostomy may be necessary in case the patient is medically unstable or in the presence of complications such as diffuse peritonitis or free perforation.

1.1.6.4. Adjuvant Chemotherapy

In stage II (node negative) disease, the benefits of chemotherapy 5-FU or capecitabine, plus/minus the addition of oxaliplatin, in increasing the 5-year survival rate are very low (2–3%) and it is not recommended [81]. Treatment decisions must be individualized based on the presence of high-risk clinicopathologic features such as fewer than 12 nodes in the surgical specimen; T4 tumour stage; presence of perforation/obstruction, poorly differentiated histology and lymphovascular or perineural invasion (Table 1.4). It is important to assess the MMR status because MMR-deficient tumours have an excellent prognosis and do not benefit from 5-FU adjuvant chemotherapy [82].

Table 1.4: Definitions of ‘high risk’ stage II colon cancer from expert groups*

	ASCO (2004)	NCCN (2014)	ESMO (2012)
T4 primary tumour	+	+	+
Inadequately sampled nodes	+ (<13)	+ (<12)	+ (<12)
Poorly differentiated tumour	+	+	+
Perforation	+	+ (localized)	+
Obstruction		+	+
LVI	+	+	+
PNI	+	+	+
Close/indeterminate or positive margins		+	
High preoperative levels of serum CEA			

LVI: lymphovascular invasion; PNI: perineural invasion; CEA: carcinoembryonic antigen.

*ie, the American Society of Clinical Oncology (ASCO), the National Comprehensive Cancer Network (NCCN), and the European Society for Medical Oncology (ESMO).

In 2015, updated data showed an increasing absolute survival benefit for oxaliplatin in stage III disease with time (67 vs 59%, P=0.043) [83]. Standard treatment include a six-month course of a combination of oxaliplatin with infusional 5-FU (FOLFOX) or with capecitabine (XELOX) [84]. Postoperative RT is not usually considered a routine component of care for completely resected colon cancer.

1.1.6.5. Management of Metastatic Disease

CRCs disseminate prevalently through the haematogenous and lymphatic system to the regional LN, liver and lungs, but can also metastasise locally through contiguous and transperitoneal spread. Because of the portal venous drainage of the colon, the first site of haematogenous dissemination is usually the liver, while the lungs are a common site if the tumour develops in the distal rectum drained by the inferior vena cava. Approximately 20% of newly diagnosed CRCs are metastatic at presentation (synchronous metastasis). In the majority, the intent of therapy is palliative, while for selected patients with limited metastatic disease, long-term survival can be achieved with metastasectomy plus removal of the primary tumour in conjunction with systemic chemotherapy. Unfortunately, only about 20–30% remain disease free. Initial therapeutic options were chemotherapy 5-FU and leucovorin based chemotherapy [85-87] that increased survival from 6 months up to 12 months compared with untreated patients. Currently, the regimens used are a combination of infusional 5-FU and leucovorin with the addition of irinotecan (FOLFIRI) [88, 89] or oxaliplatin (FOLFOX) [90, 91]; use of these combinations have resulted in improved median survival to >20 months. Addition of the vascular endothelial growth factor –A (VEGF-A) antibody bevacizumab, or the epidermal growth factor receptor (EGFR) antibodies cetuximab and panitumumab to standard regimes has further improved overall survival (OS) up to 24 months [92-95] in selected patients. Sequential exposure to all active agents gives the best overall outcomes and data from the FIRE-3 and CALGB 80405 studies showed an improvement in OS in a subset of molecularly defined patients [96].

1.1.6.6. Initial Therapy of Metastatic Disease

The first line of treatment is the most effective in terms of response rate (RR), progression free survival (PFS) and OS, especially in combination with an antibody against VEGF-A or EGFR [92, 93]. Multiple Phase III studies showed that a doublet chemotherapy regimen (FOLFOX, XELOX or FOLFIRI) is more active than monotherapy with fluoropyrimidine [89, 90, 97] or than sequential use of single agents (Table 1.5). Both FOLFOX and FOLFIRI

regimens showed similar first-line efficacy, and the decision to use one or the other should mainly be based on the expected toxicity profiles.

Table 1.5: Irinotecan and oxaliplatin-based regimens for metastatic colorectal cancer

Regimen [reference]	Irinotecan	Oxaliplatin	Leucovorin	Fluorouracil/ capecitabine	Schedule
FOLFIRI [98]	180 mg/m ² day 1		400 mg/m ² over 2 hours day 1	Fluorouracil 400 mg/m ² bolus day 1, followed by 2400 to 3000 mg/m ² over 46 hours, continuous infusion	Every 2 weeks
Douillard regimen [88]	180 mg/m ² day 1		200 mg/m ² leucovorin over 2 hours days 1 and 2 before fluorouracil	Fluorouracil 400 mg/m ² bolus then 600 mg/m ² over 22 hours days 1 and 2	Every 2 weeks
FOLFOX 4 [99]		85 mg/m ² day 1	400 mg/m ² over 2 hours days 1 and 2 before fluorouracil	Fluorouracil 400 mg/m ² bolus then 600 mg/m ² over 22 hours days 1 and 2	Every 2 weeks
FOLFOX 6 [98]		100 mg/m ² day 1	400 mg/m ² over 2 hours day 1	Fluorouracil 400 mg/m ² bolus day 1, followed by 2400 to 3000 mg/m ² over 46 hours, continuous infusion	Every 2 weeks
Modified FOLFOX 6 [85, 86]		85 mg/m ² day 1	350 mg total dose over 2 hours day 1	Fluorouracil 400 mg/m ² bolus day 1, followed by 2400 mg/m ² over 46 hours	Every 2 weeks
FOLFOX 7 [100]		130 mg/m ² day 1	400 mg/m ² over 2 hours day 1	Fluorouracil 400 mg/m ² bolus, then 2400 mg/m ² over 46 hours	Every 2 weeks
Modified FOLFOX 7(Optimox) [101]		100 mg/m ² day 1	400 mg/m ² over 2 hours day 1	Fluorouracil 3000 mg/m ² over 46 hours	Every 2 weeks
Modified FOLFOX 7(CONcePT) [102]		85 mg/m ² day 1	200 mg/m ² over 2 hours day 1	Fluorouracil 2400 mg/m ² over 46 hours	Every 2 weeks
XELOX [86]		130 mg/m ² day 1		Capecitabine 1000 mg/m ² orally twice per day on days 1 to 14	Every 3 weeks
FOLFOXIRI [103]	165 mg/m ² day 1	85 mg/m ² day 1	400 mg/m ² leucovorin over 2 hours day 1	Fluorouracil 3200 mg/m ² over 48 hours	Every 2 weeks

The combination of 5-FU, irinotecan and oxaliplatin (FOLFOXIRI) compared with FOLFIRI suggests a significantly improved outcome with FOLFOXIRI [103, 104]. Benefits of a six-month course of FOLFOXIRI included a significantly higher RR (66 vs 41%) and a greater number of secondary surgical resections of liver metastases (36 vs 12%) [103]. At a median follow-up of over 60 months, FOLFOXIRI was associated with significantly longer median PFS (mPFS) (9.8 vs 6.8 months) and OS (23.4 vs 16.7 months), with a 5-year survival rate of 15 vs 8% [104]. Patients with BRAF mutated tumours in the FOLFOXIRI plus bevacizumab arm reached an improvement in OS (24 months) when compared with the OS (16/17 months) from subgroup analysis in the CRYSTAL and FIRE-3 trials [105, 106]. This combination is particularly toxic and should only be considered in extremely fit patients.

Following response, oxaliplatin should be discontinued after 3–4 months of therapy to avoid neurotoxicity, but the infusional fluoropyrimidine, with or without bevacizumab, should be continued [107, 108]. Several trials compared different maintenance therapies compared with a drug holiday in terms of PFS and OS demonstrating that any treatment after FOLFOX plus bevacizumab as induction therapy had a better PFS than no treatment [101, 109-111]. Infusional fluoropyrimidine or capecitabine with or without bevacizumab would be more appropriate for frailer patients and the AVEX study has shown an advantage in OS in an elderly population [112].

Results from clinical trials showed that assay of RAS mutations permit the selection of individuals with RAS wild-type (WT) tumours who might benefit from agents that target EGFR. The approval for the use of cetuximab or panitumumab was initially granted after identification of KRAS exon 2 WT tumours [113] but more recent data showed that the benefit of treatment was abolished in cases with the presence of more rare mutations in KRAS exons 3 and 4 and NRAS exons 2, 3 and 4 [113, 114]. In the presence of RAS mutations, bevacizumab can be added to FOLFOX, FOLFIRI or FOLFOXIRI and used in addition to cetuximab or panitumumab in RAS WT status [115].

There are few studies testing the efficacy of bevacizumab vs cetuximab or panitumumab with FOLFOX, FOLFIRI or both. In one study comparing FOLFIRI plus cetuximab vs

FOLFIRI plus bevacizumab, the mPFS turned out to be similar (10.0 months in the cetuximab arm vs 10.3 months in the bevacizumab arm, $P=0.55$), although median OS (mOS) was significantly longer in the cetuximab arm (28.7 vs 25.0 months, $P=0.017$) [105, 116]. In one study [117], oxaliplatin based therapy with cetuximab showed a trend towards longer OS vs bevacizumab treated patients, while OS was comparable for FOLFIRI based therapy; in contrast another study showed a benefit in OS with cetuximab-FOLFIRI [105]. The PEAK study (Panitumumab Efficacy in combination with mFOLFOX6 against bevacizumab plus mFOLFOX6 in metastatic CRC (mCRC) subjects with WT *KRAS* tumours) was a Phase II study designed to address whether to include anti-EGFR vs anti-VEGF monoclonal antibodies in the first-line treatment of patients with mCRC. The primary objective was PFS and a secondary objective was to evaluate PFS and OS in *RAS* WT patients. No statistically significant PFS difference was detected in patients with exon 2 WT *KRAS* mCRC (PFS 10.9 vs 10.1 months, HR =0.87, $P=0.35$), but an improvement in OS was seen in the panitumumab arm (34.2 vs 24.3 months, HR =0.62, $P=0.009$) [118]. There are still only limited data on the benefit of adding bevacizumab to an oxaliplatin-based regimen and the available data suggest that incremental benefit is modest at best. Whether it is preferable to add cetuximab or panitumumab rather than bevacizumab to first-line chemotherapy is still unclear, since data are conflicting.

1.1.6.7. Treatment at Progression

In the absence of direct clinical trial data for second-line chemotherapies, a significant survival benefit has been shown following irinotecan-based first-line treatment with the addition of bevacizumab to FOLFOX [119]. After progression on FOLFOX or XELOX, FOLFIRI with aflibercept, a soluble 'decoy' receptor that binds to VEGF-A, VEGF-B and placental growth factor (PIGF), showed a significant increase in OS [120]. Aflibercept received FDA approval based on the placebo-controlled VELOUR trial plus FOLFIRI, in oxaliplatin-refractory mCRC patients; mOS was significantly longer in patients treated with aflibercept (13.5 vs 12.1 months) [120].

On the contrary, treatments with anti-EGFR in the second line did not show an OS benefit irrespective of the chemotherapy previously administered [121], while an increase in survival has been shown in later lines of chemotherapy for patients with RAS WT tumours, with or without irinotecan [95, 122]. In addition, the kinase inhibitor regorafenib significantly prolonged OS, albeit with little objective antitumour response when tested against best supportive care (CORRECT trial) [123]. New compounds such as TAS-102 (trifluridine and tipiracil hydrochloride) and TAS-114 (dUTPase inhibitor) that interfere with thymidylate metabolism, have shown encouraging results in Phase II trials and TS-102 showed significant OS benefit against placebo in the Phase III trial (RECURSE) in refractory mCRC [124]. After failure of all conventional 'lines of therapy', it is acceptable to re-utilize the regimen initially used in the treatment sequence since tumours may regain sensitivity to previously used drugs [125].

In the last two decades, the development of new drugs and the evaluation of the best therapy sequence and combinations of treatments have considerably increased the OS from 6 months to more than 30 months. The investigation of mechanisms of CRC carcinogenesis, secondary resistance and new molecular biomarkers will contribute to more personalised treatment in the future.

1.2. Biomarkers

Identical histological subtypes of CRCs can have different prognoses and response to treatment. Clinicopathological staging remains the mainstay of prognostication and treatment selection but there is a clear need for robust diagnostic, predictive and prognostic markers for routine clinical use [126].

Investigations into the molecular mechanisms involved in pathogenesis and progression of CRCs have demonstrated underlying genetic and epigenetic lesions that can provide important information along with clinicopathologic features, guiding treatment management in a personalised fashion (Table 1.6) [127, 128]. The most well-known genetic and epigenetic abnormalities in CRCs are chromosomal instability (CIN), MSI and methylation changes [126].

CIN is present in 85% of CRCs and is characterised by the presence of aneuploidy. It is usually mutually exclusive of MSI which presents with a normal karyotype and unique gene mutations involving the DNA Mismatch Repair (MMR) family [126]. MSI account for about 15% of CRCs, can be sporadic and are characterised by silencing of MLH1 by aberrant DNA methylation [126, 129] frequently carrying BRAF V600E mutations [130, 131] or can be hereditary as in the Lynch syndrome due to germline mutations in one of the MMR genes (MLH1, MSH2, MSH6 and PMS2).

Results from meta-analyses have shown that MSI CRCs have a better prognosis of CIN tumours [132, 133] independently of stage but, although they can be considered as prognostic markers, have not yet been included into routine practice.

Other genetic aberrations commonly found in CRCs are CpG Island Methylator Phenotype (CIMP) and global DNA hypomethylation resulting in deregulation of specific important signalling pathways such as APC/ β -catenin/WNT- β -catenin pathway, transforming growth factor β (TGF- β) pathway, EGFR/MAPK pathway and phosphatidylinositol 3-kinase (PI3K) pathway [134, 135].

Table 1.6: Molecular classification of colorectal carcinoma

Heredity	Chromosomal instability pathway	Mismatch repair pathway	Serrated/CIMP pathway		Hybrid pathway
	Hereditary and sporadic	Hereditary	Hereditary	and sporadic	Sporadic
CIMP status	Negative	Negative	High	High	Low
MSI status	MSS	MSI-H	MSI-H	MSI-L	MSI-L or MSS
Chromosomal instability	Present	Absent	Absent	Absent	Present
<i>KRAS</i> mutation	+++	+/-	-	-	+++
<i>BRAF</i> mutation	-	-	+++	+++	-
MLH1 status	Normal	Mutation	Methylated	Partial methylation	Normal
MGMT methylation	---	---	+/-	+++	++

CIMP: CpG island methylator phenotype; MSS: microsatellite stability; MSI: microsatellite instability; MSI-H: high-level microsatellite instability; MSI-L: low-level microsatellite instability; MGMT: O-6-methylguanine DNA methyltransferase; +++: present; +/-: might or might not be present; ---: absent.

Adapted from: Noffsinger AE. Serrated polyps and colorectal cancer: New pathway to malignancy. *Annu Rev Pathol* 2009;4:343 [128]

1.2.1. Signalling Pathway and Biomarkers in CRC

To date, mutant *KRAS* is the only predictive marker that has been clinically validated in the treatment of CRC, while further validations are still needed for mutant *BRAF*, *PIK3CA* and *PTEN* [136]. Research efforts are also focused on ascertaining molecular features of

CRC that can predict response to adjuvant chemotherapy such as 5-FU, irinotecan and oxaliplatin [135].

1.2.2. Transforming Growth Factor Beta (TGF- β) Pathway

Deregulation of the tumour-suppressor TGF- β signalling is very common in CRCs [137] and can involve receptor genes (TGFBR2 and TGFBR1), intra-cellular signalling pathway genes (SMAD2, SMAD4) and TGF- β super family members (ACVR2) [138-140]. SMAD4 is a tumour suppressor gene located on 18q [141], it is lost in >50% of CRCs correlating with worse prognosis [142]; SMAD4 can be deleted by the loss of the long arm of chromosome 18 (18q loss of heterozygosity; LOH). There is a strong association between 18qLOH and CIN suggesting a role as an independent prognostic marker, but further data need to validate their roles as prognostic biomarkers [135].

1.2.3. EGFR/ Ras/Raf /MAPK Pathway

KRAS is a member of the RAS family of proto-oncogenes and is mutated in approximately 40% of CRCs (codons 12 or 13). The KRAS protein is a downstream effector of EGFR signalling through the BRAF gene in the Ras/Raf/MAPK signalling pathway, promoting cell growth and survival [143, 144]. The most common BRAF mutation (10–15%) is the result of the substitution of glutamic acid for valine at codon 600 (V600E) [134] and is mutually exclusive with KRAS mutations in promoting tumourigenesis [145].

Evidence from previous studies showed that mutant BRAF could be a reliable prognostic marker of OS in Stage II and III CRCs and a marker of poor prognosis in advanced disease is association with mutant KRAS [146, 147]. The relationship between KRAS mutational status in metastatic CRC and benefit from anti-EGFR therapy has been extensively studied in four large Phase III randomized studies [148-151] establishing its use as a predictive marker for anti-EGFR mAb resistance. However, only a minority (30%) of KRAS codon 12/13 wild-type tumours respond to anti-EGFR mAb therapy [136]. Further investigations have shown mutations of BRAF V600E, PIK3CA and loss of PTEN protein expression [134] as potential markers for resistance of anti-EGFR mAb therapy, leading to the evolving use of BRAF mutation testing in KRAS-WT patients prior to treatment.

1.2.4. Phosphatidylinositol 3-kinase (PI3K) Pathway

PI3K Pathway is regulated by EGFR signalling partly via KRAS activation, and mutations are observed in up to 40% of CRCs, especially involving the PIK3CA gene (32% of CRCs) [152] and the tumour suppressor gene PTEN (30% of MSI tumours and 9% of CIN tumours) [153]. These two genes could potentially be used as predictive markers for therapies targeting the PI3K, mTORC and the MAPK pathway (Figure. 1.1) [154, 155]. Nevertheless, there is still a lack of consensus and further studies are needed to determine if these genes should be incorporated into clinical practice [156].

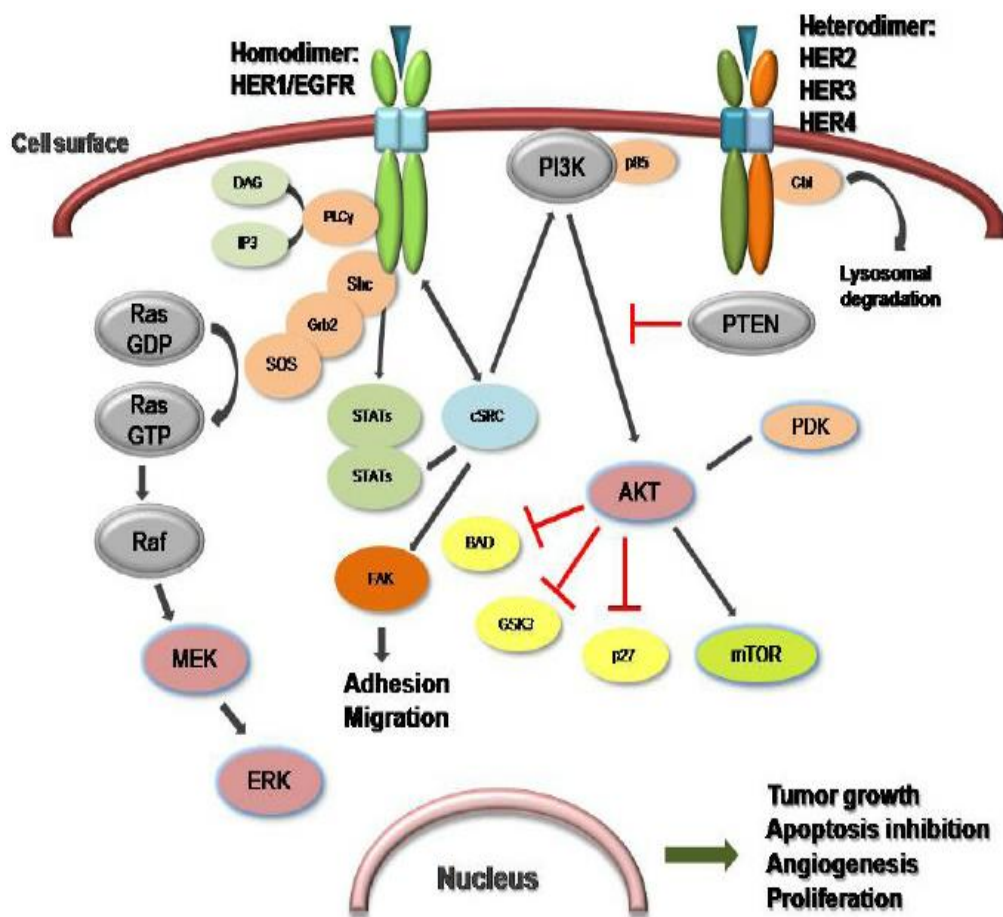


Figure 1.1: The complexity of the intracellular EGFR pathway.

Cbl, casitas B-lineage lymphoma; DAG, diacyl glycerol; EGFR, epidermal growth factor receptor; ERK, extracellular-signal-regulated kinase; FAK, focal adhesion kinase; GDP, guanosine diphosphate; Grb2, growth factor receptor-bound protein 2; GSK3, glycogen synthase kinase 3; GTP, guanidine triphosphate; HER, human epidermal receptor; IP3, inositol-1,4,5-trisphosphate; MEK, methyl ethyl ketone; mTOR, mammalian target of rapamycin; PDK, phosphoinositide-dependent kinase; PI3K, phosphatidylinositol 3-kinase; PLC, phospholipase C; PTEN, phosphatase and tensin homologue; RAS, rat sarcoma; SOS, salt overly sensitive; STATs, signal transducer and activator of transcription

Aprile G, *et al. OA Molecular Oncology* 2013;1(1):7 [157]

1.2.5. Predictive Biomarkers for Risk Stratification and Early Detection

Molecular markers could be further used in risk stratification for early-stage CRCs detection and identification of high-risk subjects. So far, germline mutations in genes

responsible of hereditary colon cancer syndromes and MSI tumour status are the most solid molecular markers. In addition, other markers for use in non-invasive colorectal cancer screening assays [158-160] have been identified such as the methylated vimentin (VIM) gene, present in the majority of CRCs (53–84%), detected with the stool-based methylated VIMENTIN (mVim) assay [161, 162]. The methylation assay is undoubtedly an area that is likely to endure rapid advances in the future.

1.2.6. Predictive Biomarkers for Chemotherapy

MSI and 18qLOH abnormalities are currently the most encouraging biomarkers for guiding adjuvant chemotherapy in CRCs, since previous studies showed adverse response to 5-FU based regimens [163-166] in patients carrying these molecular alterations. However, data from the literature showed that the tumour stage and the differences in sporadic MSI vs Lynch syndrome CRCs may also affect 5-FU resistance.

Several clinical trials are assessing the predictive value of 18qLOH and MSI including the ongoing Phase III study (NCT00217737) with 5-FU, oxaliplatin and bevacizumab on stage II CRCs [135], the Phase III study of olaparib on stage IV CRC (NCT00912743), and the retrospective analysis of 5-FU alone or in combination with irinotecan on Stage II or III CRCs (CLB-9581/CLB-89803).

High expression of Topoisomerase I (Topo I) has been found to be associated with responsiveness to the Topo I inhibitor irinotecan in a large randomized trial that compared 5-FU alone with 5-FU combined with irinotecan or oxaliplatin in advanced CRCs; validation by independent studies is required before Topo I can be used as a predictive biomarker in the clinical setting [167].

Germline polymorphisms affecting the PK and PD of chemotherapy could potentially be used as biomarkers for guiding treatment selection, even if only few of them have been appropriately validated for clinical use [168, 169]. The commercial genotyping test that has been approved by the FDA to aid irinotecan dosing checks the enzyme UDP-glucuronosyltransferase (UGT1A1), involved in the detoxification of the irinotecan metabolite SN-38. A homozygous polymorphism of the gene reduces the activity of the

enzyme affecting an inter-individual variation of the toxicity via the alternation of bioavailability of SN-38 [170, 171].

Molecular testing on CRC and identification of specific genetic or epigenetic markers can reduce medical costs and improve patient outcomes by targeting therapies on a stratified patient population. Indications for mutational analysis is likely to expand in the future and clinical trials are currently assessing the efficacy of specific inhibitors of the PI3K signalling pathway [134, 172, 173] or investigating other multikinase target inhibitors in the setting of resistance to anti-EGFR mAb therapies [174, 175]. The identification of PIK3CA mutations or PTEN loss are expected to become applicable for the treatment of CRCs as well as the detection of BRAF mutations to select a group of patients likely to respond to BRAF inhibitors in combination with anti-EGFR mAb therapy; this approach is currently being investigated (NCT00343772) [174, 175].

1.3. The Rationale for studying Circulating Tumour Cells (CTCs) in CRC

1.3.1. Background

Circulating tumour cells (CTCs) are epithelial cancer cells estimated to account for 1 cell in 10^7 circulating nucleated cells [176], and are the mediators of haematogenous metastases [177]. CTCs can be isolated from a peripheral blood draw, and used as predictive and prognostic markers [178]. CTCs are most commonly detected in higher numbers in advanced prostate cancer (60–75% of patients) compared to breast, colorectal, gastric and oesophageal cancer, while they are much less common in other tumour types [179].

In recent years the identification and characterisation of CTCs has improved in terms of sensitivity and specificity and a number of methods based on different physical and molecular properties of these cells have been described. However to date, the only FDA approved and validated detection method is the CellSearch® (Janssen Diagnostics) platform.

CellSearch detects CTCs through positive selection with antibodies against the epithelial cell adhesion molecule EpCAM and CKs that are expressed by CTCs in a broad range of

tumours such as colorectal, pancreatic, gastric, prostate, lung and neuroendocrine cancers [176, 180-185]. EpCAM detection is the most widely used approach to identify CTCs [186], however there is broad morphological and immunophenotypical variation within CTCs derived from the same tissue of origin and similarly, during epithelial to mesenchymal transition which occurs in CTCs, the expression of epithelial markers may be down-regulated and become undetectable with EpCAM-based CTC detection assays [179, 187]. Therefore, accurate detection of CTCs based on morphological and immunophenotypical profiling is still challenged.

Initial analysis of the CellSearch technology demonstrated that the prevalence of CTCs in the blood is related to tumour type and stage of disease. The first of these studies was carried out in breast cancer patients [188] and showed that ~60%–70% of metastatic breast cancer patients have ≥ 2 CTCs, whereas CTCs were very rarely observed in normal control subjects [179]. Statistically, it has been shown that patients with ≥ 5 CTCs at baseline had poorer PFS and OS than patients with < 5 CTCs [188]. Subsequent studies demonstrated similar results for metastatic prostate and colorectal cancers, with the identified threshold number needed for stratification into the poor prognosis group being ≥ 5 CTCs at baseline for prostate cancer patients, and ≥ 3 CTCs at baseline for colorectal patients [189-191].

1.3.2. Current CTC Data in Breast and Prostate Cancer

The CellSearch platform was approved for use by the US FDA in 2004 based on data generated in metastatic breast cancer [188]. Prospective, multicentre studies validated a cut-off to discriminate between favourable or unfavourable prognostic groups for PFS and OS, corresponding to a CTC count ≥ 5 per 7.5 mL of blood in breast and in prostate cancer and ≥ 3 CTCs in advanced CRCs [188-190]. On multivariate analysis, in patients with metastatic breast cancer, the CTC count at baseline and first follow-up was the strongest predictor of PFS and OS compared with other clinical and pathological factors including ER, PR, HER2 status, ECOG performance status, time to metastasis and type of therapy. Specifically, the presence of 5 or more CTCs in 7.5 mL of blood at time of diagnosis was

associated with worse outcome in terms of PFS and OS, and the level of CTCs at each follow-up time point was better than imaging in predicting PFS and OS [188, 192].

In the adjuvant setting, in early breast cancer, the presence of CTCs both before and after chemotherapy was also demonstrated to be associated with poor disease-free survival (DFS), breast cancer-specific survival and OS [193].

In castrate-refractory prostate cancer, CTC count at baseline and after treatment was the strongest predictor of OS, with greater prognostic significance than changes in PSA, symptoms and imaging, and is increasingly being incorporated into clinical trials [191, 194]. The cut-off to discriminate between favourable and unfavourable groups corresponded to CTC count ≥ 5 in 7.5 mL of blood and identified patients with a shorter OS across studies of both chemotherapy and hormonal agents [189]. Data showed that a CTC count decrease from ≥ 5 to < 5 was associated with a better prognosis and survival in contrast to a CTC count increase from < 5 to ≥ 5 [189]. Changes in CTC levels before and after treatment have also been incorporated in Phase I/II studies as an indirect PD biomarker to confirm active doses of drugs tested, further demonstrating an early indication of antitumour activity reflected by significant PSA declines modification [194].

1.3.3. Current CTC Data in CRC

In CRC, CTC count has also been demonstrated to be a prognostic and predictive factor for patients with metastatic disease. The presence of ≥ 3 CTCs at baseline and follow up, is associated with an unfavourable PFS and OS, and is the strongest independent prognostic marker compared with other clinical factors [195]. Patients with ≥ 3 CTCs at baseline had a shorter median PFS and OS with an improvement in PFS and OS if CTCs decreased from ≥ 3 to < 3 after 3–5 weeks on treatment [195, 196]. The negative impact of elevated baseline CTC count has been evaluated in a number of clinical subgroups, demonstrating a statistically inferior OS in all subgroups including line and type of therapy administered, age (≥ 65 years) and ECOG performance status [195], while PFS was statistically inferior in many but not in all factors. In more recent studies, improved detection of CTCs in mCRC patients following combined CellSearch and Adna Test® analysis (the

AdnaTest® uses an RT-PCR platform targeting transcripts for *EpCAM*, *EGFR*, *CEA* to identify tumour cells within the EpCAM-enriched cell fraction) demonstrated a significant correlation with overall survival ($P=0.046$) [197]. In a study where the use of a multigene biomarker chip for detecting CTCs for postoperative surveillance of stage I–III CRC patients was used, the sensitivity and specificity of the biochip was shown to be significantly greater for predicting postoperative relapse than elevated postoperative serum CEA levels. Moreover, the median time between positive biochip result and postoperative relapse detection was significantly earlier than that between elevated postoperative serum CEA level and postoperative relapse detection (10.7 vs. 2.8 months; $P<0.001$) and positive biochip results were strongly correlated with lower disease-free survival and OS of CRC patients (both $P<0.001$) [198]. A prospective study by Hinz *et al.* evaluated CTC or disseminated tumour cells detected using CK20 RT-PCR at the time of surgery, as well as their correlation with tumour characteristics, OS and disease free survival. This study reported that the detection of CTCs with CK20 RT-PCR was a highly specific and independent prognostic marker in patients with CRC [199]. A study evaluating the expression of epithelial and mesenchymal markers in CTCs and their clinical relevance in a large cohort of Chinese patients with CRC used the CanPatrol™ TC enrichment technique to isolate and classify CTCs. CTCs were identified in 87% of patients and three phenotypes were identified based on the expression of epithelial and mesenchymal markers: epithelial CTCs, biophenotypic (epithelial/mesenchymal) CTCs, and mesenchymal CTCs. Total, biophenotypic and mesenchymal CTCs were all shown to correlate with clinical stage, lymph node and distant metastasis [200].

These data confirm the importance of CTCs as a potential stratification factor for OS in future mCRC clinical trials, especially considering the limited number of informative stratification factors in advanced CRCs [201, 202]. In addition, CTCs provide an opportunity to interrogate the molecular characteristics of the tumour in real-time, potentially guiding therapeutic interventions.

CTCs are an attractive tumour marker for survival, likely to streamline drug development and clinical trials, both to improve efficacy, shorten timelines in development of new drugs and assessing at earlier time points whether a treatment should be discontinued.

CTC count may also be useful to detect malignancy in early stage of disease and predict the risk of early metastases or relapse raising the possible use in clinical practice to prompt a change in treatment, as well as performing molecular analysis for future personalised targeted therapy. Thus, several clinical trials are ongoing to incorporate molecular analysis and assess the utility of CTC changes to drive therapeutic modification [194].

1.3.4. The Role of CTCs in Clinical Trials

CTC assessments present an opportunity to develop new PD and PK biomarkers to evaluate drug-target inhibition and assist in making 'go' or 'no-go' decisions, especially in early drug development [203]. Minimally invasive PD assays such as the use of CTCs as a PD endpoint in monitoring the efficacy of new drugs has great advantages, allowing serial controls of drug effects while reducing the need of biopsies and the risk associated with these procedures. Therefore, longitudinal assessment of CTCs is being incorporated into clinical trials as prognostic, predictive and intermediate biomarkers of response [204]. A longitudinal approach may also enable detection of molecular changes in CTCs reflecting tumour genotype that may be driving disease resistance or progression [205]. CTC counts are currently incorporated into the treatment decision algorithm in a number of Phase III trials of metastatic breast cancer, are under evaluation to select between chemotherapy vs endocrine therapy [206], and to guide an early change of treatment.

In the adjuvant setting, trials are assessing HER2-positive CTCs in HER2-negative primary tumours and testing the role of HER2-directed therapies in these patients [206].

In the prostate cancer setting, CTC count ≥ 5 is now included in the eligibility criteria of some trials to select a poorer prognostic group of patients that may demonstrate the utility of the therapeutic agent in a more time-efficient manner [189]. However, there is bias related to inter-individual variability to consider with regard to simple CTC count, therefore future studies should also take into account the relative changes of CTC level reduction to

monitor a clinical response, instead of simply looking at changes from unfavourable (>5 CTCs) to favourable groups (<5 CTCs).

1.3.5. Molecular Characterisation of CTCs

The molecular characterisation of CTCs has strong potential to be translated into individualised targeted treatment. Various protein based assays counting HER-2 [207], the phosphorylated nuclear DNA double strand damage biomarker (γ -H2AX) [208], EGFR [209], insulin like growth factor I receptor (IGF-IR) [210] expression, AR signalling [211], and *KRAS*, *BRAF* and *PIK3CA* mutations [212, 213] in CTCs have been included into clinical trials as exploratory PD biomarkers.

The role of γ -H2AX expression on CTCs to detect PD changes after treatment has been investigated in patients undergoing clinical studies [214, 215]. A combined NCI analysis of eight National Cancer Institute Phase I and II trials in a variety of solid tumours had a population of statistically evaluable patients of approximately 30% for all trials (CTC biomarker evaluation was limited by the total number of CTCs collected from each blood sample). Data obtained from multiple trials of Topo 1 and PARP inhibitors showed that the γ -H2AX-positive CTC baseline level was less than 20% in 34/50 patients. The fraction of CTCs expressing γ -H2AX independent of changes in the total CTC count, increased in patients following treatment with different Topo 1 inhibitors alone or in combination with other drugs. Furthermore, correlations between γ -H2AX levels and overall responses were demonstrated in patients with refractory cancer in a Phase II randomized trial of the veliparib in combination with metronomic oral cyclophosphamide. This increase of γ -H2AX in CTC post-treatment compared with baseline confirms the potential utility of CTC based PD biomarker analysis in such settings [215].

More recently, the genetic characteristics of CTCs have been investigated. In CRC mutations that are being investigated in CTCs include *KRAS*, *BRAF* and *PIK3CAI*. As stated previously (Section 1.3.3), in patients with mCRC, 80% of patient blood samples were positive for CTCs and at least one of these mutations were detected in 78% of samples. High concordance rates of mutations in CTCs were observed with 78%, 74%

and 91% of cells have mutations in *KRAS*, *BRAF* and *PIK3CA*, respectively [213]. Another small study characterised *KRAS* mutations in CTCs from patients with mCRC and compared these with patients matched primary tumour samples and correlated the detected mutations with clinical and pathological features of patients. In this study, *KRAS* mutations were detected in 33% and 37.5% of CTCs and primary tumours, respectively; a significant concordance (71%, $P=0.017$) of matched cases was observed. *KRAS* mutation neither on primary tumour nor in CTCs was associated with clinical-pathological parameters analysed. The concordance between *KRAS* mutation detection between CTC and primary tumours suggests that CTCs could be used as a surrogate of primary tumours in clinical practice when the knowledge of mutational profile is required but the primary tumour is not available [212].

The possibility to provide longitudinal assessment of a tumour's molecular profile and possible causes of drug resistance using CTCs as a PD marker are very appealing and, in the future, the simple cell count or characterization of protein biomarkers on CTCs may be replaced with single cell profiling, monitoring tumour genome changes that could be associated with treatment resistance.

1.4. Gamma H2AX as a Protein Biomarker and its use in Drug Efficacy Measurements

1.4.1. Gamma H2AX: Functional Role in DNA Damage Response (DDR)

DNA lesions occur in the context of chromatin, a complex of double helix DNA enfolded with histone proteins in nucleosomes linked together by other histones [216]. Nucleosomal histones belong to four families: H2A (further subdivided in H2AZ and H2AX [217], H2B, H3 and H4, while the linker histones pertain to the H1 family [218, 219] (Figure. 1.2).

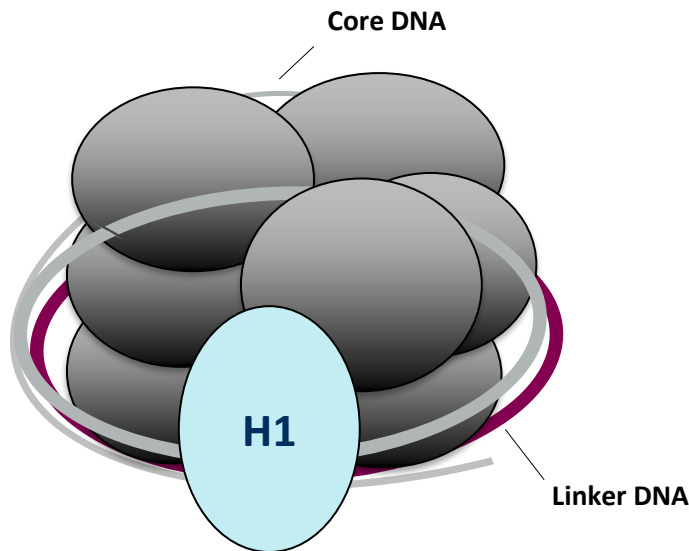


Figure 1.2: Nucleosomal histones.

Redrawn from: Stryer L, *et al. Biochemistry* 1995 (fourth ed.) [220]

The H2A family is characterised by an omega-4 serine residue, which is converted into the phosphorylated form gamma-H2AX (γ -H2AX) after double-strand break (DSB) damage [221-223]. It is essential to repair and conserve chromatin architecture immediately after DNA damage, to prevent genome instability. The DNA damage response (DDR) is primarily responsible for detecting and restoring the integrity of DNA through two major mechanisms, homologous recombination and non-homologous end joining which will be activated, and H2AX phosphorylation [224, 225]. When a DSB takes place, the tri-protein MRN complex (MRE11-RAD50-NBS1) recognizes the DNA damage and recruits and activates PI3-kinase related kinases including ataxia telangiectasia mutated (ATM), ATR (AT and Rad3-related protein) and DNA-dependent protein kinase (DNA-PK). ATM, ATR and DNA-PK phosphorylate H2AX on its c-terminal Ser139 residue [226, 227] which is crucial to activating the DNA damage response pathway, resulting in γ -H2AX which attracts the Mediator of Damage Checkpoint protein 1 (MDC1), which is also phosphorylated by ATM (Figure. 1.3). MDC1 in turn serves as a scaffold for the recruitment of other proteins required for the activation of BRCA1 by ATM, promoting cell cycle arrest and DNA repair. ATM phosphorylates other target substrates like the checkpoint protein Chk2 and p53, which are also

responsible for cell cycle arrest or apoptosis if the damage cannot be repaired. The repair of the DSB is associated with γ -H2AX dephosphorylation by the phosphatase PP2A and the removal of γ -H2AX prevents further recruitment of DDR and repair factors [217]. Cellular stress can induce a cellular response through the histone post-translational modifications (PTMs) [228], therefore the importance of identifying alterations in histone PTM homeostatic levels may generate important clinical information on the disease or on its treatment efficacy [229]. Because of its critical role in DSB repair and genome stability, γ -H2AX has recently become one of the most widely known examples of a histone PTM and the most common marker of DNA DSB damage.

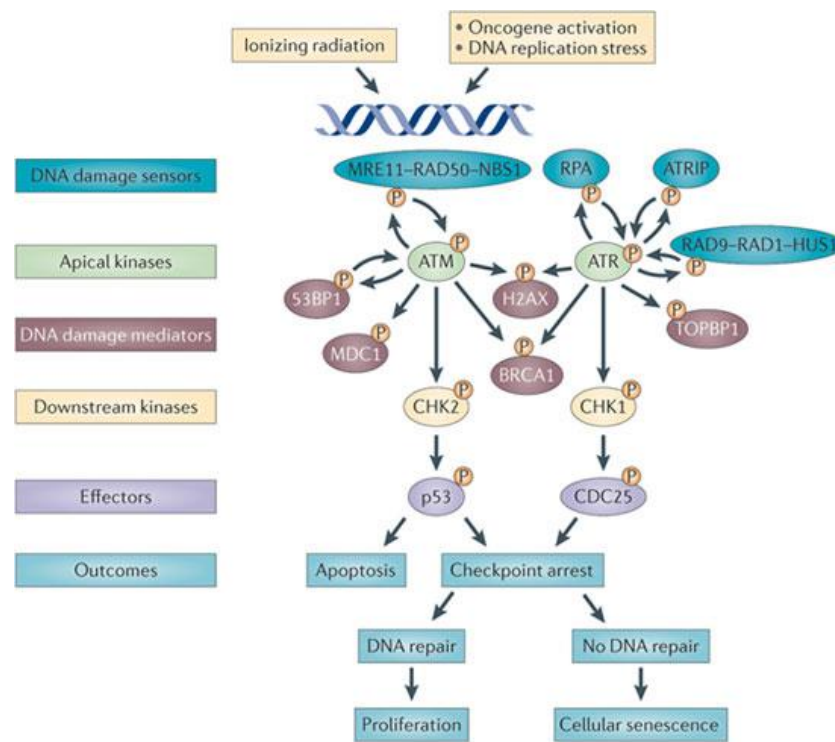


Figure 1.3: Crosstalk between chromatin state and DNA damage response in cellular senescence and cancer. The DNA damage response (DDR) pathway is composed of two main DNA damage sensors, the MRE11–RAD50–NBS1 (MRN) complex that detects DNA double-strand breaks, and replication protein A (RPA) and the RAD9–RAD1–HUS1 complex which detect exposed regions of single-stranded DNA. These sensors recruit the apical kinases ataxia- telangiectasia mutated (ATM) and ataxia telangiectasia and Rad3-related (ATR), which is bound by ATR-interacting protein (ATRIP). These in turn

phosphorylate (P) the histone variant H2AX on Ser139 (known as γ H2AX) in the region proximal to the DNA lesion.

From: Sulli G *et al. Nature Reviews Cancer* 2012;12:709–720 [230]

1.4.2. Gamma H2AX as a Protein Biomarker for DNA DSBs and its Applications

DSBs are highly cytotoxic, and this is exploited in conventional cancer treatment, with radiation therapy and chemotherapy treatments generating large numbers of DSBs. These include chemotherapeutic drugs that induce DNA cross-links or function as topoisomerase inhibitors, inducing DSB's in all cells. Cancer cells are particularly susceptible to these drugs, as they are rapidly dividing and often have inactivated components of their DNA repair machinery and deregulated cell cycle checkpoints [231]. Therefore, biomarkers for DNA damage such as γ -H2AX foci could allow *in vivo* measurement of individual response to specific treatment in real time as well as planning of treatment for each individual patient [232-235]. *In vitro* experiments using fixed mitotic cells of the Indian muntjac (*Muntiacus muntjak*) or normal human fibroblast W138 cells treated with ionizing radiation showed an increase of γ H2AX foci in the nucleus in a dose-dependent manner at early stages of DDR while DNA repair correlates time-wise with γ H2AX loss or dephosphorylation and with the decrease in number and size of the γ H2AX foci [236]. Muntjac mitotic chromosomes exhibit small γ -H2AX foci three minutes after exposure to ionizing radiation (IR) which become brighter and larger nine minutes after treatment, and reach maximal brightness and size 30 minutes following IR. These findings suggest that H2AX molecules in a small region near the DSB site are phosphorylated first, and are followed by molecules at increasing distances from the break site. Many DNA repair and/or checkpoint protein species accumulate on the growing γ -H2AX focus, which may serve to open the chromatin structure and form a platform for the accumulation of DNA damage response and repair factors [236].

Persistence of γ -H2AX foci after DNA damage indicates that some breaks remain unrepaired making γ -H2AX a potential effective PD biomarker following treatment with IR and chemotherapies. This role has been evaluated in several clinical trials [208, 237, 238]

(Table 1.7) testing drugs generating DSB DNA damage including DNA synthesis inhibitors, DNA alkylating agents, Topo I and II inhibitors [239, 240] and other therapies [239, 241-243].

Table 1.7: Non-exhaustive list of clinical studies using the γ -H2AX assay to measure the effects of chemotherapeutic drugs in cancer patients. The top of the table includes published clinical studies while the bottom part contains some studies obtained from the ClinicalTrials.gov database.

Tissues analyzed	Drug(s)	Condition	γ -H2AX detection	Phase	References
PBMCs	Clofarabine and cyclophosphamide	Refractory acute leukemias	FACS	I	[Karp JE et al. Blood. 2007;110:1762–1769]
PBMCs/tumor biopsies	SJG-136	Solid tumours	M	I	[Hochhauser D, et al. Clinical cancer research. 2009;15:2140–2147]
AML marrow blasts	Combination of tipifarnib and etoposide	AML	FACS	I	[Karp JE et al. Blood. 2007;110:1762–1769]
PBMCs	Combination of 5-azacytidine and entinostat	MDS, chronic myelomonocytic leukemia, and AML	I	I	[Fandy TE. Current medicinal chemistry. 2009;16:2075–2085]
Plucked eye-brows	Olaparib (AZD2281)	Breast cancer	M	I	[Fong PC. The New England journal of medicine. 2009;361:123–134]
CTCs/PBMCs	Combination of veliparib (ABT-888) with topotecan	Solid tumours and lymphomas	M	I	[Kummar S, et al. Cancer research. 2011;71:5626–5634.]
ClinicalTrials.gov					
Tissues analyzed	Drug(s)	Condition	γ -H2AX detection	Phase	ClinicalTrials.gov identifier
PBMCs, skin, hairs	Veliparib (ABT-888)	Breast, ovarian, pancreatic, prostate cancers; BRCA1, BRCA2 mutations carriers	N/S	I	NCT00892736
Tumor biopsies	7-t-butyl(dimethylsilyl)-10-hydroxycamptothecin	Solid malignancies	M/I	I	NCT01202370
N/A	BSI-201 (Iniparib)	Advanced solid tumours	N/S	I	NCT01161836
N/A	Combination of BSI-201 and temozolomide	Glioblastoma	N/S	I, II	NCT00687765
N/A	BSI-201 (Iniparib)	Ovarian cancer	N/S	II	NCT01033123
N/A	TH-302	Glioma	M/I	II	NCT01403610
N/A	Combination of gemcitabine, carboplatin and BSI-201	Triple negative breast cancer	N/S	II	NCT00813956
N/A	Combination of gemcitabine/carboplatin plus BSI-201	Breast cancer	N/S	III	NCT00938652

From: Ivashkevich A, *et al. Cancer Lett* 2012;Dec 31;327(1–2):123–133. [244]

Such anticancer drugs affect the mechanisms of DNA replication and H2AX phosphorylation in several ways [245-247]. ATM kinase is considered as a major physiological mediator of H2AX phosphorylation in response to DSB formation [247]. H2AX can also be phosphorylated by ATR and DNA-dependent protein kinases (DNA-PK). ATR phosphorylates H2AX in response to single-stranded DNA breaks and during replication stress, such as replication fork arrest. DNA-PK mediates phosphorylation of

H2AX in cells under hypertonic conditions and during apoptotic DNA fragmentation [247]. However, DNA damage caused by ionizing radiation leads to phosphorylation of H2AX that is mediated by all PIKK kinases, ATM, ATR, and DNA-PK [247]. In addition, DNA Topo I and II inhibitors impede DNA replication through the impact of replication forks. DNA Topo I inhibitors including SN-38, topotecan and camptothecin work predominantly in S-phase cells while DNA Topo II inhibitors, such as etoposide and mitoxantrone, generate γ -H2AX in all phases of the cell cycle [248, 249].

There are several reasons for the clinical use of γ -H2AX including its role in investigating the potential genotoxicity of a new investigational drug and the possibility to tailor treatments to patients, taking into account individual sensitivities and/or previous treatments, or as an indicator of cellular radiosensitivity to potentially predict individual responses to IR in the clinical setting [250]. γ -H2AX could be used as a biomarker to predict patient outcomes [251] and recent studies have employed γ -H2AX as a biomarker for clinical diagnosis of cancer development. High levels of γ -H2AX are present in both precancerous and cancer lesions indicating an increased level of DNA damage as a general feature of cancer development [252-254]. In addition, γ -H2AX foci have been proposed as prospective biomarkers of aging due to the accumulation of DSBs in senescing cells [250].

1.4.3. Gamma H2AX as PD Biomarkers to Monitor Drug Activity in CTCs

Currently, patient response to treatment is evaluated by imaging techniques, requiring several weeks until tumour shrinkage may be detected [214]. In addition, tumour markers may not correlate positively with tumour outcome, therefore it would be valuable to measure patient drug response at the molecular level [255]. The use of specific antibodies permits the visualization of γ -H2AX foci at individual DSB sites, allowing the efficiency of a drug in a patient to be measured by detecting changes in γ -H2AX levels before and after treatment.

Tumour biopsy is pivotal to evaluate the effect of drugs on DNA metabolism. Sequential biopsies in a clinical trial would allow following the PD effects throughout the time of

exposure to the drug being tested [214]. However, sequential biopsies may not be feasible for technical or safety reasons and are not generally acceptable for patients. Nevertheless, tumour heterogeneity due to differences in vascularity and genetic mutations may affect γ -H2AX formation and removal, confounding the relationship of γ -H2AX formation with tumour prognosis or tumour response to treatment. In addition, genetic variability may impact the expression or function of proteins that metabolize the drug or may affect the drug target itself, thereby affecting treatment efficacy. Thus γ -H2AX responses may differ among different metastases in the same patient as well as among different cells of the same tumour mass [217].

Less invasive methods based on tumour cell response through the identification of biomarkers to detect on-target drug effect during treatment can allow monitoring specific treatment to the patient.

Recently, as discussed in Section 1.3.4., the presence of CTCs in the bloodstream has been shown to predict disease progression in several cancers [256]. In addition, the characterisation of tumour type through the assessment of biomarkers in CTCs has also been used [257, 258]. CTCs isolated from peripheral blood of patients with a variety of advanced malignancies over the course of treatment with investigational agents as part of a Phase I clinical study showed increased numbers of γ -H2AX positive CTCs from 2% at baseline to 38% after a single day of treatment; this increase was irrespective of decreases in the total CTC count. Therefore, such assessments could be used to optimize cancer treatments assessing the drug effectiveness in real time [214]. In addition to the evaluation of CTCs and the expression of γ -H2AX in cells from peripheral blood of patients with a variety of advanced malignancies, there are several other tissue-based approaches that have assessed γ -H2AX in normal surrogate tissues as many chemotherapeutic agents also target the patient's normal cells [214]. Compared to tumour cells, γ -H2AX responses in normal cells may be more uniform, reproducible, and informative. Levels of γ -H2AX have been quantified by microscopy or flow cytometry in PBMCs, and by microscopy in skin biopsies, plucked hair bulbs and buccal cells. PBMCs contain low γ -H2AX focal background levels (on average less than one focus per 5–10 cells), which improve the

detection of low levels of DNA damage allowing measurement of IR doses as small as 1 mGy [214]. The major disadvantage of PBMCs is their state of terminal differentiation, which might make them less useful for studies of chemotherapeutic drugs that produce DSBs by interfering with DNA replication [214]. Another accessible tissue that does contain proliferating cells is the skin. Skin biopsies are necessary to obtain the basal keratinocytes, an issue which limits their routine use due to its invasive nature. It is noticeable in sections of skin biopsies that hair follicle cells often exhibit the largest γ -H2AX response after drug treatment [214]. An alternative and less invasive procedure for obtaining at least some of these follicle cells, is plucking hairs. A Phase I trial included the use of γ -H2AX detection in plucked eyebrow hair bulbs to confirm the effects of a PARP inhibitor *in vivo* [259]. Like plucked hairs, the use of exfoliative oral cells has been previously promoted as a non-invasive technique for cancer diagnosis [232] and for γ -H2AX detection [260].

1.4.4. Gamma H2AX assay types

Detection of γ -H2AX foci after exposure to DNA-damaging agents is a more reliable DSB marker than other repair proteins as it is formed *de novo* in the cell, it is far more sensitive than other methods in detecting DSBs and allows the distinction of the temporal and spatial distribution of DSB formation.

Other techniques such as constant or pulsed field gel electrophoresis and comet assays can only detect DSBs induced by large doses of IR (5–50 Gy), and in contrast to the Comet assay [261], the analysis of γ -H2AX foci does not involve lyses at high temperatures. Discrete nuclear γ -H2AX foci can be measured by flow cytometry, western blotting or immunofluorescence and antibodies directed against both H2AX and γ -H2AX are now commercially available [236, 262-264]. However, fluorescence microscopy is still the preferred and most sensitive method for γ -H2AX detection for clinical applications, being able to detect a single DSB, given that each break has been found to correspond to one γ -H2AX focus [244]. Analysis by microscopy may discriminate γ -H2AX responses induced by different drugs or IR, based on the different timing of interference with DNA replication. In fact, drugs that interfere with DNA replication induce foci primarily in

proliferating cells in contrast to IR that affect virtually all cells [217]. Furthermore, microscopy is more specific than flow cytometry, being able to distinguish foci from the background, allowing the analysis of tissue samples instead of single cells such as PBMCs and bone marrow cells. Other types of assays, such as electro chemiluminescent-based detection system and whole cell ELISA [244] also utilize cell and tissue extracts, however they are as yet not available for the clinic. There is therefore an ongoing demand for the development of high throughput γ -H2AX foci counting systems for clinical assays, intended to speed up analysis and automate microscopic examination [217].

1.5. Aims of this thesis

Current methods available for detection of γ -H2AX in patient samples, such as γ -H2AX immunofluorescence, FACS analysis, alkaline comet assay and immunohistochemistry, have showed limited applicability to the clinic to monitor tumour response to chemotherapy and radiotherapy as they cannot be used to evaluate γ -H2AX expression on isolated CTCs from whole blood. Therefore, γ -H2AX response to drug treatment can only be established in non-tumour cells (e.g., peripheral blood mononuclear cells).

γ -H2AX induction has been studied in cancer cells treated with different chemotherapy agents and in CTCs from patient blood samples processed using the CellSearch system in conjunction with γ -H2AX-AF488 antibody staining. γ -H2AX signal was detected as a percentage of γ -H2AX-positive CTCs per total CTCs recovered following chemotherapy [214]. However, the CellSearch platform is not designed to quantify levels of immunofluorescence and this may limit its sensitivity to detect changes in γ -H2AX phosphorylation in response to DNA damaging chemotherapy at a single cell level. The DEPArray system is a recently developed platform that combines fluorescent microscopy with cell sorting and allows quantification of the fluorescent signal. To date, it has not been used to evaluate the molecular response to therapy in CTCs.

Hypothesis

The overarching hypothesis for this thesis was that, using the DEPArray technology, γ -H2AX foci can be measured quantitatively in CTCs, and that short-term increases in γ -

H2AX foci correlate with long terms response to chemotherapy with DNA damaging agents.

To test this hypothesis, it was necessary to develop a novel assay and the experimental steps required to develop this assay are described in the results chapters as follows:

Chapter 3: To define the optimal dose of oxaliplatin and SN-38 required to induce γ -H2AX foci on human adenocarcinoma colorectal cells by performing dose-response experiments with increasing concentrations of oxaliplatin and SN-38.

Chapter 4: To define the optimal time to measure γ -H2AX foci in human adenocarcinoma colorectal cells following treatment with oxaliplatin and SN-38 at the doses determined in Chapter 3.

Chapter 5: To evaluate changes in γ -H2AX signal according to both the CellSearch System (Janssen Diagnostics) and the DEPArray™ System (Silicon Biosystems) using conditions defined by chapters 3 and 4.

Chapter 6: To test the assay in samples obtained from patients with colorectal cancer undergoing chemotherapy.

CHAPTER 2

Materials and Methods

2.1. General materials

All chemicals were from Sigma-Aldrich Co Ltd. (Dorset, UK) unless otherwise stated.

General materials used in these studies are as follows:

Lab-Tek II chamber slides (Cat. No. 154526, Thermo Fisher Scientific)

Trypsin-EDTA (Autogen Bioclear UK Ltd., Wiltshire, UK)

Haemocytometer (DHC-BO2-Burker Turk [INCYTO])

Trypan blue solution, 4%

Green 21 gauge needles (Exchange Supplies)

PBS (stored at 4°C)

Fixation buffer: 50% methanol and 50% acetone (stored at -20°C)

Permeabilization buffer: 0.5% Triton X-100 in PBS (stored at room temperature) (cell culture experiments)

Permeabilization buffer: 0.2% triton X-100 in ice cold PBS (cell suspension experiments)

Blocking buffer: 0.2% skimmed dry milk, 0.1% Triton X-100, in PBS (stored at 4°C) (cell culture experiments)

Blocking buffer: 10% FBS, 5% BSA in PBS (store at 4°C) (cell suspension experiments)

Washing buffer: 0.1% Triton X-100 in PBS (stored at 4°C)

Mouse anti-H2AX monoclonal primary antibody diluted in blocking buffer (1:1000) (Merck Millipore, UK) (stored at -20°C)

Goat anti-mouse Alexa Fluor® 488 IgG secondary antibody diluted in blocking buffer (1:1000) (Life Technologies Ltd., UK) (stored at 4°C)

Propidium iodide (PI) 2 µg/mL (stored at 4°C)

ProLong® Gold Antifade reagent and ProLong® Gold Antifade with 4',6-DAPI (Invitrogen, Life Technologies Ltd., UK)

Freezing media (FCS + 10% DMSO) (Sigma-Aldrich Co., UK)

T75 flask, 75 cm² (Sigma-Aldrich Co., UK)

Slide container (Shandon EZsingle cytofunnel)

Paraformaldehyde (PFA) 4%

1.5 mL microcentrifuge tubes (Sigma-Aldrich Co., UK)

Falcon™ 15 mL conical centrifuge tubes (Sigma-Aldrich Co., UK)

Microscope Slides (25 mm × 75 mm; Sigma-Aldrich Co.)

Phosphatebuffered saline (PBS) (stored at 4 ° C)

Bovine serum albumin

Hoechst staining 33342 (Life Technologies H3570) 10 µg/mL

Cytospin™ 4 Cytocentrifuge (Thermo scientific)

Micro Cover Glasses (24 mm x 60 mm) (VWR® SuperSlips™)

ProLong® Gold Antifade reagent and ProLong® Gold Antifade with 4',6- DAPI) (Invitrogen, Life Technologies Ltd.)

2.2. Investigational drugs

Oxaliplatin was obtained from Mayne Pharma (Raleigh, NC, USA) as an injectable aqueous 3.3 mM stock solution (12.500 µM in 2 mL). SN-38 was obtained from Mayne Pharma as an injectable aqueous solution 200 mg/1 mL. Topotecan was obtained from Sigma-Aldrich (Sigma-Aldrich) and a stock 10mM solution was made in DMSO and stored at -20°C until use. All drug stock solutions were prepared fresh for each experiment and serially diluted as appropriate for different experiment procedures. Further dilutions were made in cell-specific medium for treating cell lines.

2.3. Cells and culture conditions

The cell lines used in these experiments are detailed in Table 2.1. The human colon adenocarcinoma cell line HT-29 was initially used (Chapter 3–5) to fully characterize the DNA damage response during oxaliplatin treatment by measuring the expression levels of γ-H2AX in the cells; HT-29 cells are sensitive to the chemotherapeutic drugs 5-fluorouracil and oxaliplatin, which are standard treatment options for colorectal cancer [265]. In

addition to HT-29 cells, HCT-116 cells were also utilised (Chapter 4–5); these cells were chosen because the kinetics of oxaliplatin-induced DNA damage have previously been investigated by analysis of the expression levels of phospho-p53 (Ser-15) and γ -H2AX in HCT-116 cells [266]. Cell lines were purchased from the American Type Culture Collection (ATCC) and from the European Collection of Cell Cultures (ECACC). All cells were maintained in McCoy's 5A (modified) medium (Gibco, Thermo Fisher Scientific, Waltham, MA, USA) supplemented with 10% foetal calf serum (FBS; Gibco), 2 mM L-glutamine, and Penicillin Streptomycin antibiotics.

Cells were grown at 37°C in a 5% CO₂ humidified incubator and passaged approximately three times weekly. Adherent cell lines were passaged using 5 mL trypsin-EDTA solution (Autogen Bioclear UK Ltd., Wiltshire, UK) for 5 minutes at 37°C to detach cells. 5 mL of cell medium was added and cells were centrifuged at 350 × g for 5 minutes at room temperature. The supernatant was discarded and the cell pellet was resuspended in cell medium. Cell lines were tested for mycoplasma twice a year, and grown for approximately 30 passages, at which point new stored aliquots were used. The aliquots were prepared by freezing cells in 10% DMSO in FBS overnight at -80°C followed by long-term storage in liquid nitrogen. When needed, cell lines were defrosted quickly in a 37°C water bath, resuspended in medium, and centrifuged at 350 × g for 5 minutes. The supernatant was discarded and cells were resuspended in fresh medium.

Table 2.1: Cancer cell lines used

Cancer cell origin	Cell line	Medium
Solid	HT-29 colon cancer cell line ECACC n. 85061109	McCoy's 5A (modified)
Solid	HCT-116 colorectal cancer cell line ECACC n. 91091005	McCoy's 5A (modified)

2.4. γ -H2AX immunofluorescence staining for adherent colon cancer cell lines treated with varying concentrations of oxaliplatin and SN-38 (Chapter 3)

2.4.1. Sample preparation

HT-29 cells were prepared, counted, and plated for experiments. An aliquot of each cell line containing 8×10^4 cells/mL cells was obtained from a stock in liquid nitrogen that was quickly thawed at room temperature, and 9 mL of medium was added to each sample and pipetted into a 15-mL conical tube. Tubes were spun in a Jouan CT422 centrifuge (Thermoelectron, Basingstoke, UK) at $270 \times g$ for 5 minutes. Supernatant was poured off, the pellet was resuspended in 10 mL of medium. The whole cell sample was transferred to a T75 flask. Flasks were placed into an incubator (37°C , 5% CO_2) overnight for the cells to attach.

Cells were assessed for confluency under the microscope. Once they reached 80% to 90% confluence, they were split to enable growth and multiplication to continue. The medium was poured off, and 5 mL of trypsin (Autogen Bioclear UK Ltd., Wiltshire, UK) was pipetted into the flask, which was incubated for 5 minutes at 37°C and 5% CO_2 . Once incubated, trypsin was pipetted off, added to 10 mL of McCoy's 5A (modified) medium containing 10% FCS in a 15 mL conical tube, and centrifuged at $270 \times g$ for 5 minutes. The supernatant was poured off and the cell pellet was resuspended in 10 mL of complete medium. A variable amount of the suspension, according to the size of the cell pellet, was pipetted into sterile T75 flask. Cells were split again once they neared confluency. This was repeated until cells were ready to use for the following experiments. Cells were only used if they were at the point of reaching confluency, as this indicated they were in the exponential phase of growth.

2.4.2. Treatment *in vitro* with oxaliplatin or SN-38

HT-29 cells were treated *in vitro* with varying concentrations of oxaliplatin to determine the dose required for peak induction of γ -H2AX foci in the nuclei.

Cells were counted with a haemocytometer. The coverslip was placed over the counting surface before loading the cell suspension. After cells were trypsinized, they were suspended in fresh media, gently passed a few times through a syringe needle, and diluted so the cells or other particles did not overlap each other on the grid. To distinguish between dead and viable cells, a sample was diluted (dilution factor 1:1) with trypan blue stain which uses a diazo dye that selectively penetrates cell membranes of dead cells, colouring them blue. 10 μ l of the cell suspension was pipetted into one of the V-shaped wells of the haemocytometer and gently expelled under the coverslip covering the mirrored surface. Two samples were loaded on the haemocytometer, one into each of the two grids. The full grid on a haemocytometer contains nine squares, each of which is 1 mm². The central counting area of the haemocytometer contains 25 large squares and each large square has 16 smaller squares. The cells that were counted were on the lines of two sides of the large square to avoid counting cells twice. The cells were counted inside the four large corner squares and the middle one. The loaded haemocytometer was placed on the microscope stage and cells were systematically counted in the selected squares so that the total count was approximately 100 cells, the minimum number of cells needed for a statistically significant count. If a cell was overlapping a ruling, it was counted as 'in' if it overlapped the top or right ruling, and 'out' if it overlapped the bottom or left ruling. Once the total cell count was obtained, the cell concentration was calculated from the following formula: Total cells/mL = Total cells counted \times dilution factor \times 10,000 cells/mL # of squares.

Each well of a 4-well LAB-TEK II chamber slides was plated with 4×10^2 cells in 1 mL complete medium. Cells were left to adhere overnight and then treated with oxaliplatin or SN-38. Oxaliplatin or SN-38 were diluted in McCoy's 5A (modified) medium to obtain concentrations of 0 μ M, 1 μ M, 5 μ M, and 10 μ M; 1 mL total volume per well was pipetted into each well containing cultured cell lines at 80% to 90% confluence. After 2 hours incubation, the drug was removed and the cells were washed with cold PBS.

For SN-38 treated cells, the concentrations of drug used and the time of exposure induced a gradual increase in γ -H2AX and irreparable DNA damage was observed (Section 3.4).

Therefore, the experiments were repeated using lower SN-38 concentrations (0 μ M, 0.01 μ M, 0.05 μ M, 0.5 μ M and 1 μ M) with a shorter incubation period of 1 hour.

2.4.3. Immunofluorescence Staining

2 mL of methanol-acetone (50:50) was added to each well for 8 minutes at 4°C to fix the cells. Plates were washed twice with PBS and permeabilised with 2 mL/well of permeabilisation buffer (0.5% Triton X-100 in PBS) for 15 minutes at room temperature.

Blocking buffer (0.2% skimmed milk, 0.1 % Triton X-100 in PBS) was added at 2 mL/well and cells were incubated overnight at 4°C followed by two cold PBS washes.

Immunofluorescence staining was carried out with cold solutions, maintained at 4°C, and in subdued lighting, unless otherwise stated. Cells were incubated overnight at 4°C with primary mouse monoclonal anti-phospho- γ -H2AX antibody (Millipore) (dilution of 1:1000 in blocking buffer, 0.5 mL/well). Cells were washed three times with cold washing buffer (0.1% Triton X-100 in PBS). Cells were then incubated with the secondary antibody Alexa Fluor 488 (Life Technologies) diluted in blocking buffer for 4 hours at room temperature in the dark. Slides were washed three times with cold washing buffer (0.1% Triton X-100 in PBS), counterstained with 2 μ g/mL of PI for 2 minutes at room temperature in the dark, rinsed with distilled water for 30 minutes, then allowed to dry in the dark.

Cell chambers were removed with a slide tool and two drops of ProLong® Gold Antifade Mountant (Life Technologies) was added to each well, which was then covered with a coverslip (24 x 60 mm) and sealed with transparent nail polish. The slides were left for 30 minutes at room temperature. Finally, the slides were stored at 4°C in a light-proof box until analysis.

2.4.4. γ -H2AX foci detection

γ -H2AX foci in single cells were measured using a Leica SPE2 (488 nm laser (Alexa)/432 nm laser (PI)) confocal microscope equipped with a prism and a detector device to select the spectral range from 430–750 nm. The TCS SPE control box contains four solid state

lasers: 488, 532, and 635 nm, the standard excitation wavelengths for most common dyes and a 405 nm laser, for nuclear staining.

All laser foci were positioned at only one point in the focal plane from excitation to detection. Foci were visualised and analysed by Volocity Acquisition/Visualization Software version 5.5 (Perkin Elmer, UK). The parameters, including camera exposure, sensitivity, and background, were set according to the controls of each experiment and applied to each drug treated sample. For each sample, a minimum of 50 cells were analysed.

The correct objective was selected in the software and the light path was switched to laser. The imaging resolution was set to 1024 × 1024 and the speed to 600 Hz. The sequential scanning mode was selected and the laser power gain and PMT (photo-multiplier tube) offset was adjusted for the first, second, third, and fourth sequence if required. The top and bottom of the z-stack was set up, the images were scanned. To save the images, series, process, and visualization 3-D projection were selected and all images were scanned twice (one for each channel). Duplicate images were created with the overlay channel selected to merge the images. Images were processed and further split in two channels (red and green [RG]), forming two grey scale images; one for each channel. The grey scale images were saved for analysis with CellProfiler software and merged again with the native Fiji function.

2.4.5. CellProfiler Software

CellProfiler software (available from www.cellprofiler.org) was used to process, identify objects in selected compartments, and quantitatively measure phenotypes from large sets of images automatically that can be exported for further analysis. Advanced algorithms for image analysis are available as individual modules that can be placed sequentially to form a pipeline, which is then used to identify and measure biological objects and features in images, particularly those obtained through fluorescence microscopy.

2.4.6. Image analysis using CellProfiler Software

Original images obtained with the Leica SPE2 (488 laser (Alexa)/432 laser (PI)) confocal microscope were loaded into the CellProfiler Pipeline software for use with the following module categories:

- File processing: image input, file output
- Image processing
- Object processing: identification of the object of interest
- Collection of measurements from the object of interest
- Data tools: measurement exploration, measurement output

Images were opened with the CellProfiler Image Tools. An image set of 50 cells for each drug dose were used for analysis. During 'Primary Object Identification', nuclei stain channel one (red input image) was selected for nuclei identification. The diameter of each nucleus was measured with the CellProfiler Image Tools (60 pixel units) and the typical diameter range was set between 35–150 (Min–Max) pixel units for object identification.

Foci stain channel two (green input image) was selected for γ -H2AX foci identification. The diameter was measured with the CellProfiler Image Tools (10 pixel unit) and the typical range was set between 35 and 150 pixel units for object identification. Objects outside the diameter range were automatically discarded (Figure. 2.1).

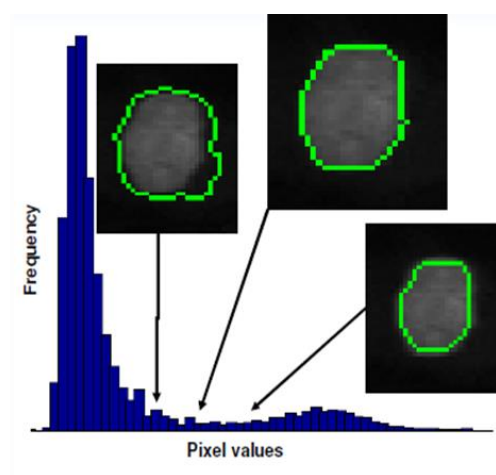


Figure 2.1: Foci identification using CellProfiler foci stain channel two (green input image)

The threshold method selected for channel one (nuclei) was Otsu Global, which allows a readily identifiable foreground/background, while the Background method was preferred for channel two (foci), since it is more appropriate for images where most of the image was comprised of background. In the Object Separation Module, clamped objects were distinguished by intensity. These methods were chosen using the Test Mode, which allows the user to view the results of all setting combinations.

Objects to export were selected and their individual measurements were saved.

Experiments were performed once for the DR and the γ H2AX foci were expressed as mean γ H2AX foci/cell \pm SE in 50 cells per experiment.

2.5. Time course experiments in colon cancer cell lines treated with oxaliplatin or SN-38 (Chapter 4)

2.5.1. Drug Treatment

Cells were treated *in vitro* with 5 μ M of oxaliplatin for 2 hours or with 0.01 μ M of SN-38 for 1 hour to establish the time of peak induction of γ -H2AX foci/nucleus. The time course experiments with oxaliplatin and SN-38 were carried out at 1, 2, 4, 6, 8, 18 and 26 hours and were repeated three times each for validation purposes.

2.5.2. Treatment *In vitro* with Oxaliplatin or SN-38

Six sets of 4-well chamber slides were plated with 1 mL of an 8×10^4 cells/mL suspension of HT-29 or HCT-116 cells in each well chamber and left to adhere overnight.

Oxaliplatin or SN-38 were added to McCoy's 5A (modified) medium to obtain a final dilution of 5 μ M or 0.01 μ M, respectively. 1 mL of total volume per well of drug was pipetted into each well (media without oxaliplatin/SN-38 was used as a control) containing cultured cell lines at 80% to 90% confluence that were incubated for 2 or 1 hours, respectively, at 37°C in 5% CO₂.

Oxaliplatin or SN-38 was removed and cells were washed twice with PBS. Cells were fixed, permeabilised, blocked, and incubated with primary and secondary antibody as described in Section 2.4.2.

2.5.3. Immunofluorescence Staining, γ -H2AX Foci Detection and Image Analysis using CellProfiler Software

Immunofluorescence staining, γ -H2AX foci detection and image analysis using CellProfiler Software are described in Sections 2.4.3–2.4.6.

2.6. Development of the Protocol for quantification of γ H2AX intensity using the CellSearch System (Janssen Diagnostics) and the DEPArray™ System (Silicon Biosystems) (Chapter 5)

2.6.1 The CellSearch System (Silicon Biosystems)

CellSearch is an automated enrichment and immunocytochemical detection system for CTCs that has been approved by the US Food and Drug Administration for routine clinical use in metastatic breast, prostate and colorectal cancer patients. CellSearch enables the immunomagnetic detection and enumeration of CTCs in peripheral blood through a ferrofluid-based capture reagent of nanoparticles with a magnetic core and antibodies targeting the EpCAM antigen for capturing and identification with fluorescent staining reagents of CTCs. Anti-CKPE is specific for the intracellular protein cytokeratin (specific for epithelial cells), while DAPI stains the cell nucleus, and leukocytes are selected with an anti-CD45-APC. The CellSearch Epithelial Control Cell Kit contains single-use bottles of fixed cells from a breast carcinoma cell line (SKBR-3) and control cells. Sample processing by the CellTracks Autoprep® System processes and optimizes the sample preparation protocol for use with the CellSearch Epithelial Cell and Epithelial Control Cell Kits.

The CellSearch Profile Kit is designed to complement research on CTCs allowing standardized and automated immunomagnetic collection and enrichment from whole

blood of the cells that can be further processed offline with several research methods. Analysis and enumeration of CTCs and control cells are performed using the CellTracks Analyzer II with the Linux operating system. When sample processing is complete, images are presented in a gallery format for final cell classification. CTCs are identified based on morphology and immunophenotype defined as EpCAM+, CK+, DAPI+, and CD45-.

2.6.2. DEPArray™ System (Silicon Biosystems)

The DEPArray system (Di-Electro-Phoretic Array system; Silicon Biosystems Bologna, Italy), is a semiautomated system based on application of dielectrophoresis (DEP) principles that allows the isolation of CTCs and other rare cells from mixed-cell populations [267] (Figure. 2.2). After an enrichment phase, CTCs were fluorescently labelled and loaded into the DEPArray cartridge, inserted into the DEPArray system and automatically injected into the main chamber. The cartridge electrodes create a dielectric field that trap CTCs in electric cages generated. A six-channel fluorescent microscope and CMOS camera enabled the identification of single cells that express the desired pattern of fluorescent markers and are moved to a 'parking area' through an automated process. Cells could be further recovered individually or in groups into a PCR tube in a medium suitable for downstream analysis. The CellBrowser software analysed each cell image, selecting them from a population of cells using a multi-parametric fluorescence and brightfield criteria. Cells trapped in the electronic cages were selected based on specific selection criteria (perimeter, diameter, circularity measures and desired fluorescence patterns) through the brightfield channel and visual inspection. Cells can be recovered from the DEPArray cartridge directly to cell culture plates allowing genomic and expression analysis down to the single cell level (Figure 2.2).

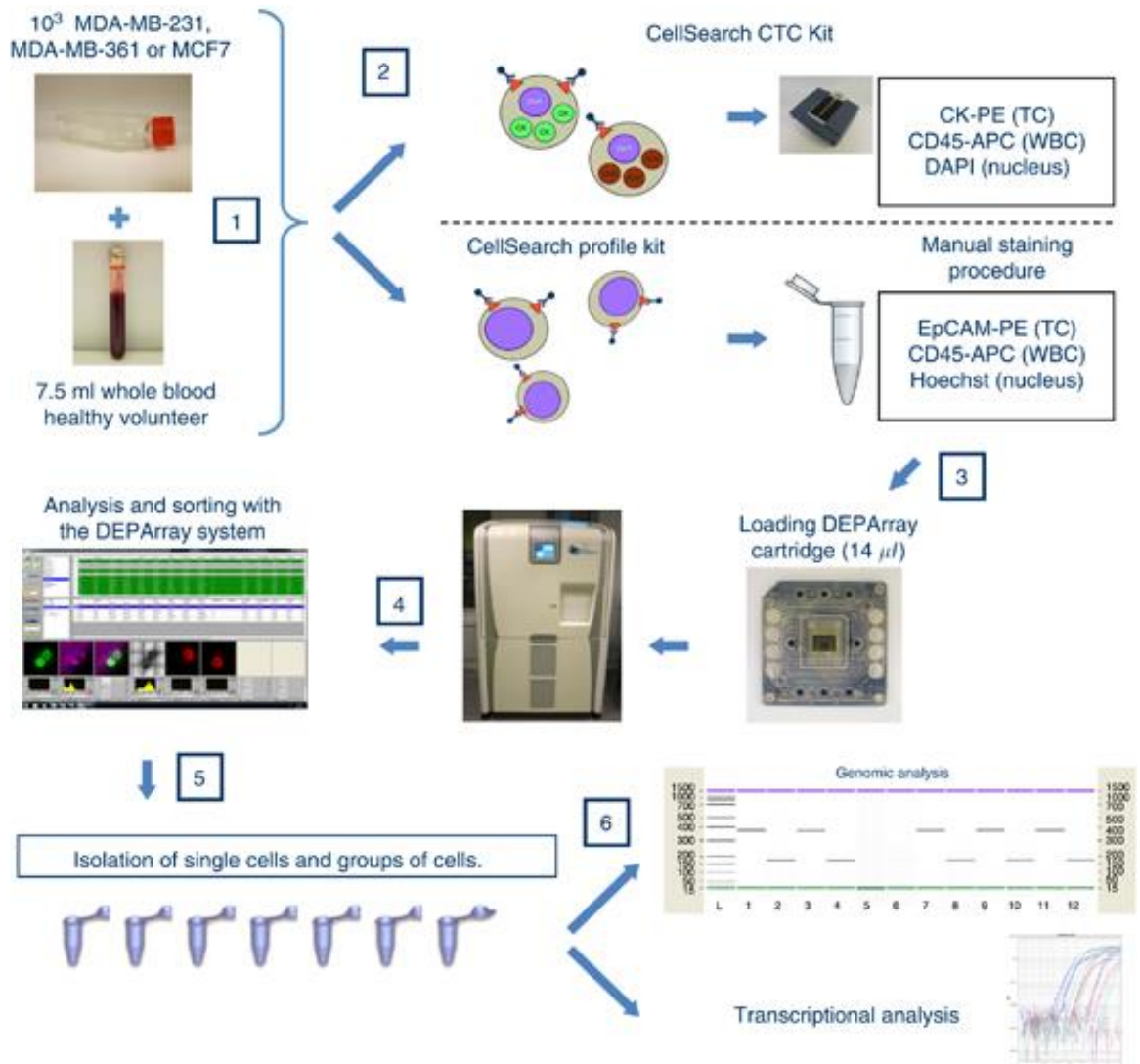


Figure 2.2: Schematic of CellSearch and DEPArray system experimental workflow.

Step 1: Tumour cells of three different human cultured breast cancer cell lines were spiked in healthy donor blood at a concentration of 10^3 tumour cells per 7.5 ml whole blood. Step 2: Tumour cells were immunomagnetically enriched using either the CellSearch CTC kit or the CellSearch Profile kit followed by a manual staining procedure. Step 3: Cells were reconstituted in a final volume of $14 \mu\text{l}$ and loaded in a DEPArray cartridge. Step 4: Analysis and sorting procedures were performed on the DEPArray system. Step 5: Single cells and groups of cells of interest were isolated with the DEPArray system. Step 6: Mutation or transcriptional analysis of isolated tumour cells.

From: Peeters DJ *et al.* *Br J Cancer* 2013. 108(6):1358–1367 [268]

2.6.3. γ -H2AX immunofluorescence staining for adherent colon cancer cell lines treated with oxaliplatin, SN-38 or topotecan

Materials, investigational drugs, cell sample and culture conditions, γ -H2AX immunofluorescence staining, foci detection and analysis are described in Sections 2.1–2.4.

2.6.4. Treatment with Oxaliplatin or SN-38

Twelve sets of four well chamber slides were plated up with 1 mL of 8×10^4 /mL of HT-29 and HCT-116 cells each, and left to adhere overnight. Cells were treated *in vitro* with 5 μ M of oxaliplatin for 2 hours or 0.01 μ M of SN-38 for one hour and fixed after 2–4 hours as previously established by the results of the dose response and time course experiments (Chapters 3 and 4).

2.6.5. Treatment with Topotecan

To provide further validation of the methods developed additional experiments were performed using cells treated with the Topo I inhibitor topotecan; the use of an additional Topo I inhibitor would allow confirmation as to whether the methods developed using the Topo I inhibitor SN-38 were appropriate.

Cells were treated with 1 μ M topotecan hydrochloride for 2 hours at 37⁰C in the presence of 5% CO₂ or were left as untreated control cells. This dose of topotecan and the time of exposure to treatment were chosen as they have previously been shown to induce γ -H2AX in HT-29 cells [214]. After treatment cells were washed, trypsinised and resuspended in PBS. Cell number and viability were determined by trypan blue assay, and the cells stored in freezing medium in 1 mL 1×10^5 cell/mL aliquots until analysis.

2.7. γ -H2AX Immunofluorescence Staining Protocol for Suspension Cells (Chapter 5)

2.7.1. Cell Treatment

HT-29 and HCT-116 colon cancer cells were plated in T75 flasks at a density of 8×10^4 /ml and left to adhere overnight. Oxaliplatin (5 μ M), SN-38 (0.01 μ M) were prepared as previously described and 1 ml of each was added to a separate 15 ml Falcon conical centrifuge tube containing 1 ml of HT-29 or HCT116 cultured cells and left for 2 and 1 hours, respectively, as determined from previous experiments (Chapters 3 and 4). The Falcon conical tubes were centrifuged at 1500 rpm (430 g) for 5 minutes at room temperature and the samples were washed three times with PBS.

2.7.2. γ -H2AX Immunofluorescence Staining

1 mL PBS was added to the cells and gently mixed by hand. Cells were fixed with 2 mL ice-cold 4% PFA, mixed by hand and incubated for 5 minutes at room temperature. The samples were centrifuged at 1500 rpm (430 g) for 5 minutes at room temperature, the supernatant was discarded. Cells were washed three times for 5 minutes in ice-cold PBS and the samples were again centrifuged at 1500 rpm (430 g) for 5 minutes. The supernatant was discarded leaving 200 μ l of PBS containing the cell pellet which was transferred into 1.5 mL microcentrifuge tubes (Sigma-Aldrich Co.). Microcentrifuge tubes were placed into a Shandon EZ single cytofunnel (one sample at the time), kept in a diagonal position and spun at 650 rpm for 5 minutes in a cytospin machine. Samples were permeabilised in ice-cold permeabilisation buffer (permeabilisation buffer: 0.2% triton x-100 in ice-cold PBS) for three minutes at room temperature then washed three times for 5 minutes each in ice-cold PBS. Samples were blocked with blocking buffer (10% FBS, 5% BSA in PBS) for 1 hour at room temperature. Unless otherwise stated, immunofluorescence staining was performed with the slide tray in fridge to minimise movement of slides, with a reservoir of water at the bottom to provide humidity and reduce antibody evaporation from slide during incubation. On each slide, a circular rim was drawn

with a radius of approximately 1 cm around edge of cells. 90 µl of the primary γ -H2AX antibody (Mouse anti-H2AX monoclonal primary antibody diluted in blocking buffer (1:1000) (Merck Millipore, UK) (stored at -20°C) 1:500 in 1% FBS in PBS) was pipetted into the gap marked with the pen ink, fully covering the cells and incubated at 4°C overnight. Slides were washed with cold-ice PBS three times. When the cells were dry 90 µl of the secondary antibody (AF-488 goat antimouse IgG 1:500 in 1% FBS in PBS) was added and the slides were incubated for 1 hour in the dark at room temperature. The slides were washed three times for 5 minutes each with ice-cold PBS and then stained with Hoechst 33342 (10 µg/mL; Life Technologies H3570) for 30 minutes in the dark and further washed as described above. Slides were rinsed in distilled water twice to remove salts from PBS, protecting them from light and were then allowed to dry in the dark. Once dry, the pen barriers were removed, 25 µl of Prolong Gold (Invitrogen, Life Technologies Ltd.) was added to the area above and below the cells and then covered with micro cover glasses (24 x 60 mm; VWR SuperSlips) to ensure coverage of the whole area traversed by cells and Prolong Gold. The edges were sealed with clear nail varnish and the slides were stored at 4°C until analysis.

2.8. Materials and Methods for CellSearch System (Janssen Diagnostics)

(Chapter 5)

2.8.1. Materials for CellSearch Epithelial Cell Kit

γ -H2AX antibody (Anti-phospho-Histone H2A.X (ser139), clone JBW301, FITC conjugated) (Merck, catalogue number 16-202A) diluted to 57 µg/mL in Bond primary antibody diluents

CK-PE (CK-Phycoerythrin) (CK-PE antibody) (Abcam)

Dapi (4'-6-Diamidino-2-phenylindole) (ThermoFisher Scientific)

CD45-APC (CD45-Allophycocyanin) (CD45-APC Antibody) (ThermoFisher Scientific)

Anti-EpCAM Ferrofluid (Janssen Diagnostics): Contains a suspension of 0.022% magnetic particles conjugated to a mouse monoclonal antibody specific for the cell surface marker

EpCAM present on epithelial cells in a buffer containing 0.03% BSA and 0.05% ProClin® 300 preservative.

Staining Reagent (Janssen Diagnostics): Contains 0.0006% mouse monoclonal antibodies specific to cytokeratins conjugated to phycoerythrin (PE); 0.0012% mouse anti-CD45 monoclonal antibody conjugated to APC in buffer containing 0.5% BSA and 0.1% sodium azide.

Nucleic Acid Dye (Janssen Diagnostics): Contains 0.005% 4', 6-DAPI and 0.05% ProClin® 300.

Capture Enhancement Reagent (Janssen Diagnostics): Contains 0.02% proprietary reagent for controlled ferrofluid aggregation, 0.5% BSA, and 0.1% sodium azide in buffer.

Permeabilisation Reagent (Janssen Diagnostics): Contains 0.011% proprietary permeabilisation reagent and 0.1% sodium azide in buffer.

Cell Fixative (Janssen Diagnostics): Contains 25% proprietary fixative ingredients, 0.1% BSA, and 0.1% sodium azide in buffer.

2 × 110 mL bottle Dilution Buffer (Janssen Diagnostics): Contains buffer with 0.1% sodium azide.

CellSearch Conical Centrifuge Tubes (15 mL) and Conical Tube Caps (Janssen Diagnostics)

Cartridges and Cartridge Plugs (Janssen Diagnostics)

CellSave Preservative Tubes (Janssen Diagnostics)

CellTracks Autoprep System (Janssen Diagnostics)

CellTracks Analyzer II (Janssen Diagnostics)

CellSearch Epithelial Cell Control Kit (Janssen Diagnostics)

CellTracks Autoprep Instrument Buffer (Janssen Diagnostics)

Horizontal swing out style rotor (swing bucket) centrifuge capable of 800 × g

Test tube racks

Calibrated micro-pipettes and tips

2.8.2. Method for CellSearch System (Janssen Diagnostics)

2.8.2.1. Sample Preparation

From the peripheral blood draw of healthy volunteers, (National Research Ethics Service Committee, NRES, London, Bloomsbury, 12/LO/1654). 7.5 mL of blood was collected in CellSave tubes, mixed by inversion (x5) and combined with 6.5 mL of Dilution Buffer (CellSearch CTC Kit, Cat No 7900001) in a 15 mL conical tube and again mixed by inversion (x 5). The sample was centrifuged at 800 g for 10 minutes at room temperature and processed on the CellTracks Autoprep system (Cat No 9541) within one hour of sample preparation. A CTC Control Sample (CellSearch CTC Control Kit, Cat No 7900003) was prepared for each run and stored at 4°C. Prior to analysis the control sample was allowed to reach room temperature, vortexed for 5 seconds to mix, inverted five times then added to a 15 mL conical tube and placed on the CellTracks AutoPrep system for analysis. The CellSearch platform has a 4th channel (FITC) that allows molecular analysis to be performed.

The γ -H2AX antibody (Merck) was diluted to 57 μ g/mL in Bond primary antibody diluent and loaded into position 1 of the reagent carrier. This concentration was based on methods taken from publications by the Division of Cancer Treatment and Diagnosis at the National Cancer Institute (<http://dctd.cancer.gov/>).

Once on the CellTracks Autoprep system, the plasma and buffer layer were aspirated from the blood sample. To obtain a magnetic separation, ferrofluids containing nanoparticles with a magnetic core surrounded by a polymeric layer coated with antibodies to EpCAM were then added and incubated leaving unbound cells and plasma that were eventually aspirated out.

The presence of CTCs was identified with the addition of staining reagents and permeabilisation buffer to fluorescence label the immunomagnetically labelled cells. The fluorescent reagents that were added were cytokeratins 8, 18, 19 (CK-PE), 4' 6-DAPI and an antibody to CD45 conjugated to allophycocyanin (CD45-APC; Janssen Diagnostics). CK-PE is specific for epithelial cells, marking the intracellular protein cytokeratins, DAPI stains the cell nucleus and CD45-APC is specific for leukocytes.

Cells were then resuspended in the MagNest cell presentation fixture, characterised by a strong magnetic field responsible to move the magnetically-labelled target cells to the outward edge of the cartridge, where they distributed uniformly over the analysis surface and were oriented for analysis at a single focal depth. The cartridge containing stained CTCs was then removed, left in the dark for 20 minutes and finally inserted into the CellTracks Analyzer II (Cat No 9555 RUO), a four-colour semi-automated fluorescence microscope, for scanning.

2.8.2.2. CTC Analysis and Enumeration Using the CellSearch Method

On the CellTracks Analyzer II, the cartridges along with the control were scanned capturing image frames covering the entire surface of the cartridge and displaying tumour cells positive for cytokeratin and DAPI that were reviewed by the operator afterwards.

The CellTracks Analyzer II presented the images with overlays of CK-PE and DAPI signals to show whether the nuclear and cytokeratin staining were consistent with a tumour cell. The objects in the CK-PE filter channel were required to be a round or oval intact cell, at least 4 microns in diameter with a nuclear area smaller than the cytoplasmic area and more than 50% of the nucleus needed to be visibly surrounded by the cytoplasm. Sometimes, an image could appear very bright as results of a spectral spillover in the CK-PE channel that was creating a visible cytoplasmic image in the CD45-APC channel. This could still be classified as a tumour cell if it maintained negativity for CD45 and positivity for CK-PE, differentiating from leukocytes that would be positive for CD45-APC and DAPI but negative for CK-PE. Artefacts were recognised as appearing with the same shape in all channels. All samples were reviewed by two trained laboratory staff, as well as myself.

The Autoprep and the following steps were performed using the manufacturer's instructions summarised as follows:

- Autoprep was switched on
- 'run batch' was selected
- CTC Kit was loaded into reagent carrier

- The instructions on Autoprep to set up batch were followed, User Defined Marker was selected and γ -H2AX was entered.

When completed, cartridges were removed and stopper was inserted. Cartridges were laid flat in the dark for 20 minutes before scanning on the CellTracks Analyzer II. System verification of the Analyzer II was performed and control and sample cartridges were scanned. Cartridges were automatically imaged with the following filters:

PE (CK-PE Antibody)

Dapi (nuclear marker)

APC (CD-45- APC Antibody)

FITC for 4th channel marker (γ -H2AX, 3 seconds exposure).

Controls were analysed to check that Low and High cell populations fell within the expected range (one control was run per day of sample processing). Cells were analysed with the criteria for identifying CTCs as previously mentioned. γ -H2AX positive cells were selected by nuclear FITC staining. Cartridges were stored in the dark at 4°C for future analysis (DEPArray) or contents transferred to 50% glycerol for -20°C storage.

2.8.3. Validation of the CellSearch System protocol for Detection of γ -H2AX on CTCs

Validation of the assay used in this thesis for the detection of γ -H2AX on CTCs using the CellTracks Autoprep System and the CellTracks Analyzer II was conducted in the laboratories of the UCL ECMC GCLP Facility, UCL Cancer Institute between 01.06.2013 and 30.06.2013. Development and validation of a new biomarker detection assay with these systems is limited. The CellTracks Autoprep System is fully automated and the only parameter which can be changed is the concentration of the antibody, which was set at 57 μ g/mL. The only parameter which can be changed on the CellTracks Analyzer II is the exposure time for the FITC channel, which was set at 3 seconds. Both settings are based on methods taken from publications by the Division of Cancer Treatment and Diagnosis at the National Cancer Institute (<http://dctd.cancer.gov/>).

Healthy donor blood was spiked with HT-29 colon adenocarcinoma cells. Cells were left untreated, or treated either with 1 μM topotecan hydrochloride for 2 hours at 37°C in the presence of 5% CO_2 , or with 5 Gy X-ray with 30 minutes post-incubation. The doses of topotecan and Gy X-ray and the time of exposure to treatment were chosen as they have previously been shown to induce $\gamma\text{-H2AX}$ in CTCs from peripheral blood [214, 269].

2.8.3.1. Method Validation

Three validation runs were performed on different days. For each validation run, 4 x 7.5 mL healthy donor blood was collected in CellSave tubes. Prepared aliquots of HT-29 cells were thawed and washed in 10 mL PBS. Cells were then pelleted by centrifugation at 1500 rpm for 5 minutes, before being resuspended in 10 mL PBS. 50 μL of one of the following four cell suspensions (~500 cells per suspension) was added to 7.5 mL healthy donor blood:

- Healthy donor blood (blank)
- Healthy donor blood spiked with untreated HT-29 cells
- Healthy donor blood spiked with topotecan treated HT-29 cells
- Healthy donor blood spiked with X-ray irradiated HT-29 cells.

For each run, four samples from one healthy donor and a CellSearch CTC control sample were run using a CellSearch Circulating Tumour Cell Kit on the CellTracks Autoprep System and the CellTracks Analyzer II. Different healthy donors were used for each of three validation runs. $\gamma\text{-H2AX-FITC}$ antibody was used on sample numbers 2–4 at 57 $\mu\text{g}/\text{mL}$. Exposure time for the fourth channel was set at 3 seconds on the CellSearch Analyser II. The criteria to define a CTC were as described previously.

Acceptance criteria for detection of $\gamma\text{-H2AX}$ were:

- Samples spiked with untreated cells must be $\leq 3\%$ positive for $\gamma\text{-H2AX}$
- Samples spiked with treated cells must be $\geq 10\%$ positive for $\gamma\text{-H2AX}$.

2.9. Materials and Methods for the DEPArray™ System (Silicon Biosystems)

(Chapter 5)

2.9.1. Materials for the DEPArray™ System (Silicon Biosystems)

DEPArray™ A300K disposable cartridge

Ultrasonic bath (Sonorex)

Manipulation buffer SB115

Sterile holder (e.g., Petri dish)

P20 Eppendorf R pipette (2-20 µl)

LoRetentionR dualfilter Eppendorf tips 20 µl Eppendorf

LoRetentionR dualfilter Eppendorf tips 1000 µl Eppendorf

0.2 µm filter

Lint-free cloth

2.9.2. Methods for the DEPArray™ System (Silicon Biosystems)

2.9.2.1. Sample Preparation and Buffer Compatibility

The buffer compatibility and the downstream application of the recovered cells by the DEPArray system was chosen according to the sample type, in this case live cells (Table 2.2).

Table 2.2: Downstream application and manipulation buffers

Sample	Downstream application	Manipulation buffer
Live cells	Cell culture	Complete culture medium
	Immunofluorescence, other applications	Complete culture medium
	DNA/RNA analysis	Complete culture medium
Fixed cells	<i>Ampli 1</i> ™ whole genome amplification kit	SB115 (Silicon Biosystems spa)
	FISH or other downstream molecular analyses	SB115 (Silicon Biosystems spa)

The appropriate DEPArray parameters were selected to define the set-up execution. A single cell suspension was prepared for each sample, and the total number of cells and staining were analysed using a fluorescent microscope. The presence of cell debris or large cell clusters was also evaluated as they can decrease the success of cell manipulation and the total number of cells to be loaded in the DEPArray A300K cartridge (version 1.3.0).

HT-29 and HCT-116 cells were prepared as discrete cells as described in Section 2.4 and 2.7 followed by the CellSearch Sample Pre-Processing Protocol for the DEPArray System. Cells were washed with 1 mL of SB115 buffer, and sealed with parafilm. Cells were centrifuged at 1000 g for 5 minutes at room temperature using a swinging-bucket rotor. The supernatant was removed and put into labelled tubes for storage until the end of analysis and 1 mL of manipulation buffer was added to the remaining cells; centrifugation and removal of the supernatant was then repeated. The cell pellet was reconstituted in an adequate volume of buffer, mixed well and counted using a Burker's Hemocytometer. A percentage of the sample loaded in the DEPArray A300K cartridge was analysed by the system and an aliquot of the cell culture medium (830 μ l) was prepared and equilibrated at room temperature. After equilibration, 2 x 900 μ l of SB115 buffer was filtered with 0.2-micron filter and then degassed for 10 minutes on full power using a Bath Ultrasonic QS5 (BAT 1904; Scientific Laboratory Supplies).

2.9.2.2. Cartridge Loading

The DEPArray A300K cartridge was placed in a sterile Petri dish in preparation for loading. The DEPArray A300K cartridge was opened and 830 μ l of sonicated de-gassed SB115 medium was added to chamber B and 14 μ l of the cell sample was added to chamber S. The volume was checked before loading, adjusted by centrifugation (14100 rcf) in a fixed rotor centrifuge for 30s, in order to leave approximately 10 μ l PBS containing the cell pellet. The DEPArray A300K cartridge was inserted in the machine. The SB115-30K-rev3 or SB115-16K-rev3 parameters were selected (SB115-30K was preferable to get a good distribution of cells; 16K was used in cases where cell numbers were <20,000; Table 2.3).

Appropriate temperature and other parameters were selected as indicated in the DEPArray System Protocol. The filters/channels for the sample scanning and Bright field required for DEPArray functionality were selected (i.e. add or remove FITC):

Filter 1 = target filter i.e. for PE Cytokeratin.

Filter 2 = -ive/other i.e. APC for CD45

Filter 3 = DAPI for DNA – UV filter (to prevent photo bleaching)

Filter 4 = Bright field

Fluorescent channels were chosen to analyse the images of all the events detected. Images were analysed by creating a Region of Interest (ROI) in correspondence to the positive label and were further processed in order to obtain information on fluorescent and morphological parameters displayed at the Cell Browser (Section 2.9.3).

To remove particles detected more than once during image analysis, the Duplicate Compare was selected and the appropriate parameters were used:

PE – Gain 2%, Exp 100,000, Signal detection Faint

APC – Gain 2%, Exp 300,000, Signal detection Faint

DAPI – Gain 1%, Exp 100,000, Signal detection Bright

FITC 1 - Gain 1%, Exp 100,000, Signal detection Faint

FITC 2 – Gain 4%, Exp 800,000, Signal detection Faint

Scan Area 'Full' was selected followed by Sorting Mode 'Standard'. The sample was observed while loading to avoid loading failure, in which case manual recovery was performed.

After analysis the execution was stopped and the DEPArray A300K cartridge removed. The cell sample volume was readjusted to 14 µl as before and loaded with the buffer in a new DEPArray A 300K cartridge. The system automatically performed the Calibration and the Sample Load steps. The Cage Parameters Programme (manipulation buffer and the cage pattern) was selected using the parameters described in Table 2.3.

Table 2.3: DEPArray Programme Parameters

Sample	Total cells in 13–14 μl, n	Button selection	Manipulation buffer
Live cells	n <20,000*	PBS-16k-rev3	Cell culture medium
	20,000 \leq n <40,000*	PBS-30k-rev3	
	40,000 \leq n \leq 100,000	PBS-30k-rev3	
Fixed cells	n <20,000*	SB115-16k-rev4	SB115
	20,000 \leq n <40,000*	SB115-30k-rev3	
	40,000 \leq n \leq 100,000	SB115-30k-rev3	

*Range recommended for single-cell sorting execution

After automatic calibration and sample loading, image analysis started automatically. There are two steps during this process: Chip scan and Image Analysis steps. The Chip scan step consisted of scanning the chip using fluorescence and bright field channels allowing the images (events) acquired to be counted and their position inside the chip to be calculated. In addition, morphological and intensity measurements were extracted from the scanned images. Following the Chip scan and Image Analysis steps, events were detected based on an image thresholding algorithm that was selected during the Cell Sorting Execution Start Up in the Chip Scan Setting form. The acquired images were cropped in areas of 3 x 3 electrodes around every event detected creating, for each scan filter build, an image gallery displayed at the Cell Browser step (Section 2.9.3). Particle geometries, morphological measurements and intensity were obtained and analysed in the Image Gallery. Measurements were carried out for each detected event on the ROI and calculated based on the intensity of fluorescence signals. The analysis was performed in all fluorescence channels to get the correct measurements for each filter (Figure 2.3). If a duplicate particle was detected in the overlapping area between two images, it was removed.

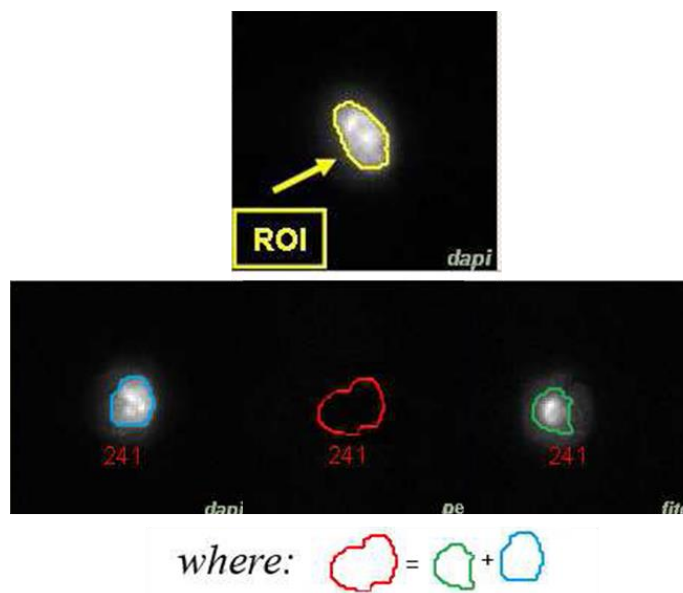


Figure 2.3: An example of a *use case* in which the DEPAArray analysis is performed using DAPI and FITC channels without the PE channel: for PE, merging of the ROIs found in the DAPI and FITC channels (red ROI in the centre crop) was used for measurement calculations.

2.9.3. Cell Browser

The Cell Browser software allows the identification, selection and assignment of particles of interest to user-defined groups. The particles are retrieved as input and the cells are produced as the output. The input population included the particles produced by the Image Analysis step and identified using a unique ID code. When the Cell Browser step was initiated the input population was displayed in the Table Analysis mode while the morphological and fluorescence intensity measures were displayed in the Image Gallery Bar. The particles of interest were selected after the creation of groups for processing with Recovery Manager.

A Cell Browser group was used to categorize different cell populations, and the cells were sorted based on different characteristic such as intensity fluorescence and morphological trait. Several parameters were used to classify the input particles based on cell morphology and label signals, which were calculated during the detection of the fluorophore intensities. The trapping parameters were:

- In Cage: allowed the identification of the particles correctly trapped in the cage, suitable for the cell routing
- In Grid: allowed the automatic removal of unstained contaminants from the cell population and evaluation of distance between the barycentre of the particle and the electrode centre.

Morphological parameters were:

- Circularity: roundness of the particle
- Perimeter: perimeter in microns of the ROI
- Diameter: circumference of the circle extrapolated from the area in microns.

The perimeter and diameter were calculated on the ROI based on fluorescence detection. As a result, the measurements do not correspond to the actual dimensions of the entire cell.

Intensity parameters were:

- Mean intensity: mean of all gray levels measured within the ROI (usually selected for diffused cell staining in the nucleus, cytoplasm or on the cell plasma membrane, e.g. pancytokeratins, DAPI)
- Max intensity: maximum of all gray levels measured within the ROI preferentially used for a punctuate cell staining in the nucleus, cytoplasm or on the cell plasma membrane
- Mean intensity with background subtraction: indicate how much the cell contrasts with the background.

The Histogram Analysis mode was initially used to filter the particles captured by the dielectrophoretic field displaying the distribution frequency of selected parameters using a histogram graph. The Population Filter and the Plotted Parameters tool were used to select the input populations and parameters to plot. For each histogram, gating cursor bars were

used to select the output subpopulation. At each selection process, the *Gated Particles Counter* showed the total number of particles represented and the number that were gated. Once the analysis and selection were complete, the subpopulations could be further analyzed. The gating process described above reduced the number of particles that needed to be visually examined and represented the particles that were captured by the dielectric field (low APC signal, high FITC signal and high circularity FITC). The Scatter Plot Analysis mode was used to display the gated subpopulation as a collection of points in a scatter plot, plotting one parameter related to the positive marker (e.g. *mean_intensity_PE*) and the other related to the negative marker (e.g. *mean_intensity_FITC*). Each point displayed in the scatter plots represented one or more particles which could be displayed as gallery images. The output subpopulation was gated and loaded in Table Analysis mode where it was possible to individually view particles that met the desired characteristics and assigning them to the appropriate group. Once a group was created, the individual cells were reviewed and visually confirmed that they were single cells with the desired morphology.

During the exporting of the data the system automatically acquired all the images that had been selected, creating an Image Gallery for each cell acquired. A panel of selected cells were displayed (Figure 2.4); the first column showed the cell ID, the second column displayed the name of the selected group and the remaining columns showed the Image Gallery channels as created in the Cell Browser. To view the visible attributes of the particles, this parameter was selected with the appropriate parameters to display (e.g. *mean_intensity_dapi* and *mean_intensity_pe*; Figure 2.5). High resolution images of cells for recovery were taken if required using the 20x objective and saved (one for each fluorescence channel and bright field channel).

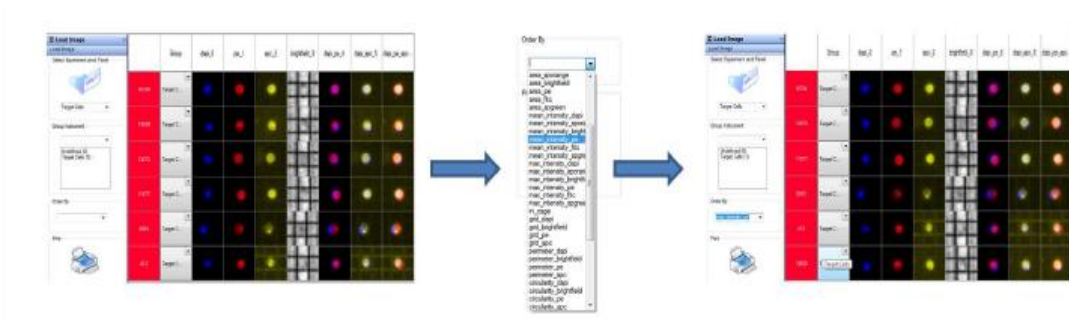


Figure 2.4. Example of the Image Gallery created in the Cell Browser

	Group	depi_0	pe_1	apc_2	brighfield_3	depi_pe_4	depi_apc_5	depi_pe_apc...	mean_intens...	mean_intens...
16734	Target C...								43.32	93.46
13633	Target C...								44.71	90.71
13671	Target C...								47.4	90.04
11677	Target C...								47.3	92.65
8580	Target C...								53.47	90.21
412	Target C...								45.57	93.36

Figure 2.5. Example of the visible attributes of the particles created in the Cell Browser

2.9.3.1 Cell Routing and Recovery

The cells selected at the Cell Browser were moved across the chip active area in order to be recovered for downstream analysis. The Cell Routing and Recovery steps were performed using the automatically activated Recovery Manager™ as follows:

Park Routing: cells to be routed were selected from the groups created at the Cell Browser and moved by the system from the Main Chamber to the Park Chamber. In the Camera Live section the movement of the cells was followed in real time. While in process, the tubes were added to required positions. All cells were checked to confirm they had routed successfully using DAPI filter to see the presence of nuclei where cells should be.

The Recovery supports for the downstream analysis were selected along with the recovery positions for the collection of target cells. Before starting the collection of cells, the

Washing step and a Priming Recovery of clean buffer was performed to clean the Exit or Recovery Chamber. The number of drops to recover was automatically selected by the software. In the Recovery Support section the option Set Priming Recovery Position was selected. In the Exit and Recovery section, the Group name or Cell ID was selected to the desired position. After the recovery positions were defined, the Exit routing was activated and the first recovery support to collect target cells was inserted into the DEPArray Machine. After the cells had been transferred to the Recovery section they were washed, Priming Recovery was then performed which eliminated putative sources of contaminations (e.g. cell debris, not selected cells, etc.) present in the Exit Chamber. The tubes containing the cells of interest were closed and carefully labelled and the cartridge was removed. During recovery a PDF panel of recovered cells was created from the Cell Browser and a printable report was saved.

The data obtained during the cell sorting with the DEPArray could be analysed off-line and elaborated using the Cell Browser software with the DEPArray in Post Processing mode. Every time a New Post Processing Session was created all settings (histograms, scatter plots, etc.), particle populations and selections were restored from the original data. Backup software allowed experimental and user data to be saved on an external backup unit allowing for data processing and elaboration. Data automatically generated, during sorting executions, or during post processing (e.g. cells scan images, and/or cells panels) were exported.

2.10. Materials and Methods for CellSearch Sample Pre-Processing Protocol for the DEPArray System (Silicon Biosystems) (Chapter 5)

2.10.1. Materials for CellSearch Sample Pre-Processing Protocol for the DEPArray System (Silicon Biosystems)

Manipulation buffer SB115

BSA 2% (Sigma-Aldrich; Order no: A3059-10G) in PBS 1X (Gibco; Order no: 20012-019)

Protein Lobind Tube 1.5 mL (Eppendorf; Order no: 0030.108.116)

Gel Loading Tip Round (Corning; Order no: 4853)

Swinging-bucket Rotor Centrifuge

2.10.2. Methods for CellSearch Sample Pre-Processing Protocol for the DEPArray System (Silicon Biosystems)

2% BSA solution was prepared in PBS 1X (Gibco Order no: 20012-019) from lyophilized powder, essentially globulin and protease free, $\geq 98\%$ and stored at 4°C while a bottle of DEPArray Sample Manipulation Buffer (6 mL) was thawed at room temperature. Two aliquots of 325 μL of DEPArray Sample Manipulation Buffer were prepared in 1.5 mL tubes. One aliquot of 1.5 mL of PBS mL was also prepared as a control. Three separate 1.5 mL Lo-Bind tubes were labelled, one with the Sample ID and one each with Supernatant 1 and Supernatant 2. The CellSearch Cartridge was opened. A 200 μL gel-tip was loaded onto a P200 pipette (set at 200 μL) and was slowly pipetted five times in the PBS-BSA 2% aliquot to coat the tip with PBS-BSA. The tip was then dipped into PBS solution to coat the external surface, leaving the tip empty. The 200 μL pre-rinsed gel-tip was used to withdraw the sample from the CellSearch Cartridge. The sample was resuspended by pipetting and transferred from the CellSearch cartridge to a clean 1.5 mL sample tube. 325 μL of manipulation buffer was transferred from one of the two aliquots to the CellSearch Cartridge. The buffer was thoroughly resuspended inside the CellSearch cartridge by repeatedly pipetting against the inner surface and all the fluid was then transferred to the Sample Tube. This step was repeated with the second prealiquoted 325 μL of manipulation buffer. The Sample tube was centrifuged at 1000 g for 5 minutes in a swinging-bucket rotor. The supernatant was withdrawn over the pellet leaving approximately 30 μL of supernatant over the cell pellet. The supernatant was transferred to a new LoBind tube (identify it as 'Supenatant 1') and stored until DEPArray analysis.

1 mL of DEPArray Sample Manipulation Buffer was added to the sample without resuspending and the same process was followed leaving about 10 μL of fluid over cell pellet, and transferred in a new LoBind tube that was stored until DEPArray analysis. The total volume required was 14 μL ; the pellet was resuspended with manipulation buffer and

the sample volume was measured and adjusted with manipulation buffer. If the volume was higher than 14 μl , the sample was centrifuged for 5 min at 300 g and the extra volume was removed.

2.10.3. DEPArray Analysis of γ -H2AX expression in treated and untreated colon cancer cells

The buffer compatibility and the downstream application of the recovered cells by the DEPArray System was chosen according to the sample type (live cells) (Section 2.9.2.2.) and the DEPArray set-up execution system was selected according to the manufacturers protocol. Cells were prepared using standard protocols (CellSearch Sample Pre-Processing Protocol for DEPArray System; see Section 2.9).

The cartridges containing the cells were loaded and the scan filters selected. After automatic calibration and sample loading, the Chip scan step and Image Analysis step started automatically followed by the cell selection workflow. A Cell Browser group was used to categorise different cell populations, and cells were sorted based on different characteristic such as intensity fluorescence and morphological trait.

Several parameters were used to classify the input particles based on cell morphology and label signals, which were calculated during the detection of fluorophore intensity. The cells selected by the Cell Browser were moved across the active area of the chip in order to be recovered appropriately for downstream analysis.

Three colon cancer cell samples were treated (sample 1, treated with SN-38 [0.01 μM], sample 2, untreated control, sample 3, treated with oxaliplatin [5 μM]) and were analysed as trial experiments to set up the workflow on the DEPArray System as follows:

- **Step A:** CTC enumeration with CellSearch system: The required exposure time for γ -H2AX with FITC identification was 3 seconds, as previously identified and validated in Section 5.2 After the CellTracks Analyzer II scan the sample was processed in the DEPArray system.

- **Step B:** sample analysis with the DEPArray System: Optimisation of the optical parameter to detect γ -H2AX signals and the Cell Browser workflow scheme for target cell identification were performed as described in Section 2.9.3.

To maintain the CellSearch System set up, an exposure time (FITC) of 800 ms and gain 4X was selected.

2.10.4. γ -H2AX Staining for Suspension Cells and Slide Preparation for Validation with Fluorescence Microscopy

After fixation with PFA 4%, cells were split into two samples, one sample was centrifuged in the Cytospin machine on the slide in the slide container (Shandon EZ single cytofunnel) while the other half was left in suspension to be further processed with the DEPArray platform. Following permeabilisation and blocking (Section 4.3), the suspended cells and slides were stained (or left unstained) with primary (Mouse anti-H2AX monoclonal) and secondary antibody (Goat anti-mouse Alexa Fluor 488 IgG). Cells were analysed with confocal microscope and Cell Profiler software as described previously.

2.11. Methods for the Clinical Application and Characterisation of CTCs (Chapter 6)

2.11.1. Development of the CTC Protocol

The Research Ethics Committee (REC) submission, Site-Specific Information (SSI) form and Research and Development (R&D) submissions were uploaded and completed via the Integrated Research Approval System (IRAS) and were approved by the local REC (National Research Ethics Service Committee, NRES, London, Bloomsbury, 12/LO/1654) and by the Local Trust Research and Development department at University College of London Hospital (UCLH).

Patient information was confidential by assigning a unique identification number for each patient and the study data and medical record was processed using computerised methods to assign appropriate coding; access to patient data was restricted. The protocol allowed two vials (15 ml) of the blood volume to be taken pre-chemotherapy and two vials

(15 ml) post-infusion of oxaliplatin or irinotecan to allow adequate blood volume for CTC enumeration and molecular analysis via the CellSearch platform.

2.11.2. Patient Selection and Consent

Patients with metastatic colorectal cancer who were to start chemotherapy with FOLFOX (chemotherapy containing oxaliplatin) or FOLFIRI (chemotherapy containing irinotecan) were consented into the study to investigate γ -H2AX expression in CTCs (National Research Ethics Service Committee, NRES, London, Bloomsbury, 12/LO/1654). They were identified from the weekly UCLH colorectal-oncology MDT meetings, as well as from the LOC database where it was possible to select the outpatient list of candidates who were scheduled to initiate chemotherapy. A written permission to approach patients scheduled for chemotherapy in outpatient clinics at LOC was previously obtained by their Consultants and the list was reviewed weekly by myself to identify potential patients.

Patients older than 18 years who had a confirmed histopathological diagnosis of colorectal cancer and signed informed consent were eligible for the study. Patients were excluded if they had already started a new cycle of chemotherapy with FOLFOX or FOLFIRI; previous treatment with these chemotherapies was allowed.

2.11.3. Sample and Patient Information Collection

Blood samples for CTC isolation, enumeration and analysis were taken pre- and post-infusion of FOLFOX or FOLFIRI on day 1 Cycle 1. Peripheral blood samples of up to 10 ml were collected in four CellSave Preservative tubes (Cat No 7900005; Veridex LLC, NJ, U; two tubes pre- and two tubes post-chemotherapy). Samples were anonymised and transported from the UCLH or the LOC outpatients department to the UCL Cancer Institute, where they were received by GCP and GCLP trained personnel (Victoria Spanswick, Leah Ensell, Helen Lowe). Each specimen was processed within 96 hours of being received, as per the CellSearch and UCL Cancer Institute lab protocols.

Clinical data including demographic, clinicopathologic information, details of previous lines of treatment and disease recurrence were collected on patients from the UCLH or LOC (MOSAIQ) patient information system.

2.11.4. Sample Preparation and Analysis

Blood was processed for CTC enrichment and enumeration as described in Section 2.8.2 using the CellSearch platform. Anti-phospho-Histone H2AX (ser139), clone JBW301, FITC conjugated antibody (Millipore) was used on all samples after having been validated for use in cell lines and CTCs at the UCL Cancer Institute, as described in Section 2.8.

2.12. Statistical Analyses

Data are presented as mean (+/- standard deviation or standard error). Graphical summaries of the detection of γ -H2AX expression on treated and untreated cell lines (HT-29 and HCT-116) are presented. Where data were sufficient, statistical analyses were performed for the detection of γ -H2AX expression on treated and untreated cell lines (HT-29 and HCT-116) using an unpaired T-test on mean FITC intensity (representing γ -H2AX expression) either using raw data or FITC intensity minus the background intensity. A significant difference between treatment groups was determined to be $p < 0.05$.

For the clinical application and characterisation of CTCs from patients with CRC, the number of patients selected was in the range of 15–20. Previous studies demonstrated a general low [270] CTC detection rates and counts in the CellSearch system in mCRC and a much lower yield of CTCs in this tumor type compared with breast or prostate cancer [188, 190]. In one study for the metastatic CRC patients ($n = 413$), the median CTC counts per 7.5 mL peripheral blood was 0 [190, 270].

Due to the low rate and variability of CTC detection in patients with CRC we could not predict the number of patients to enroll in order to detect a sufficient number of CTCs to demonstrate an effective methodology. This was an exploratory clinical study and no formal statistical calculation of sample size was performed.

CHAPTER 3

Defining the dose response in colon cancer cell lines treated with varying concentrations of oxaliplatin and SN-38

3.1. Introduction

DSBs in chromatin are characterized by histone H2AX phosphorylation on Ser-139 (γ -H2AX) that can be visualized by immunofluorescence microscopy shortly after induction as discrete nuclear foci [271, 272], with each focus representing a single DSB [272]. The number and intensity of foci per nucleus correlates with the dose of the agent used to induce the DSBs [273] and has recently been proposed as a PD biomarker following treatment with topo I inhibitors, including topotecan [214, 244]. As detailed in Section 1.2.6., finding faster and non-invasive methods to assess the effect of chemotherapeutic agents on tumour cells during the course of treatment can allow for an immediate determination of the effect of a drug on its putative target. γ -H2AX induction has been recently investigated in CTCs from patients receiving treatment to monitor the PD effects of anticancer therapies over treatment cycles [214]. The number of γ -H2AX-positive cells was assessed using the CellSearch system in conjunction with γ -H2AX-AF488 antibody staining and was expressed as a percentage of γ -H2AX positive CTCs.

γ -H2AX-positive CTCs were identified in all post-treatment samples and persisted during treatment, although there was individual variability in the number of CTCs collected post-treatment. However, an assay to quantify γ -H2AX expression in individual CTCs is currently not available.

A feasibility study was therefore conducted to quantify differences in γ -H2AX signal intensity in colon cancer cells pre- and post-treatment using both the CellSearch System (Janssen Diagnostics) and the DEPArray System (Silicon Biosystems).

Human colon adenocarcinoma cancer cell lines were initially treated with different concentrations of oxaliplatin and SN-38 to identify the dose that induced the highest number of γ -H2AX foci/nucleus for evaluation in time course experiments (Chapter 4).

3.2. Results

3.2.1. Dose Response in HT-29 Colon Cancer Cells treated with Oxaliplatin

Dose response experiments were conducted to determine the dose and time of exposure to oxaliplatin and SN-38 needed to induce significant levels of γ -H2AX. This information was required for subsequent time course experiments (Chapter 4).

As detailed in Chapter 1, oxaliplatin, a platinum-based chemotherapy agent, exerts its cytotoxic effect in colorectal cancer cells mostly by inducing DNA damage [274] and apoptosis. Once oxaliplatin is activated in the plasma to form di chloro (DACH) platinum compounds, it exerts the majority of its effects on genomic DNA, creating adducts and inducing DSB through three types of crosslinks: DNA intra-strand crosslinks, DNA inter-strand crosslinks, and DNA–protein crosslinks.

The kinetics of oxaliplatin-induced DNA damage was investigated in a previous study [266] by analysis of the expression levels of phospho-p53 (Ser-15) and γ -H2AX. Oxaliplatin treatment induced phosphorylation and upregulation of γ -H2AX in a concentration- and time-dependent manner in human HCT-116 colorectal cancer cells and was found to be associated with p53-dependent and independent pathways, but not with G2/M or S phase arrest.

Expression levels of γ -H2AX were measured in HT-29 cell lines in order to fully characterize the DNA damage response during oxaliplatin treatment (Section 2.3–2.4, Figure. 3.1). γ -H2AX accumulation was detectable in oxaliplatin treated cells following 2 hours incubation and the highest peak of foci was obtained with 10 μ M of oxaliplatin, a significant increase in γ -H2AX expression was observed in all oxaliplatin treated cells compared with control treated cells (Table 3.1; Figure. 3.2). Untreated cultures also expressed phosphorylated H2AX, consistent with the fact that H2AX is normally phosphorylated during DNA replication [275].

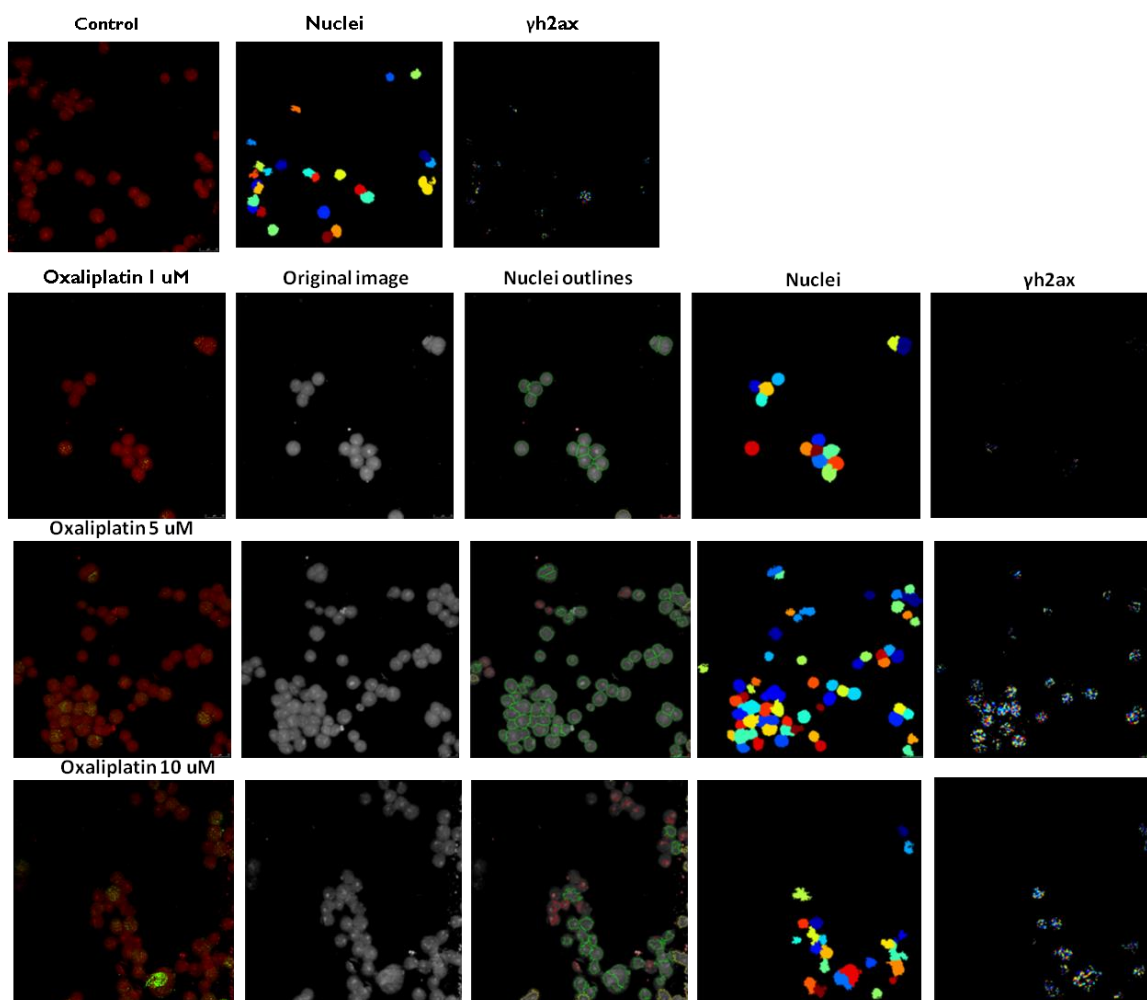


Figure 3.1: Expression levels of γ -H2AX measured in HT-29 cell lines in response to oxaliplatin treatment using CellProfiler Software. Images show the identified cells (red), the original obtained image (grey), nuclear outlines (green) over the original image, isolated nuclei (identified with different colours to identify individual nuclei), and γ -H2AX positive nuclei.

Table 3.1: Expression of γ -H2AX in HT-29 cell lines treated with oxaliplatin

	Control (oxaliplatin 0 μM)	Oxaliplatin 1 μM	Oxaliplatin 5 μM	Oxaliplatin 10 μM
No. of cells (n=1)	50	46	50	50
γ -H2AX foci	241	465	521	598
Mean γ -H2AX foci/cell	4.82	10.11	10.42	11.96
Standard deviation	7.43	10.75	9.76	14.86
T-test (versus control)		0.0034	0.0009	0.0016

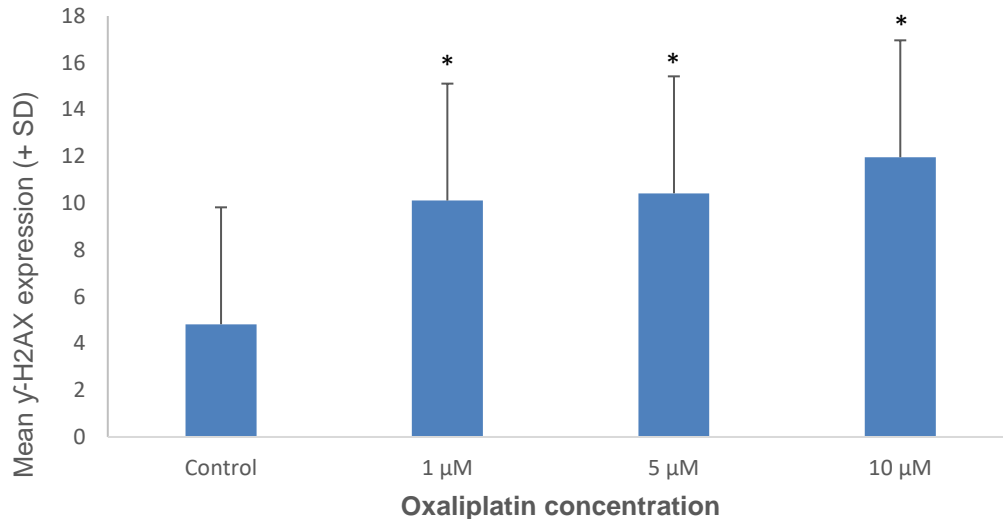


Figure 3.2: Expression levels of γ -H2AX in HT-29 cell lines treated with oxaliplatin. Results of one experiment expressed as mean foci per cell + SD from a minimum of 50 cells. Asterisks indicate a significant difference ($P < 0.05$) between treatment and control.

3.2.2. Dose Response in HT-29 Colon Cancer Cells Treated with SN-38

As discussed in Chapter 1, irinotecan (CPT-11) is an analogue of camptothecin (CPT). The mechanism of action of the pro-drug CPT-11 involves the inhibition of topo I, a nuclear enzyme involved in DNA structure preservation. The active form of CPT-11, SN-38, binds to topo I and prevents its interaction with transient DNA breaks during replication, resulting in the formation of cleavable complexes. Replication fork collision with cleavable complexes during S-phase is the major cytotoxic mechanism of topoisomerase inhibitors in dividing cells [276]. These complexes are converted to permanent DNA DSBs which activate the DNA damage checkpoint response to promote cell cycle arrest, thus preventing the replication of damaged DNA (G1/S checkpoint) or mitosis (G2/M checkpoint) [277].

HT-29 colon cancer cells were initially treated with increasing concentrations of SN-38 (1, 5, and 10 μ M). However, at the concentrations and time of exposure used, γ -H2AX levels continued to increase in treated cells with the extent of DNA damage, and it was not possible to perform statistical analysis on these samples. The continuous induction of DNA

DSBs was likely due to successive rounds of endoreduplication and attempts by each new endoreduplicated population to replicate DNA.

Subsequently, the HT-29 cell line was treated with lower concentrations of SN-38 (0.01, 0.05, and 0.5 μM) for 1 hour. $\gamma\text{-H2AX}$ accumulation was significantly increased at 1 hour in the 0.01 and 0.05 μM -treated cultures when compared with control treated cells (Figure 3.3; Figure. 3.4, Table 3.2). Untreated cultures also had minor levels of phosphorylated H2AX, consistent with the fact that H2AX is normally phosphorylated during DNA replication [275].

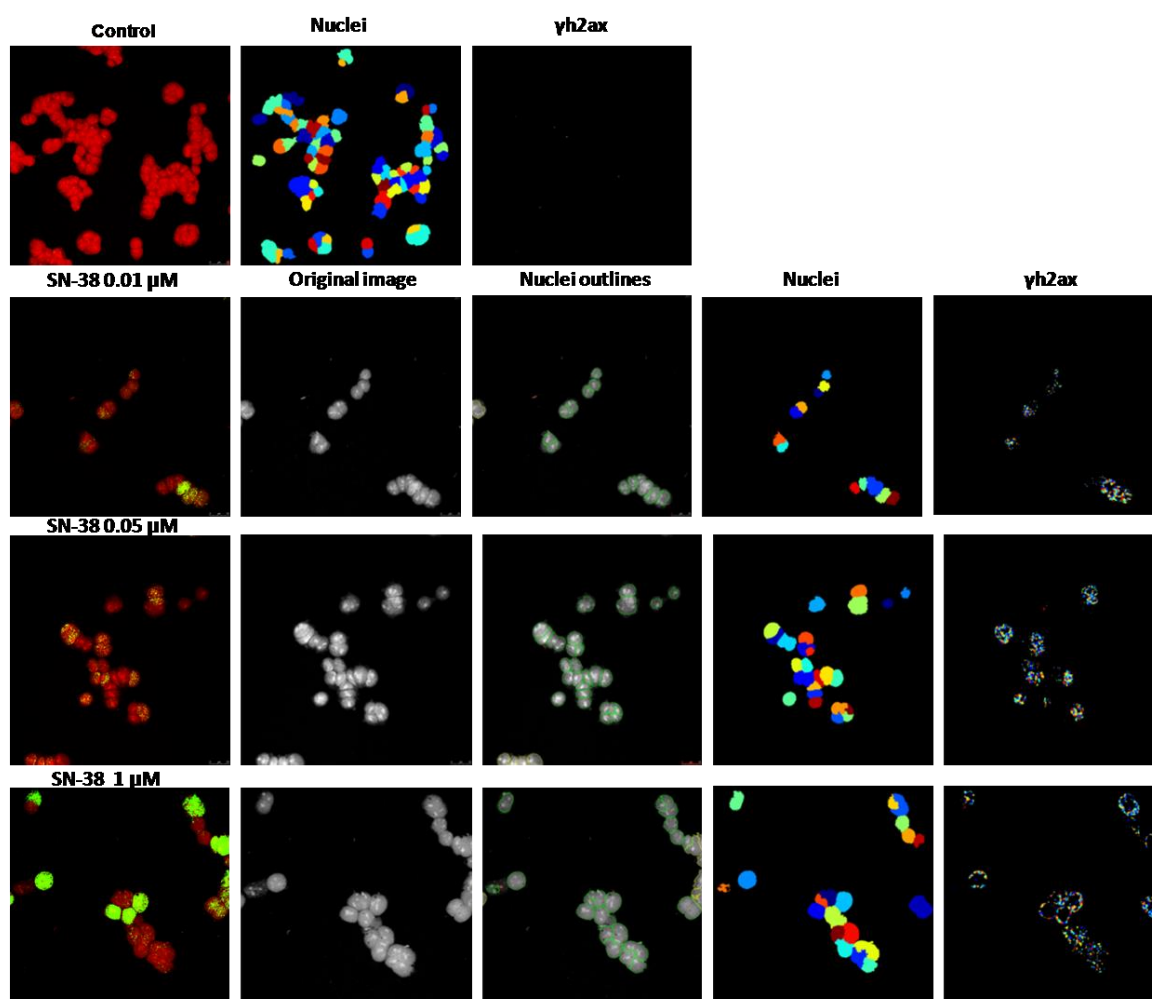
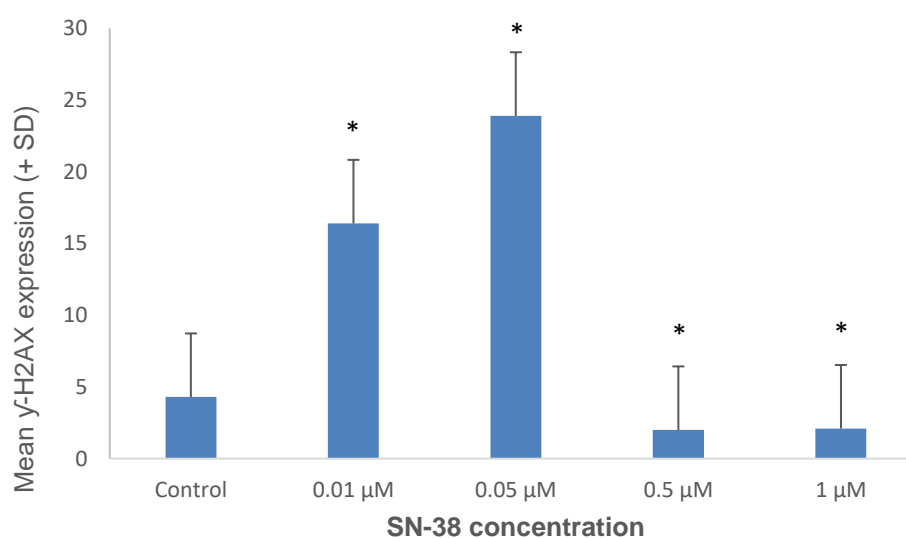


Figure 3.3: Expression levels of $\gamma\text{-H2AX}$ measured in HT-29 cell lines in response to SN-38 treatment using CellProfiler Software. Images show the identified cells (red), the original obtained image (grey), nuclear outlines (green) over the original image, isolated nuclei (identified with different colours to identify individual nuclei), and $\gamma\text{-H2AX}$ positive nuclei.

Table 3.2: Expression levels of γ -H2AX in HT-29 cell lines treated with SN-38

	Control (SN-38 0 μ M)	SN-38 0.01 μ M	SN-38 0.05 μ M	SN-38 0.5 μ M	SN-38 1 μ M
No. of cells (n=1)	50	50	50	50	50
γ H2AX foci	215	822	1196	102	104
Mean γ H2AX foci/cell	4.3	16.4	23.9	2.0	2.1
Standard deviation	6.54	6.83	5.80	1.67	1.69
T-test (versus control)		6.32^{-15}	5.81^{-29}	0.012	0.012

**Figure 3.4:** Expression levels of γ -H2AX in HT-29 cell lines treated with SN-38. Results from one experiment expressed as mean foci per cell + SD from a minimum of 50 cells. Asterisks indicate a significant difference ($P < 0.05$) between treatment and control.

3.3. Conclusions

The formation of γ -H2AX foci was investigated in human adenocarcinoma HT-29 colorectal cells by performing dose response experiments with increasing concentrations of oxaliplatin and SN-38. As shown in Figures 3.3 and 3.4, an increased number of γ -H2AX

foci were observed after treatment with oxaliplatin and SN-38, in agreement with previous studies that showed that H2AX was phosphorylated in response to DNA DSBs induced by DNA topo I cleavage complexes [276] and oxaliplatin [266]. In colorectal cancer cells, treatment with 1, 5, and 10 μM oxaliplatin for 2 hours generated more $\gamma\text{-H2AX}$ foci than in untreated cells (Figure 3.2). However, the same concentrations and time of exposure to SN-38 yielded more foci per cell; 1, 5, and 10 μM SN-38 induced diffuse DNA damage, which was detectable with immunofluorescence analysis and was due to continual DNA DSBs. It is possible that the different responses observed between the same concentrations of oxaliplatin and SN-38 in HT-29 cells is because the IC₅₀ of oxaliplatin is greater than that of SN-38 (22.17 vs 1.93, respectively [278]). Consequently, HT-29 cells were incubated with lower concentrations of SN-38 and foci were detectable and significantly increased after 1 hour of drug exposure at the 0.01 and 0.05 μM SN-38 doses, when compared with the untreated control (Figure 3.4). Based on the results of these dose escalation experiments, the final concentrations that were selected for the time course experiments (Chapter 4) were 5 μM and 0.01 μM for oxaliplatin and SN-38, respectively. The tumour suppressor p53 protein is a transcription factor inducing cell cycle arrest, senescence, and apoptosis under cellular stress. Dysregulation of *p53* tumour suppressor gene is one of the most frequent events contributing to the transformation of CRC, as well as the aggressive and metastatic features of CRC. Different types of *p53* mutations play a pivotal role in determining the biologic behaviour of CRC, such as invasive depth, metastatic site and even the prognosis of patients [279]. The HT-29 cell type has been reported to express a mutated *p53* gene whereas the HCT-116 cell line does not [280]. As the *p53* gene mutation in HT-29 cells may affect the response to treatment the time course experiments (Chapter 4) will assess both cell types.

CHAPTER 4

Time course experiments in colon cancer cell lines treated with oxaliplatin or SN-38

4.1. Introduction

In Chapter 3, the optimum concentration of oxaliplatin and SN-38 for peak induction of γ -H2AX foci was established in HT-29 human colon adenocarcinoma cancer cell lines. Using these concentrations, time course experiments were performed to establish the kinetics of γ -H2AX foci formation.

4.2. Results

4.2.1. Time Course Experiments in HCT-116 and HT-29 Colon Cancer Cells Treated with Oxaliplatin

Expression levels of γ -H2AX were measured in HT-29 and HCT-116 cell lines at different time points in order to fully characterize the DNA damage response peak during oxaliplatin treatment. Two CRC cell lines were used in these studies to allow for any differences in response to treatment or γ -H2AX expression that may occur because of the *p53* status of the cell; the HT-29 cell type has been reported to express a mutated *p53* gene whereas the HCT-116 cell line does not [280].

In response to DNA DSBs, activated ATM is reported to phosphorylate H2AX at Ser-139 [281]. The number of foci-positive cells and the intensity of γ -H2AX foci was detected at early time points following addition of the drug in both cell lines relative to their respective untreated controls (Figures 4.1–4.3 and 4.5–4.7, Table 4.1) and remained detectable throughout the experimental period. In HCT-116 cells, within 1 hour of treatment, punctate foci rapidly peaked and were maintained until 6 hours post dose, after which a gradual decline of γ -H2AX foci was observed (Figure. 4.2). After 26 hours of treatment, γ -H2AX foci largely disappeared and returned to the baseline distribution. In HT-29 cells, a rapid increase of punctate foci was observed by 1 hour post treatment which gradually increased to peak 6 hours post treatment, after which a gradual decline of γ -H2AX foci was observed.

At 26 hours post treatment γ -H2AX foci were still increased compared with baseline (Figure. 4.4).

Foci represent active DNA repair sites [282] and γ -H2AX loss or dephosphorylation correlates time-wise with DNA repair [214]. Untreated cultures also expressed phosphorylated H2AX, consistent with the fact that H2AX is normally phosphorylated during DNA replication (18).

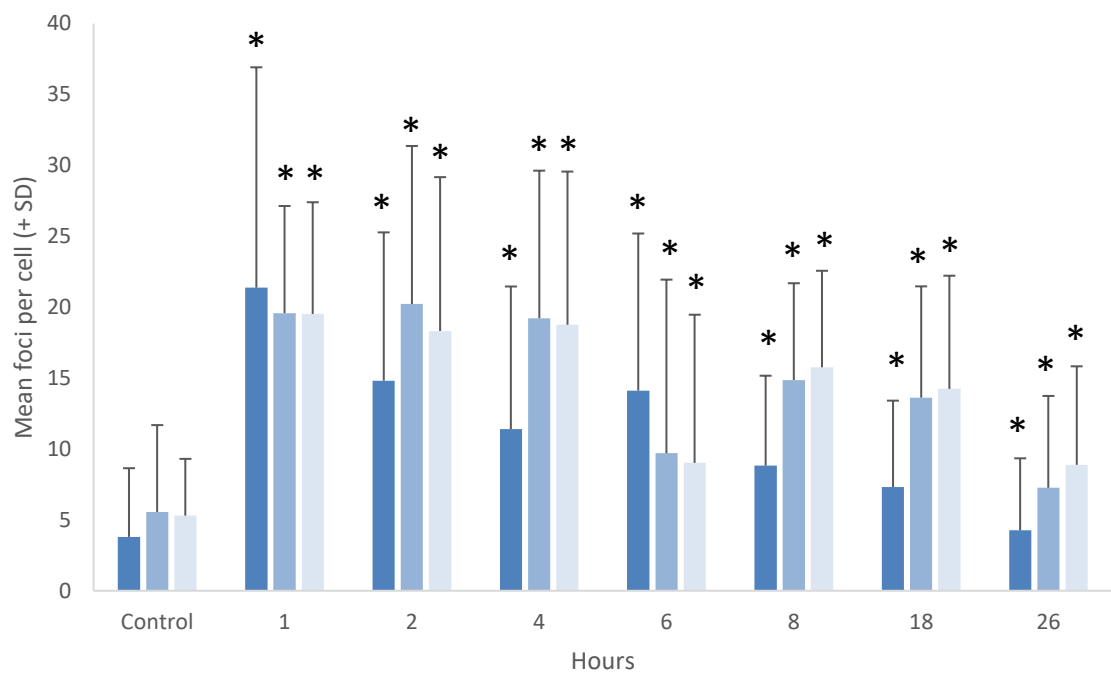


Figure 4.1. Intra-assay variation in γ -H2AX foci induction and detection in HCT-116 cells treated with 5 μ M oxaliplatin. Triplicate validation of the same experiment shown with blue shading. Results are expressed as mean foci per cell + SD from a minimum of 50 cells. Asterisks indicate a significant difference ($P < 0.05$) between time point and control for corresponding experiment.

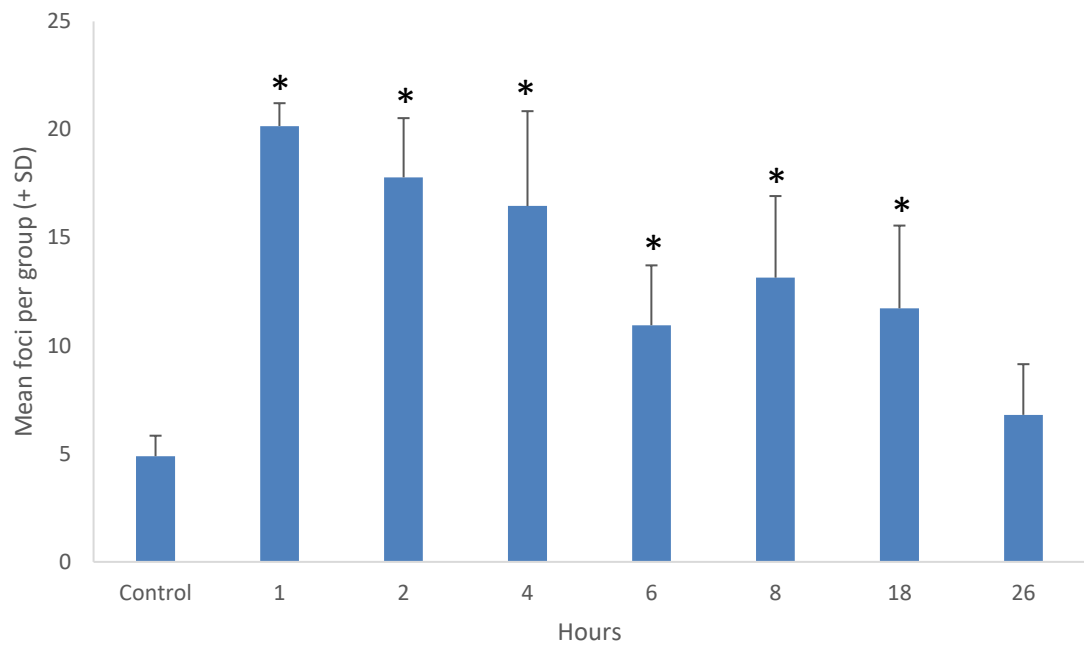


Figure 4.2. Inter-assay variation in γ -H2AX foci induction and detection in HCT-116 cells treated with 5 μ M oxaliplatin. Results are expressed as mean (of triplicate experiments shown in Figure 4.1) foci per group + SD. Asterisks indicate a significant difference ($P < 0.05$) between time point and control.

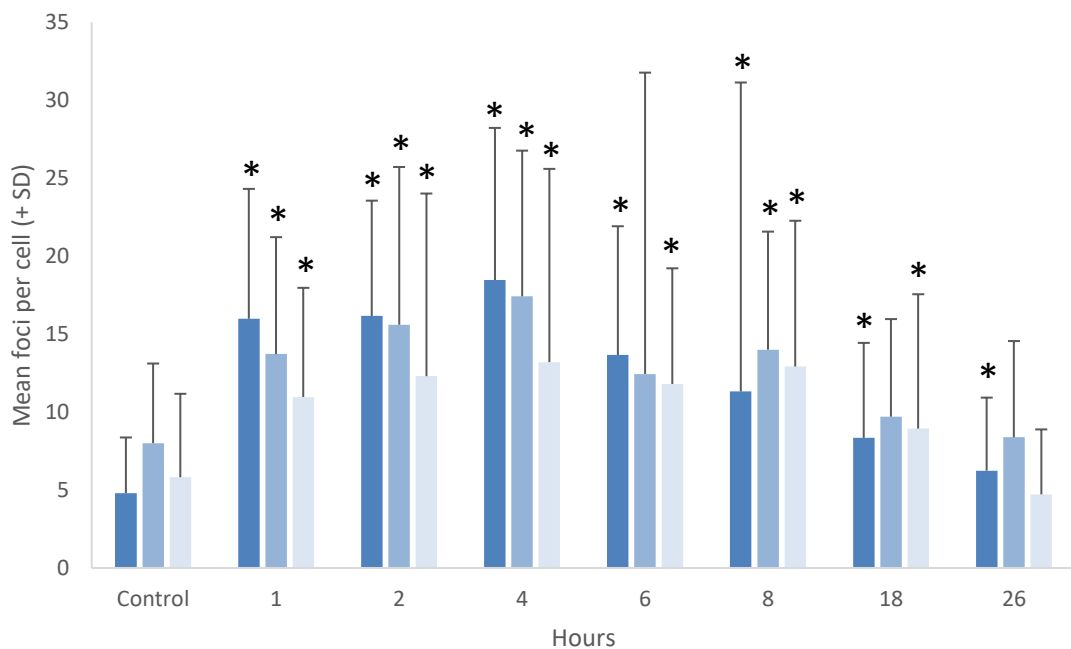


Figure 4.3. Intra-assay variation in γ -H2AX foci induction and detection in HT-29 cells treated with 5 μ M oxaliplatin. Triplicate validation of the same experiment shown with blue shading. Results are expressed as mean foci per cell + SD from a minimum of 50 cells. Asterisks indicate a significant difference ($P < 0.05$) between time point and control for corresponding experiment.

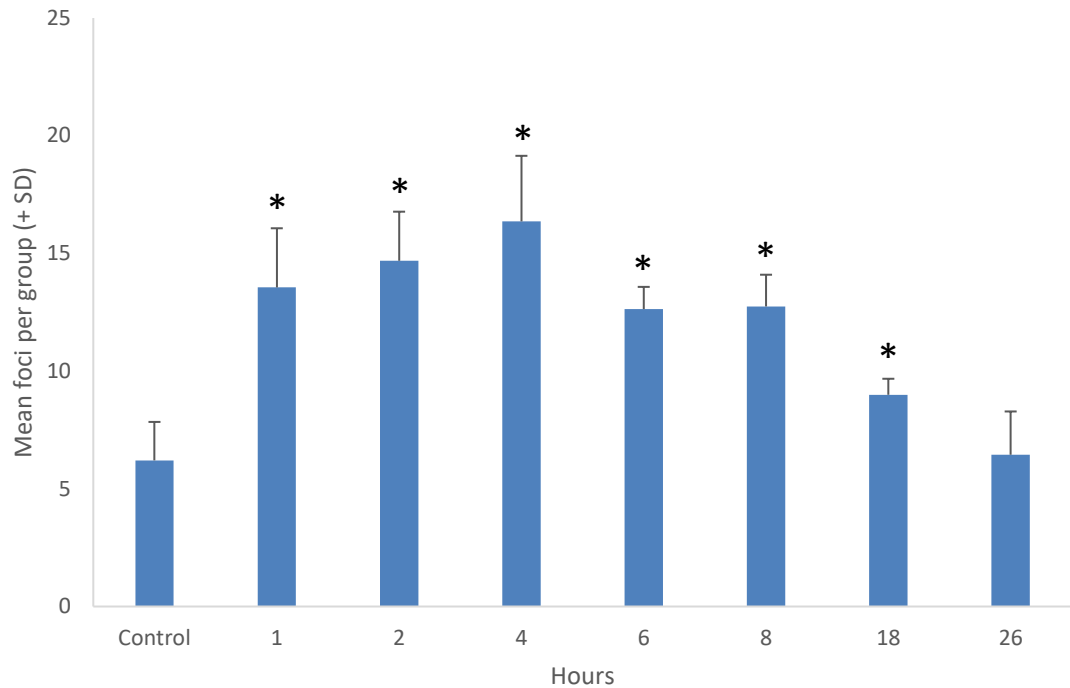


Figure 4.4. Inter-assay variation in γ -H2AX foci induction and detection in HT-29 cells treated with 5 μ M oxaliplatin. Results are expressed as mean (of triplicate experiments shown in Figure 4.3) foci per group + SD. Asterisks indicate a significant difference ($P < 0.05$) between time point and control.

4.2.2. Time Course Experiments in HT-29 and HCT-116 Colon Cancer Cells Treated with SN-38

Expression levels of γ -H2AX were also measured in HT-29 and HCT-116 cell lines at different time points in order to fully characterize the DNA damage response peak following SN-38 treatment. As with oxaliplatin treated cells, the number of foci-positive cells and the intensity of γ -H2AX foci was detected at early time points following addition of the SN-38 in both cell lines relative to their respective untreated controls (Figures 4.5 and 4.7, Table 4.1) and remained detectable throughout the experimental period. In HCT-116 cells, within 1 hour of treatment, punctate foci rapidly peaked and increased until 6 hours post dose, after which a gradual decline of γ -H2AX foci was observed (Figure 4.6). At 26 hours post treatment γ -H2AX foci were still increased compared with baseline. In HT-29 cells, a rapid increase of punctate foci was observed by 1 hour post treatment which was maintained

until 6 hours post treatment, after which a gradual decline of γ -H2AX foci was observed (Figure 4.8).

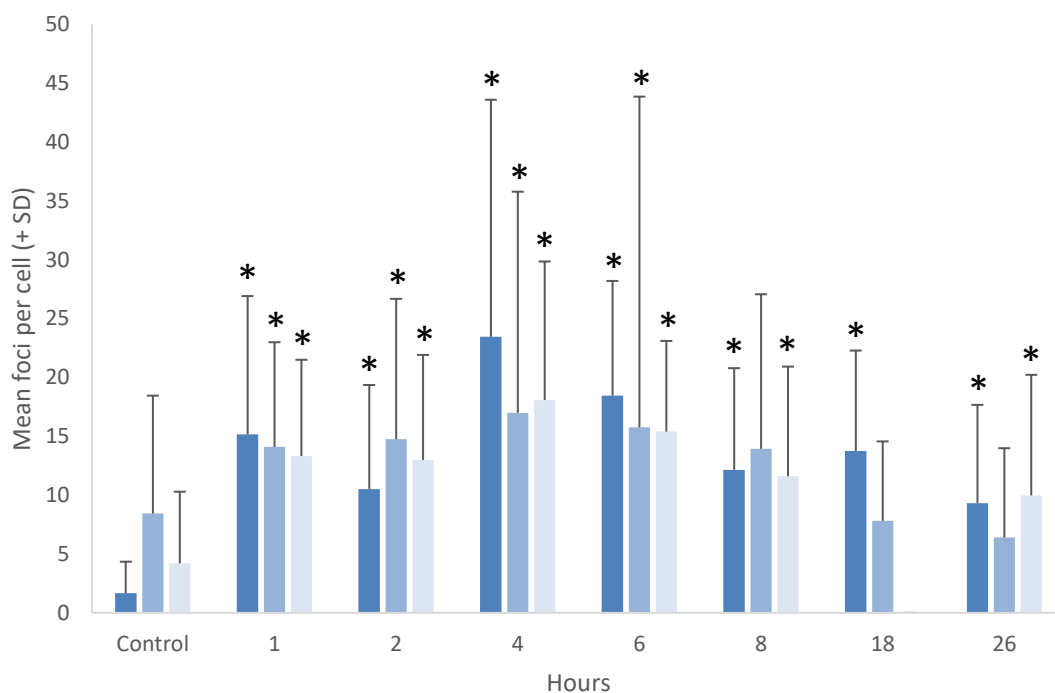


Figure 4.5. Intra-assay variation in γ -H2AX foci induction and detection in HCT-116 cells treated with 0.01 μ M SN-38. Triplicate validation of the same experiment shown with blue shading. Results are expressed as mean foci per cell + SD from a minimum of 50 cells. Asterisks indicate a significant difference ($P < 0.05$) between time point and control for corresponding experiment.

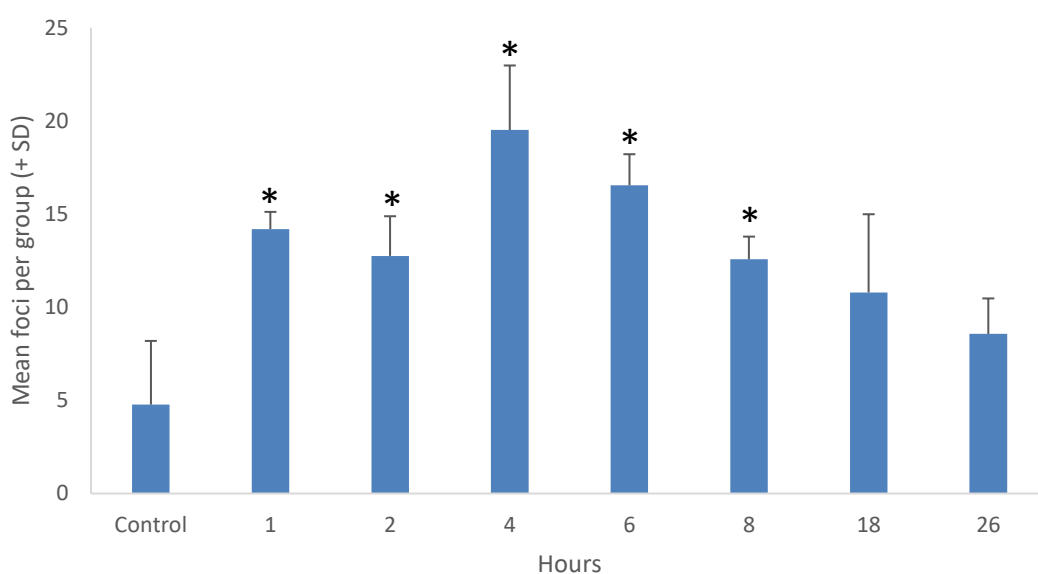


Figure 4.6. Inter-assay variation in γ -H2AX foci induction and detection in HCT-116 cells treated with 0.01 μ M SN-38. Results are expressed as mean (of triplicate experiments shown in Figure 4.5) foci per group + SD. Asterisks indicate a significant difference ($P < 0.05$) between time point and control.

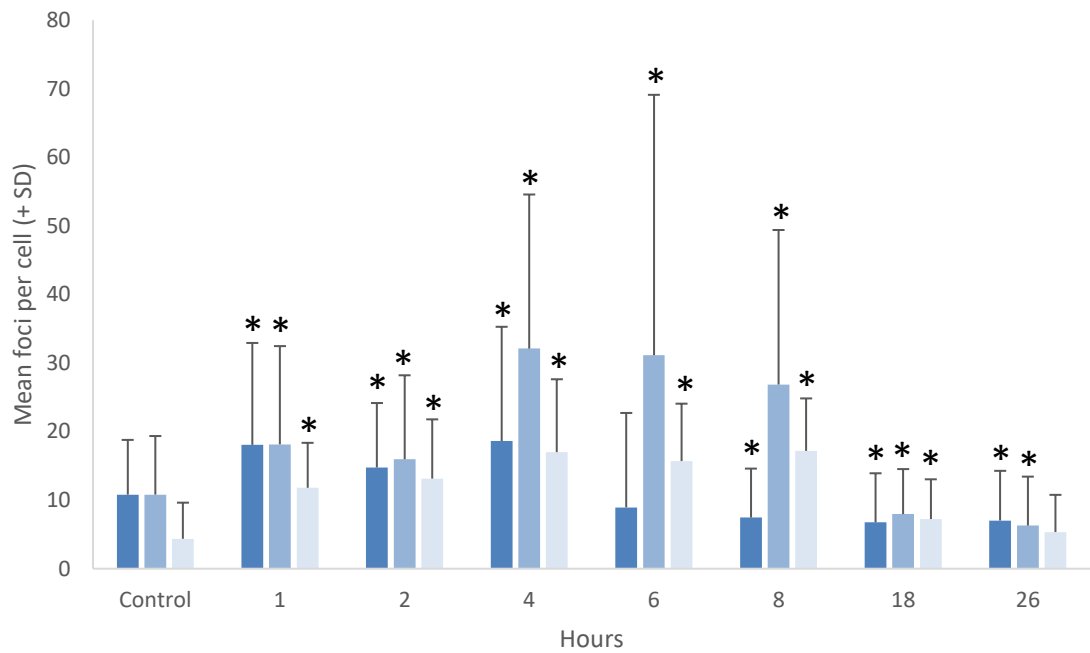


Figure 4.7. Intra-assay variation in γ -H2AX foci induction and detection in HT-29 cells treated with 0.01 μ M SN-38. Blue shading represents repeated validation of the same experiment. Results are expressed as mean foci per cell + SD from a minimum of 50 cells. Asterisks indicate a significant difference ($P < 0.05$) between time point and control for corresponding experiment.

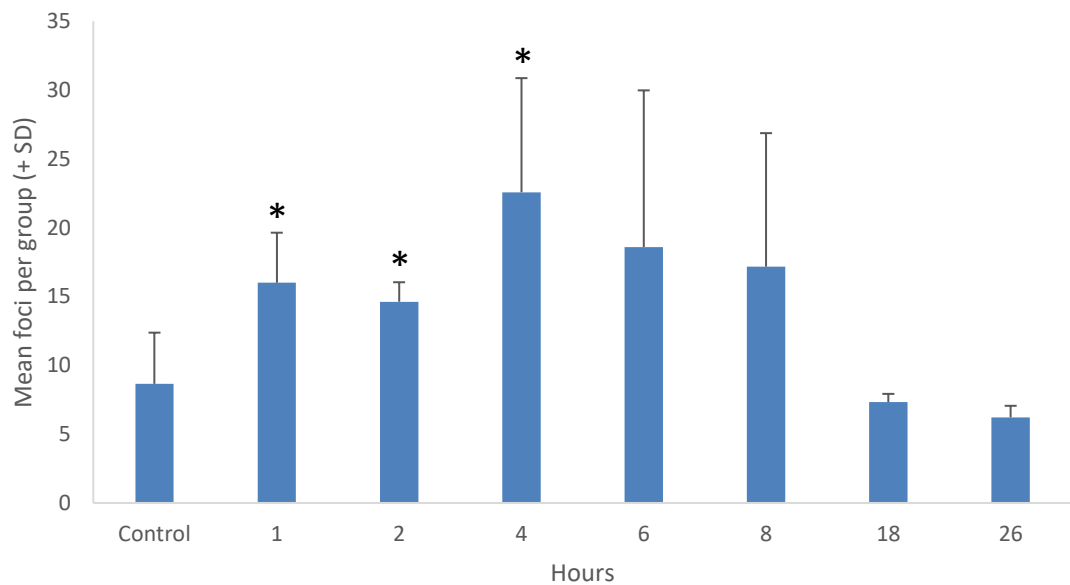


Figure 4.8. Inter-assay variation in γ -H2AX foci induction and detection in HT-29 cells treated with 0.01 μ M SN-38. Results are expressed as mean (of triplicate experiments shown in Figure 4.7) foci per group + SD. Asterisks indicate a significant difference ($P < 0.05$) between time point and control.

Table 4.1. Inter-assay variation in γ -H2AX foci induction and detection following time course experiments*

		Hours						
	Control	1	2	4	6	8	18	26
HCT-116 cells treated with 5 μM oxaliplatin								
Mean foci/group	4.89	20.16	17.79	16.46	10.95	13.15	11.73	6.80
Standard deviation	0.95	1.06	2.74	4.39	2.77	3.77	3.83	2.34
T-test		<0.0001	0.004	0.020	0.025	0.028	0.041	0.146
HT-29 cells treated with 5 μM oxaliplatin								
Mean foci/group	6.21	13.55	14.69	16.36	12.63	12.75	8.99	6.45
Standard deviation	1.63	2.51	2.09	2.79	0.94	1.35	0.68	1.84
T-test		0.009	0.003	0.005	0.004	0.003	0.041	0.437
HCT-116 cells treated with 0.01 μM SN-38								
Mean foci/group	4.77	14.19	12.75	19.51	16.54	12.57	10.79	8.57
Standard deviation	3.42	0.92	2.13	3.46	1.67	1.22	4.20	1.91
T-test		0.017	0.017	0.003	0.007	0.023	0.120	0.094
HT-29 cells treated with 0.01 μM SN-38								
Mean foci/group	8.65	16.00	14.62	22.57	18.59	17.17	7.32	6.22
Standard deviation	3.72	3.64	1.42	8.29	11.38	9.70	0.60	0.84
T-test		0.035	0.047	0.042	0.133	0.132	0.300	0.187

*Data are shown for triplicate experiments except for HCT-116 cells treated with 0.01 μ M SN-38 at 18 hours which are from duplicate experiments.

4.3. Conclusions

γ -H2AX foci formation was investigated in human adenocarcinoma HT-29 and HCT-116 colorectal cells by performing dose response experiments using increasing concentrations of oxaliplatin and SN-38 (Chapter 3; HT-29 cells only) and time course experiments to study temporal differences in γ -H2AX signal intensity post treatment.

As shown in Figures 4.1–4.8, an increased number of γ -H2AX foci formations were observed after treatment of the cells with oxaliplatin and SN-38 in agreement with previous studies [283].

In colorectal cancer cells, treatment with 5 μ M oxaliplatin and 0.01 μ M SN-38 at different time points (0, 1, 2, 4, 6, 8, 18 and 26 hours) caused a sustained increase of γ -H2AX foci positive cells detected from early time points in both cell lines relative to their respective untreated controls, confirmed by three inter and intra-assay validations (Figures 4.1–4.8, Table 4.1). The rise of foci was observed between two and six hours post-treatment, after which they gradually decreased returning close to the baseline distribution at 26 hours due to DNA repair.

Minor differences were observed between the two CRC cell lines in response to treatment with oxaliplatin and SN-38; in both cells, there was a rapid peak to a mean of \sim 10 foci/group in the first hour post-treatment which plateaued at a steady rate until 18 hours post-dose where the mean γ -H2AX foci/group declined to \sim 10 (7.32-11.73), and 6-8 foci/group by 26 hours post dose (6.22-8.57). Oxaliplatin and SN-38 are pharmacologically distinct and have different mechanisms of action. Various mechanisms of action are ascribed to oxaliplatin however like other platinum-based compounds, oxaliplatin exerts its cytotoxic effect mostly through DNA damage by causing DNA lesions (crosslinks), arresting DNA synthesis and through the inhibition of messenger RNA synthesis [274]. The active form of SN-38, irinotecan, inhibits the action of topo I, preventing relegation of the DNA strand by binding to the topo I-DNA complex. The formation of a cleavable drug–topo I–DNA complex results in lethal double-strand DNA breakage and cell death [284]. These differences in the mode of action of the drugs resulting in DNA damage may contribute to the minor differences in the formation of γ -H2AX foci that were nevertheless observed. As

noted previously, the genetic status of the different cell lines may also contribute to differences observed between the two cell lines used; the presence of *p53* gene mutations (as well as *BRAF* mutations) in HT-29 cells [280] may result in the cells responding to treatment differently. Indeed, differences in response to treatment have been observed for patients with *p53* mutations; in the Phase 2 EXPERT-C trial, which added cetuximab in the adjuvant setting for high-risk stage II rectal cancer patients, exploratory retrospective analysis suggested *p53* mutation status did predict benefit from cetuximab [285].

Based on the results of these experiments, we decided that the best time for CTC collection on patients would have been 2 hours post infusion of FOLFOX or FOLFIRI. This time was chosen for several reasons: 1. γ -H2AX induction was observed with both cell lines and treatments at this time point; 2. 2 hours post-infusion would avoid patients having to undergo a prolonged stay in the hospital following completion of their treatment. The amount of γ -H2AX induction 2 hours following treatment was therefore evaluated to determine if valuable data for their quantification using the CellSearch and DEPArray platform could be obtained (Chapter 5).

CHAPTER 5

Development of the Protocol for quantification of γ -H2AX intensity using the CellSearch System (Janssen Diagnostics) and the DEPArray™ System (Silicon Biosystems)

5.1 Introduction

γ -H2AX's role as a biomarker for DNA damage has been extensively studied and its utility in the clinical setting has been demonstrated by several studies [236-238, 271]. Detection of γ -H2AX foci after exposure to DNA-damaging agents is a more reliable DSB marker than other repair proteins as it is formed de novo in cells, it is far more sensitive than other methods in detecting DSBs at clinically relevant doses and allows the distinction of the temporal and spatial distribution of DSB formation. An assay to measure patient drug response at the molecular level could permit a faster assessment of patient response, without the need to wait several weeks [217, 286] for tumour response/stability using imaging techniques.

Tumour biopsies are pivotal to evaluate the effect of drugs on DNA metabolism [214]. However, the time course to evaluate PD responses would require patients to undergo several biopsies, which is unfeasible. Less invasive methods based on collection of CTCs in the bloodstream pre- and post-treatment, and the monitoring of drug on-target effects such as changes in γ -H2AX levels directly on CTCs is currently under investigation [214]. Presently, several techniques for γ -H2AX detection are available including constant or pulsed field gel electrophoresis, comet assays [251], flow cytometry, western blotting [262] and immunofluorescence with antibodies directed against both H2AX and γ -H2AX. However, fluorescence microscopy is the preferred and most sensitive method for γ -H2AX detection for clinical applications as it is able to detect a single DSB [244]. Analysis by microscopy may discriminate γ -H2AX responses induced by different drugs based on the different timing of interference with DNA replication and, unlike flow cytometry, can distinguish foci from the background allowing the analysis of tissue samples rather than single cells. Other types of assays, such as chemoluminescent-based detection [287] and

whole cell ELISA [288] also utilise cell and tissue extracts, however they are not yet available in the clinic setting.

There is therefore an ongoing demand for the development of a high throughput γ -H2AX foci-counting system for clinical utilisation to allow a faster analysis and automated microscopic examination [214, 244, 288].

γ -H2AX induction has recently been studied in cancer cells treated with different chemotherapy agents and in CTCs from patient blood samples processed using the CellSearch® System in conjunction with γ -H2AX-AF488 antibody staining. γ -H2AX signal was detected as percent γ -H2AX-positive CTCs per total CTCs recovered following chemotherapy [214]. However, at present this is still an unmet need since the current methods available for the detection of DNA damage in patient samples have showed a limited applicability in the clinic to monitor tumour response to chemotherapy.

It is still unknown whether γ -H2AX in CTCs will correlate with clinical efficacy, and clinical trials are currently investigating the correlation between drug effects on disease progression to γ -H2AX-positive CTCs. Examples of such studies include NCT00576654 and NCT01386385 which are evaluating the effect of veliparib in combination with chemotherapies in advanced solid tumours or advanced non-small cell lung cancer, respectively. Based on the current data, and on the lack of a system that allows a quantification of the γ -H2AX signal induction post treatment in CTCs from patients with mCRC, we investigated the feasibility of a quantitative assay using both the CellSearch System (Janssen Diagnostics) and the DEPArray System (Silicon Biosystems) with the aim of measuring and identifying differences in signal intensity caused by induction of γ -H2AX in treated and untreated cancer cells, for use as an early indicator of response to treatment.

5.2. Validation of the CellSearch System to detect γ -H2AX induction in treated CRC cells spiked into peripheral blood from healthy donors: Results

Validation of the assay developed for the detection of γ -H2AX on CTCs using the CellTracks Autoprep System and the CellTracks Analyzer II was previously performed in the laboratories of the UCL ECMC GCLP Facility, UCL Cancer Institute between 1 – 30 June 2013 (Section 2.8.3) by Victoria Spanswick, Leah Ensell and Helen Lowe using healthy donor blood that was spiked with untreated, topotecan treated or X-ray irradiated HT-29 cells. These experiments have been included into this thesis as they provide important background information for the subsequent work that was performed on blood samples from patients with CRC (Chapter 6). Figure 5.1 shows an example of the images that are provided from the CellTracks Analyzer II. The CellTracks Analyzer II also provides data on the overall number of CTCs present within the sample as well as the number and percentage of CTCs which are positive for γ -H2AX. Tables 5.1–5.4 show the data from the spiked peripheral blood of three healthy volunteers. The data demonstrate that the methodology used can consistently identify the overall number of CTCs, with the overall number over all the spiked experiments ranging from 266–399 with 0–2 cells identified in untreated control blood samples. For blood spiked with only HT-29 cells, low numbers of CTCs positive for γ -H2AX were detected, all of which were below the pre-defined threshold of $\leq 3\%$ positive for γ -H2AX. In blood that was spiked with HT-29 cells X-ray irradiated or treated with topotecan had CTCs positive for γ -H2AX above the pre-defined acceptance threshold of $\geq 10\%$ positive for γ -H2AX.

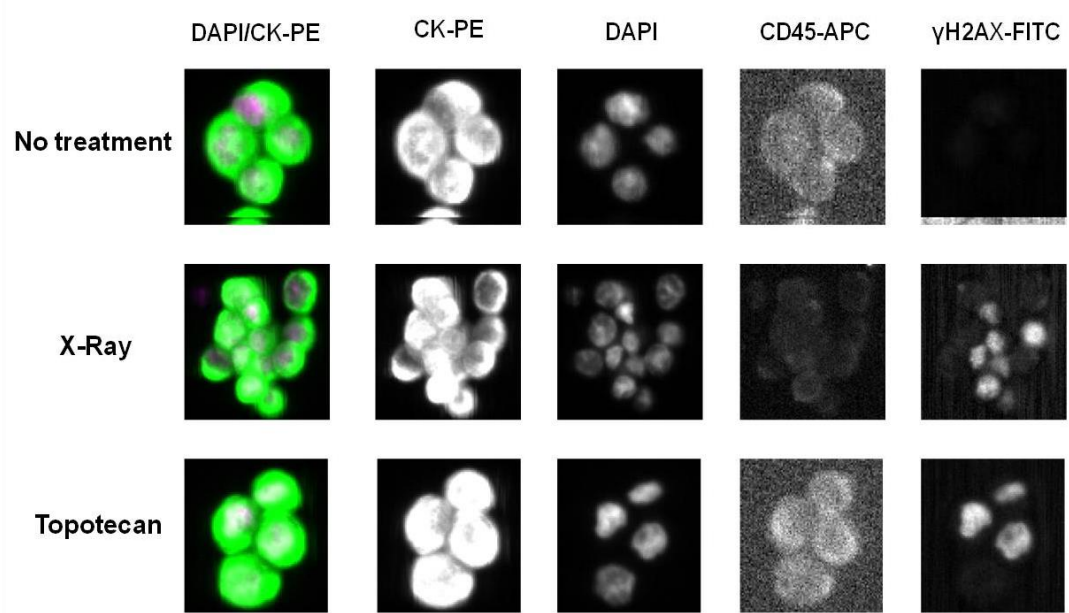


Figure 5.1: Detection of γ -H2AX induction in whole blood samples spiked with HT-29 treated tumour cells using the CellSearch Analyzer II. HT-29 cells were treated with either 5 Gy X-ray (30 minutes incubation) or 1 μ M topotecan (2 hour incubation) to allow maximum γ -H2AX induction. Cells were stained with anti- γ -H2AX antibody.

Table 5.1 Validation run 1 results

Sample ID	γ H2AX-AF488 antibody concentration	Number of tumour cells	Unassigned events	Tumour cells positive for γ -H2AX	Tumour cells positive for γ -H2AX (%)
Blank	n/a	1	58	n/a	n/a
HT-29	57 μ g/mL	339	148	9	2.65
Topotecan	57 μ g/mL	399	189	115	28.82
X-ray	57 μ g/mL	326	168	110	33.74

Table 5.2 Validation run 2 results

Sample ID	γ H2AX-AF488 antibody concentration	Number of Tumour Cells	Unassigned events	Tumour cells positive for γ -H2AX	Tumour cells positive for γ -H2AX (%)
Blank	n/a	0	29	n/a	n/a
HT-29	57 μ g/mL	266	148	7	2.63
Topotecan	57 μ g/mL	312	124	141	45.19
X-ray	57 μ g/mL	391	130	168	42.97

Table 5.3 Validation run 3 results

Sample ID	γ H2AX-AF488 antibody concentration	Number of tumour cells	Unassigned events	Tumour cells positive for γ -H2AX	Tumour cells positive for γ -H2AX (%)
Blank	n/a	2	69	n/a	n/a
HT-29	57 μ g/mL	350	181	8	2.29
Topotecan	57 μ g/mL	370	156	132	35.68
X-Ray	57 μ g/mL	382	108	134	35.08

Table 5.4 Combined validation run results

Sample ID	γ H2AX-AF488 antibody concentration	Mean number of tumour cells	Mean unassigned events	Mean (+/- SE) tumour cells positive for γ -H2AX	Tumour cells positive for γ -H2AX (%)
Blank	n/a	1	52	n/a	n/a
HT-29	57 μ g/mL	318	159	8 (0.6)	2
Topotecan	57 μ g/mL	360	156	129 (7.6)	37
X-Ray	57 μ g/mL	366	135	137 (16.8)	37

5.2.1. Validation of the CellSearch System to detect γ -H2AX induction in treated CRC cells spiked peripheral blood from healthy donors: Conclusions

Acceptance criteria for detection of γ -H2AX, as set by the NCI, state that untreated cells must be $\leq 3\%$ positive for γ -H2AX and treated cells must be $\geq 10\%$ positive for γ -H2AX. All three validation runs performed met these pre-defined validation criteria confirming that the γ -H2AX antibody used for these experiments (Anti-phospho-Histone H2A.X (ser139), clone JBW301, FITC conjugated) is appropriate for use with the CellSearch Circulating Tumour Cell (CTC) Kit and the CellTracks Autoprep System at a concentration of 57 $\mu\text{g}/\text{mL}$ (Stock antibody diluted 1:32 in Bond primary antibody diluent). Exposure for the fourth channel should be set at 3 seconds on the CellTracks Analyzer II.

5.3. Colon cancer cells treated with oxaliplatin and SN-38 enriched by CellSearch System and analysed by DEPArray using two exposure times

DR and TC experiments were performed on HT-29 and HCT-116 colon cancer cells to define the dose of oxaliplatin and SN-38, and the time required to obtain the highest peak of γ -H2Ax induction in colon cancer cells as described in Chapters 3 and 4. To reproduce the analytical process for CTCs, we evaluated γ -H2AX signal using both the CellSearch System (Janssen Diagnostics) and the DEPArray System (Silicon Biosystems).

HT-29 cells (at a concentration of 8×10^4 cells/mL) were incubated with oxaliplatin 5 μM or SN-38 0.01 μM for 2 hours and 1 hour, respectively. Control cells were untreated. Cells were maintained in suspension after washing and trypsinization. Fixing, permeabilisation, blocking, and staining with γ -H2AX antibody were performed as described in Chapter 2.

5.3.1. CTC Detection and Analysis on CellTracks Analyser II

The CellTracks Analyser II displays CTC candidate Images generated after a blood specimen has been processed on the CellTracks Autoprep System. A CTC was defined as being positive for CK-PE and nuclear staining (DAPI), negative for leukocyte staining

(CD45-APC) and as having the correct morphology, and CK-PE and DAPI overlay to be characterised as a tumour cell.

Treated and untreated HT-29 colon cancer cells were spiked into 7.5 ml of peripheral bloods that was mixed and combined with 6.5 ml of dilution buffer (CellSearch CTC Kit) and processed on the CellTracks Autoprep system along with CTC Control Sample (CellSearch CTC Control Kit). The γ -H2AX antibodies used in this experiment (Mouse anti-H2AX monoclonal primary antibody and Goat anti-mouse Alexa Fluor 488 IgG secondary antibody) were not the recommended antibodies for the CellSearch System, however they were compatible for analysis in the 4th channel (FITC) of the CellSearch platform.

Once on the CellTracks Autoprep system, the presence of CTCs was identified with the addition of the staining reagents CK-PE, DAPI, CD45-APC and permeabilisation buffer. The cartridge containing stained CTCs was then inserted into the four-colour semi-automated fluorescence microscope CellTracks Analyzer II. Images were presented in a gallery format for final cell classification and were reviewed by the operator and myself. Cells were defined as positive for γ -H2AX on the CellSearch System according to the previously validated assay. For oxaliplatin and SN-38 treated cells, 15.28% and 18.37% were classified as positive for γ -H2AX, respectively, compared with 5.10% for untreated controls (Figure 5.2).

The CellSearch Cartridge was opened, the cells were withdrawn using a 200 μ l gel-tip pre-rinsed in order to reduce cell loss and transferred to the DEPArray machine. This process involved a series of cell manipulation steps such as centrifugation, volume adjustment and resuspension of the samples that could reduce the total number of final cells for analysis.

A

Sample ID: Oxaliplatin		Cartridge ID: 01290263			Patient ID: gH2AX	
Event	Frame	DAPI/CK-PE	CK-PE	DAPI	CD45-APC	gH2AX
1483	159					
1522	165					
1524	165					
1533	166					
1545	167					
1549	167					
1553	168					

B

Sample ID: SN38		Cartridge ID: 01290255			Patient ID: gH2AX	
Event	Frame	DAPI/CK-PE	CK-PE	DAPI	CD45-APC	gH2AX
43	10					
75	14					
120	16					
124	16					
131	17					
133	17					
140	17					

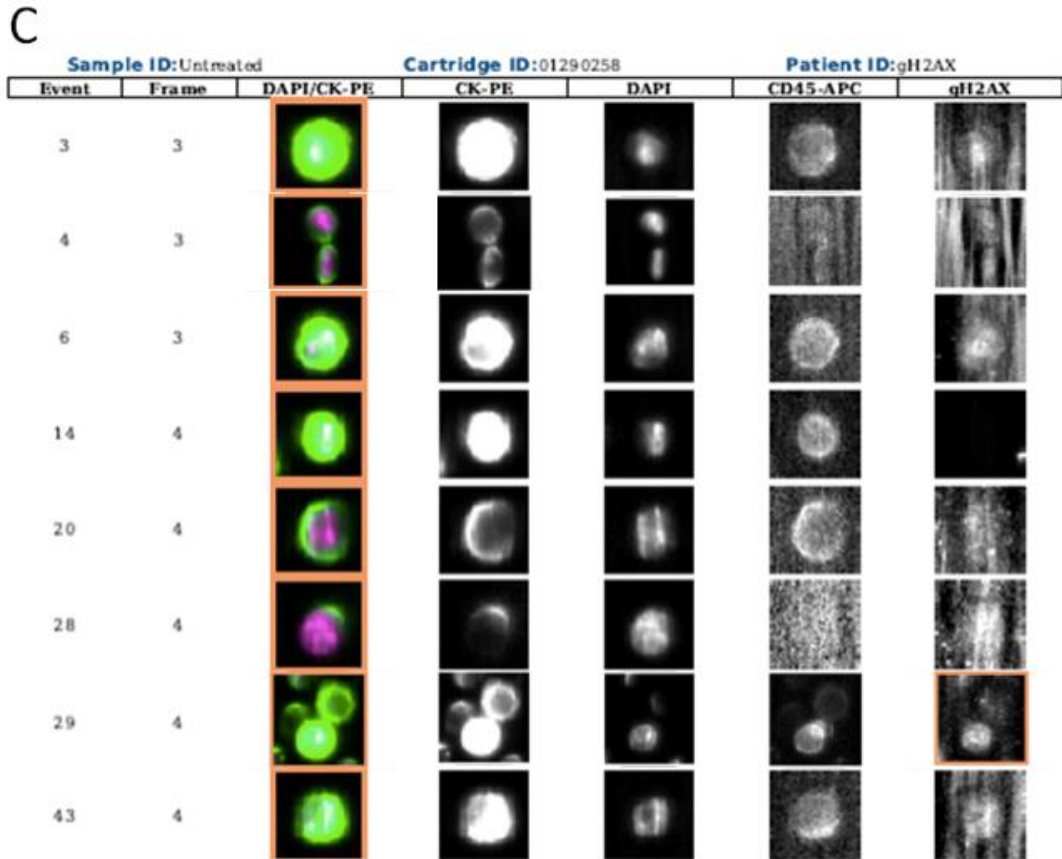


Figure 5.2. HT-29 cells treated with (A) oxaliplatin, (B) SN-38 and (C) untreated control: CellTracks Analyser CTC candidate images demonstrating the criteria for CTC analysis. DAPI/CK-PE represents cells stained with CK-PE with the cell nuclei (DAPI) overlaid; CK-PE represents cells stained only with CK-PE; DAPI represents cell nuclei; CD45-APC represents haematopoietic origin; γ H2AX represents staining for γ -H2AX molecular characterisation. Images with an orange box are positive for nuclear γ -H2AX staining.

5.3.2. DEPArray System Analysis of Colon Cancer Cells Treated with SN-38

The data obtained during the cell sorting executed with the DEPArray System were analysed off-line with the Cell Browser where fluorescent particles were measured and cells were selected and identified for PE+/DAPI+/APC-.

From the analysis of the first sample treated with SN-38 and run with DEPArray platform, 165 PE+/DAPI+/APC- cells were identified out of 860 particles detected. Most of the PE+/DAPI+/APC- cells did not show a clear positivity in the FITC channel resulting in a low number of cells being identified as CTCs. DEPArray analysis allowed the identification of only six putative target cells and only one cell presented a good signal background ratio (Figure 5.3, Table 5.5; id=3794-last row). The images of the other five putative target cells appeared grainy as a consequence of the low FITC signal/background ratio.

	PE	FITC	DAPI	BR	Mean Intensity	
					FITC	bgsub_FITC
cell_id = 1964 row_num = 1					2707.78	1421.43
cell_id = 1731 row_num = 2					2740.68	1470.31
cell_id = 4915 row_num = 3					2823.37	1525.99
cell_id = 148 row_num = 4					2961.17	1664.7
cell_id = 4328 row_num = 5					3050.26	1791.84
cell_id = 3794 row_num = 6					3786.51	2478.01

Figure 5.3. DEPArray images of PE+/DAPI+/APC- colon cancer cells following treatment with SN-38.

Rows show the cell ID, columns display the name of the *Channel Selection* the cell belonged to with respective values. Cells in rows one to five appear coarse as a consequence of the low FITC signal/background ratio. Cell number id=3794 (row six) presented a good signal background ratio.

Table 5.5. DEPArray signal (FITC channel) and background gray levels of PE+/DAPI+/APC- colon cancer cells following treatment with SN-38

	Cell ID					
	1964	1731	4915	148	4328	3794
Signal	~1421	~1470	~1525	~1664	~1791	~2478
Background	~1286	~1270	~1297	~1296	~1258	~1308

5.3.3. DEPArray system analysis of untreated control colon cancer cells

For this analysis, two different exposure times for the identification of the signal/background ratio of γ -H2AX (FITC) were selected:

- FITC I: 100 ms and gain 1X (standard set up used in the DEPArray System for the identification of FITC background signal)
- FITC II: 800 ms and gain 4X (to maintain CellSearch System set up).

Out of 1101 particles detected, 192 PE+/DAPI+/APC- cells were identified. FITC II measurement results were comparable with the value obtained for SN-38 treated cells. One cell (id=540) presented a good signal/background ratio (signal 3272 gray levels, background 1479 gray levels; Figure 5.4, Table 5.6), however it was comparable with the putative target cells identified in the SN-38 treated cells. The other cells showed a small difference between the signal and the background as for SN-38 treated cells.

	pe_0	fitcii_1	fitci_2	dapi_3	brightfield_4	mean_inte nsity_fitci	mean_inte nsity_fitcii	mean_inte nsity_bgsu b_fitci	mean_inte nsity_bgsu b_fitcii
cell_id = 4039 row_num = 1						395.78	3091.63	60.3	1711.43
cell_id = 3716 row_num = 2						411.64	3505.31	80.14	2083.13
cell_id = 3426 row_num = 3						383.15	2854.57	51.66	1449.29
cell_id = 540 row_num = 4						462.02	4751.27	135.53	3272.03
cell_id = 481 row_num = 5						403.88	3435.36	75.39	2022.28
cell_id = 392 row_num = 6						415.27	3619.34	82.77	2153.19

Figure 5.4: DEPAarray images of untreated PE+/DAPI+/APC- colon cancer cells. The rows show the cells ID, the columns display the name of the *Channel Selection* the cell belongs with respective values. Only one cell (id 540) showed good signal background ratio.

Table 5.6. DEPAarray signal and background gray levels of untreated PE+/DAPI+/APC- colon cancer cells

	Cell ID					
	4039	3716	3426	540	481	392
Signal	~1711	~2083	~1449	~3272	~2022	~2153
Background	~1380	~1422	~1405	~1479	~1413	~1466

In this control experiment FITC II could not be taken into account because it was not introduced during the analysis of the SN-38 treated cells, and in the oxaliplatin treated cells (data not shown) the FITC II was not saved and selected for analysis, therefore the data of FITC I and FITC II in positive and negative controls were not available for comparison.

The validation of the DEPArray analyses by Silicon Biosystems detailed in this section are shown in Table 5.7.

Table 5.7. Validation of the DEPArray analysis by Silicon Biosystems

	Sample 1 (treated with SN-38)	Sample 2 (control)
No. particles detected	860	1101
No. particles PE+/DAPI+/APC-	165	192
No. cells with good signal/background ratio	1	1

5.3.4. Discussion and Conclusions: colon cancer cells treated with oxaliplatin and SN-38 run with the DEPArray platform after CellSearch System using two different exposure times

On the CellTracks Analyzer II, the cell cartridges along with the control cartridge were scanned displaying tumour cells positive for cytokeratin and DAPI, which were reviewed by two trained laboratory staff, myself and Silicon Biosystems. CTCs were identified based on morphology, positivity for CK-PE and DAPI and negativity for CD45-APC. The CellTracks Analyzer II presented the images with overlays of CK-PE and DAPI signals to show whether the nuclear and cytokeratin staining were consistent with a tumour cell. The objects in the CK-PE filter channel were required to be a round or oval intact cell, at least 4 microns in diameter, a nuclear area smaller than the cytoplasmic area and more that 50% of the nucleus needed to be visibly surrounded by the cytoplasm. It was however possible for an image to appear very bright as results of a spectral spillover in the CK-PE channel creating a visible cytoplasmic image in the CD45-APC channel; if this occurred it could still be classified as a tumour cell if it was negative for CD45 and positive for CK-PE, differentiating the cell from leukocytes that were positive for CD45-APC and DAPI but

negative for CK-PE. Artefacts were recognised as appearing with the same shape in all channels.

The rate of γ -H2AX positive cells after treatment with oxaliplatin or SN-38 and CellSearch analysis was low: 177 cells out of the 1158 (15.28%) cells treated with oxaliplatin and 217 cells out of 1181 (18.37%) cells treated with SN-38 were detected as being γ -H2AX positive compared with 5.10% for the untreated controls. In many of the positive cells, the stain for γ -H2AX was faint (Figure 5.2 [A-C]). A possible explanation for this is 1. the use of different treatment protocols for the fixation and staining of the cells, and 2. the different antibodies (Mouse anti-H2AX monoclonal primary antibody (Merck Millipore) and Goat anti-mouse Alexa Fluor 488 IgG secondary antibody (Life Technologies Ltd.) rather than the anti-phospho-Histone H2A.X (ser139), clone JBW301, FITC conjugated (Millipore) normally used and validated for γ -H2AX detection by CellSearch; however, the antibodies were compatible for analysis in the 4th channel (FITC) of the CellSearch platform.

The CellSearch System allows detection of the FITC stain in the nuclei of the cells if they were γ -H2AX positive, but the distinct foci were not visible due to the low magnification limitation of the CellSearch System platform (20x).

The parameter selection process of the DEPArray 'Sorting Mode' was initially set as 'Standard'. Optimal exposure time (μ s) for label detection and the gain were set up as per protocol (Section 2.9.2). The Filter Wheel was set at the default value and the FITC was selected for the event detection. Fluorescent channels were chosen for analysis of images through a ROI in correspondence to the label positivity that was further processed and displayed at the Cell Browser. Exposure time and gain parameters for signal detection were displayed on a Gray Level Histogram. Frame by frame analysis of the intensity of the detected signals was performed through image visualisation modalities that distinguished background signal from positive signals. The Chip Scan setting was chosen for the fluorescence channels and the exposure time and gain (noise to background ratio) were set for each channel. During image analysis, the images acquired from the chip scan were further counted, their position inside the chip was calculated and morphological and intensity measurements extracted from the scanned images. The presence of cell debris

or large cell clusters were evaluated as this could potentially decrease the success of cell manipulation within the system and the number of total cells loaded in the DEPArray A300K cartridge. The chip was scanned using fluorescence and the bright field channels were set allowing the images (events) acquired to be counted and to extract morphological and intensity measurements from the scanned images. The selected cells were visually checked to avoid false objects in the recovery chambers and detection was changed as required.

This initial experiment was performed to verify the workflow on the DEPArray system and the exposure time and gain (noise to background ratio) was initially set up as required and checked for each channel.

Events were detected based on an image threshold algorithm (or detection engine) and the particle geometry intensity was analysed in the image gallery and calculated based on the intensity of fluorescence signals. Analysis was performed in all fluorescence channels to obtain correct measurements for each filter (Figures 5.3–5.4). Cells were sorted based on different characteristic such as intensity fluorescence, morphological trait and intensity parameters.

Initially, it was decided to set up the mean intensity with the background subtracted to provide an estimation of the ratio of the signal to background, indicating how much the cells contrast with the background. The particles captured were filtered by the histogram analysis mode using a histogram graph. The input populations and their parameters were plotted, and the output sub-population was selected reducing the number of particles that needed to be visually examined in the table analysis mode, representing the particles that were captured by the dielectric field (low APC signal, high FITC signal and high circularity FITC). The scatter plot analysis mode was used to display the gated subpopulation (*In Cage*), as a collection of points in a scatter plot; plotting one parameter related to the positive marker (e.g. *mean_intensity_PE*) and the other one related to the negative marker (e.g. *mean_intensity_FITC*). Once a group was created, the individual cells were reviewed and visually confirmed that they were single cells and that they had the desired morphology. CTC and WBC groups were defined using sliders – plot of mean intensity PE

(x axis) was chosen against mean intensity APC (y axis). The desired group and table order were selected by mean intensity PE or mean intensity APC. All cells were checked to be routed successfully using the DAPI filter to confirm the presence of nuclei where cells should be located. Finally, the cells required for recovery were selected and routed to the exit chamber eliminating any sources of contaminations such as cell debris or unselected cells.

With the initial standard set up for the identification of FITC background signal (FITC I: 100 ms and gain 1X) the analysis of the SN-38 treated sample run using the DEPArray platform did not show a clear positivity in the FITC channel for most of the PE+/DAPI+/APC- cells. Only six putative target cells (Figure 5.3) were identified and only one (id=3794) showed a good signal background ratio. Therefore, we analysed the untreated control with FITC I (100 ms and gain 1X) and FITC II (800 ms and gain 4X), in order to maintain the CellSearch System set up to 3 seconds. FITC II measurement results in the untreated control cells (Figure 5.4) were comparable with the values obtained in SN-38 treated colon cancer cells (Figure 5.3), and the majority of the other cells showed small differences between the signal and the background. In this experiment FITC II could not be taken into account because it was not introduced in SN-38 or oxaliplatin cells (data not shown because the FITC II analysis was not saved and selected for analysis), therefore the data for FITC I and FITC II in positive and negative controls were not available for comparison.

With the set-up required for the identification of the FITC signal after the CellSearch scan, a clear discrimination between cells expressing or not expressing γ -H2AX was not observed due to a possible bleaching of the cells as a consequence of the cartridge scanning (Section 2.9.2.2). As a result, no difference in signal intensity between the treated and untreated cells could be found. The long exposure time and gain required increased the level of the background resulting in a low signal/background ratio.

The results from this study led to the initiation of the following study, the aim of which was to identify the most appropriate Cell Browser parameter and the actual value of scan settings to be used for the evaluation of label intensity, taking into account:

- Potential variability in signal detection due to the detection system of the machine

- Optical parameters that may require a different set-up based on the cell type and labels used for cell staining
- Reagents used for sample preparation (e.g. cell fixatives and cell permeabilisation solutions) that could give a different background level intensity
- Biological variability between samples; optimisation based on the expression level of the target protein which may differ from sample to sample
- High background due to sample preparation.

The optical parameter optimisation applied to detect discrimination between background and positive signals required different set-ups for the Cell Browser:

1. The first step was to identify the background level intensity for each channel (a range between 271 [Minimum] and 322 [Maximum] gray levels was normally detected by the DEPArray machine). This signal was considered background because the range of gray levels was narrow and the distribution of gray levels was centred in the middle of the graph. Depending on the sample type and reagents used for the sample preparation, the background level could change.
2. The second step was to identify the positive signal for each channel (a range between 274 [Minimum] and 5997 [Maximum] gray levels was normally detected by the DEPArray machine).

To detect a bright or faint signal, a short or long exposure time was indicated, respectively, and the gain should not be selected to avoid saturation of the signal. A signal was considered positive when the range of gray levels had an intensity higher than the background, which could be fainter or brighter depending on the optical parameter set-up. To achieve positive information for cell imaging, the maximum gray level should not be higher than 10000–14000 (raw data not shown). Measurements were calculated based on the intensity of fluorescence signals for every detected event and the data were analysed using the mean intensity with background subtraction parameter. Due to time constraints,

we were unable to perform additional confirmatory experiments for treated and untreated SN-38 cells.

5.4. Colon cancer cells treated with SN-38 or oxaliplatin, run directly on the DEPArray platform using two different exposure times, validated with cytospin and fluorescence microscopy

In order to investigate further the potential application of the DEPArray platform, a second experiment was performed using untreated colon cancer cells (HT-29) as a negative control, and HT-29 cells treated with oxaliplatin (5 μM) or SN-38 (0.01 μM) directly with the DEPArray platform (without pre-enrichment by CellSearch; Figure 5.5) using two different exposure times (Section 5.3.3). Cells were treated as described in Chapter 2.

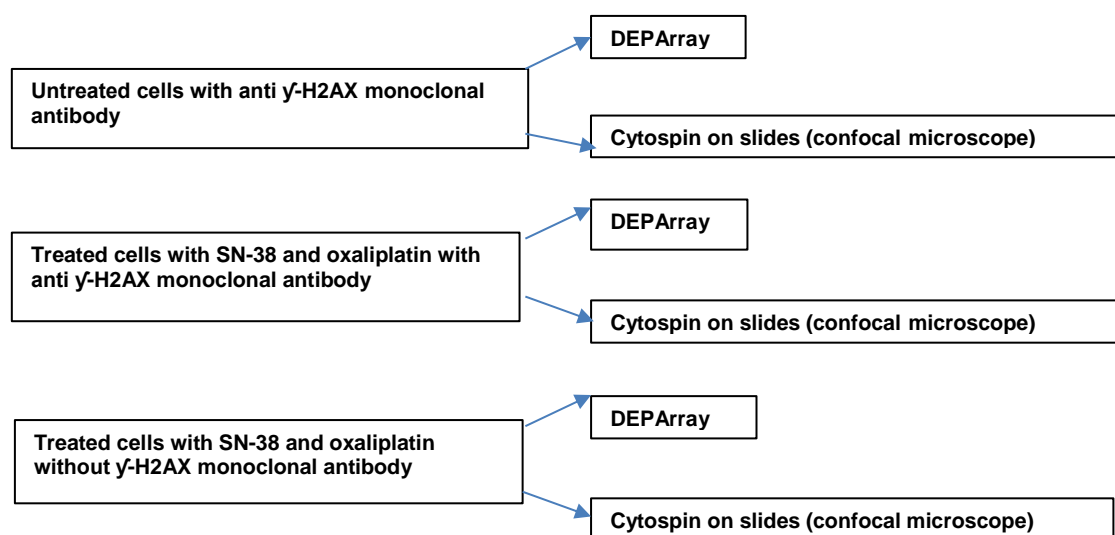


Figure 5.5. Overview of the experiments for colon cancer cells treated with oxaliplatin 5 μM or SN-38 0.01 μM and run directly on the DEPArray platform followed by validation experiments with cytospin and fluorescence microscopy

Experiments were performed in triplicate and in parallel, treating the cells exposed to the drugs with and without antibody labelling for γ -H2AX (mouse anti-H2AX monoclonal primary antibody [Merck Millipore], and goat anti-mouse Alexa Fluor® 488 IgG secondary

antibody [Life Technologies Ltd.]), followed by validation of the γ -H2AX signal with fluorescence microscopy (Leica SPE2 confocal microscope; Figure 5.6–5.7).

HT-29 cells were exposed to SN-38 and oxaliplatin with and without antibody labelling for γ -H2AX. Slides were analysed with Leica SPE2 confocal microscope and data analysis performed using CellProfiler Software (Chapter 2).

As discussed previously, the high exposure time and gain required with the validated set-up for CellSearch analysis (3 seconds) could have caused a poor fluorescent signal detection due to signal bleaching, resulting in an increased level of background and a low signal/background ratio.

NON TARGET CELLS

	Group	pe_0	fitci_1	fitcii_2	apc_3	brightfield_4	pe_fitci_5	pe_fitcii_6	mean_int ensity_fit ci	mean_int ensity_fit cii	mean_int ensity_bg sub_fitci	mean_int ensity_bg sub_fitcii
cell_id = 28 row_num = 1	TARGET								637.21	6285.06	303.72	4755.69
cell_id = 69 row_num = 2	TARGET								530.01	4902.32	198.52	3422.98
cell_id = 21 row_num = 3	TARGET								459.04	3827.92	127.55	2284.71
cell_id = 210 row_num = 4	TARGET								583.68	8945.53	251.22	7375.14

Figure 5.6: DEPAarray images of untreated PE+/DAPI+/APC- colon cancer cells (HT-29).

The rows show the cell ID, the columns display the name of the Channel *Selection* the cell belongs with respective values.

TARGET CELLS

	Group	pe_0	fitci_1	fitcii_2	apc_3	brightfield_4	pe_fitci_5	pe_fitcii_6	mean_int ensity_fit ci	mean_int ensity_fit cii	mean_int ensity_bg sub_fitci	mean_int ensity_bg sub_fitcii
cell_id = 85 row_num = 1	TARGET								874.49	10424.59	540.01	8938.36
cell_id = 208 row_num = 2	TARGET								1131.91	12184.56	791.5	10549.43
cell_id = 202 row_num = 3	TARGET								1315.91	14129.76	970.53	12416.5
cell_id = 79 row_num = 4	TARGET								1709.93	14836.39	1376.5	13343.29

Figure 5.7: DEPAarray images of SN-38 0.01 μ M treated PE+/DAPI+/APC- colon cancer cells (HT-29). The rows show the cell ID, the columns display the name of the Channel *Selection* the cell belongs with respective values.

5.4.1. DEPAarray system analysis of SN-38 or oxaliplatin treated colon cancer cells

Suspended HT-29 cells treated with SN-38 or oxaliplatin and stained using antibody labelling for γ -H2AX (Section 2.10.4) were processed as per standard DEPAarray analysis (Section 2.8.3.1) and compared with the untreated control group using two different exposure times for FITC:

- FITCI (100 ms and gain 1X)
- FITCII (800 ms and gain 4X).

Raw data were analysed using an unpaired T-test on mean intensity minus background for FITCI and FITCII. The treated cells showed a significantly increased intensity of FITC staining compared with the untreated control group: mean 363 vs mean 220 ($P < 0.0001$) for FITCI, and mean 5521 vs mean 4365 ($P < 0.0040$) for FITCII (Table 5.8–5.9, Figure 5.8).

Table 5.8: HT-29 cells treated with SN-38 0.01 μ M compared with the untreated control group and run into the DEPArray machine. Data analysis was performed with unpaired T-Test on mean intensity minus background for FITCI.

Unpaired t-test FITC1: 100 ms

	FITCI gray intensity for cells treated with SN-38 (22)	FITCI gray intensity for untreated cells (254)
Mean	362.85	220.54
Standard deviation	324.58	94.98
Standard error	69.18	5.96
<i>P</i> value and statistical significance: The two-tailed <i>P</i> value is <0.0001; confidence interval: the mean of treated FITC1 minus untreated FITC1 = 142.31; 95% confidence interval of this difference: from 86.28 to 198.351; intermediate values used in calculations: t=4.999, df=274; standard error of difference=28.46		

Table 5.9: HT-29 cells treated with SN-38 0.01 μ M compared with the untreated control group and run into the DEPArray machine. Data analysis was performed with unpaired T-Test on mean intensity minus background for FITCII.

Unpaired t-tests FITCII: 800 ms

	FITCII gray intensity for cells treated with SN-38 (n=22)	FITCII gray intensity for untreated cells (n=254)
Mean	5521.49	4364.97
Standard deviation	3472.34	1575.11
Standard error	740.30	99
<i>P</i> value and statistical significance: The two-tailed <i>P</i> =0.0040; confidence interval: the mean of treated FITC2 minus untreated FITC2 = 1156.52; 95% confidence interval of this difference: from 372.05 to 1941.00; intermediate values used in calculations: t=2.90, df=274; standard error of difference=398.48		

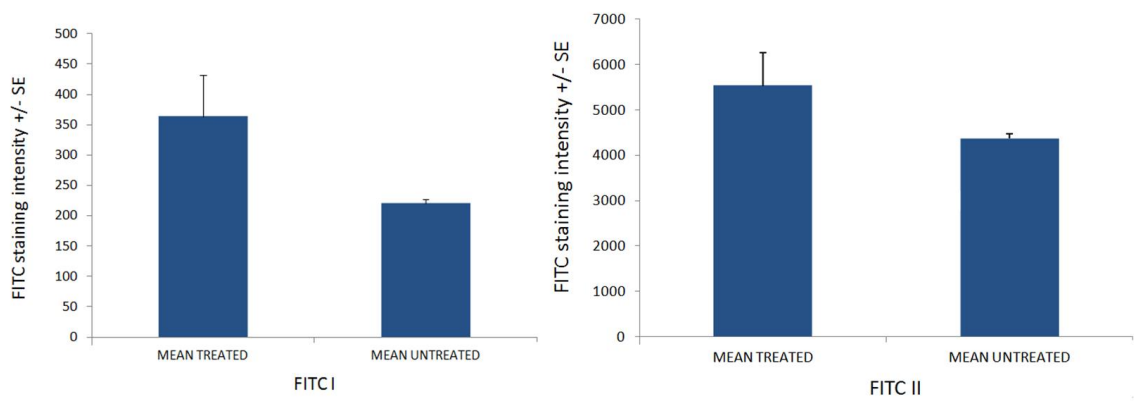


Figure 5.8: HT-29 cells treated with SN-38 0.01 μ M compared with an untreated control group using two different exposure times for FITC I (100 ms and gain 1X) and FITCII (800 ms and gain 4X). Data are expressed as mean of triplicate experiments \pm SE. The treated group showed a significantly increased intensity of FITC staining compared with the untreated control group: mean 363 vs mean 220 ($p < 0.0001$) for FITCI, and mean 5521 vs mean 4365 ($p < 0.0040$) for FITCII

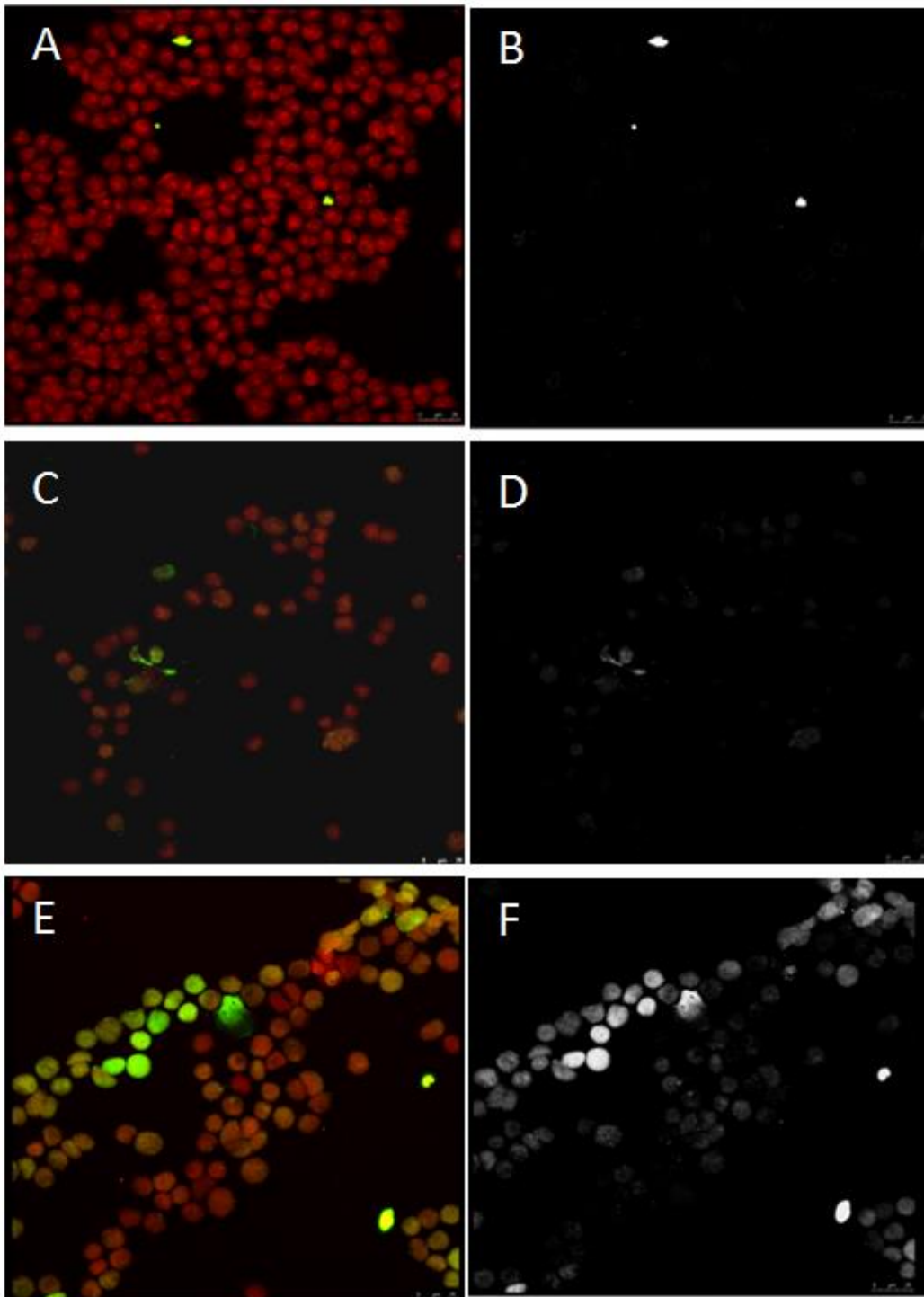


Figure 5.9: Validation of the γ -H2AX signal with fluorescence microscopy using HT-29 cells exposed to SN-38 with and without antibody labelling for γ -H2AX.

A and B represent HT-29 cells treated with SN-38 without anti-H2AX antibody staining; C and D represent untreated HT-29 cells stained with anti-H2AX; E and F represent HT-29 cells treated with SN-38 and stained with anti-H2AX. A, C and E show nuclei stain (channel one: red input image) selected for nuclei identification; B, D and F, show foci stain (channel two: green input image) selected for γ -H2AX foci identification.

Slides were analysed with Leica SPE2 confocal microscope and data analysis performed using CellProfiler Software.

For oxaliplatin treated cells, the majority of treated cells were lost during the washing and spinning steps and the total number of cells available for analysis were insufficient for validated analysis (Figure 5.10).

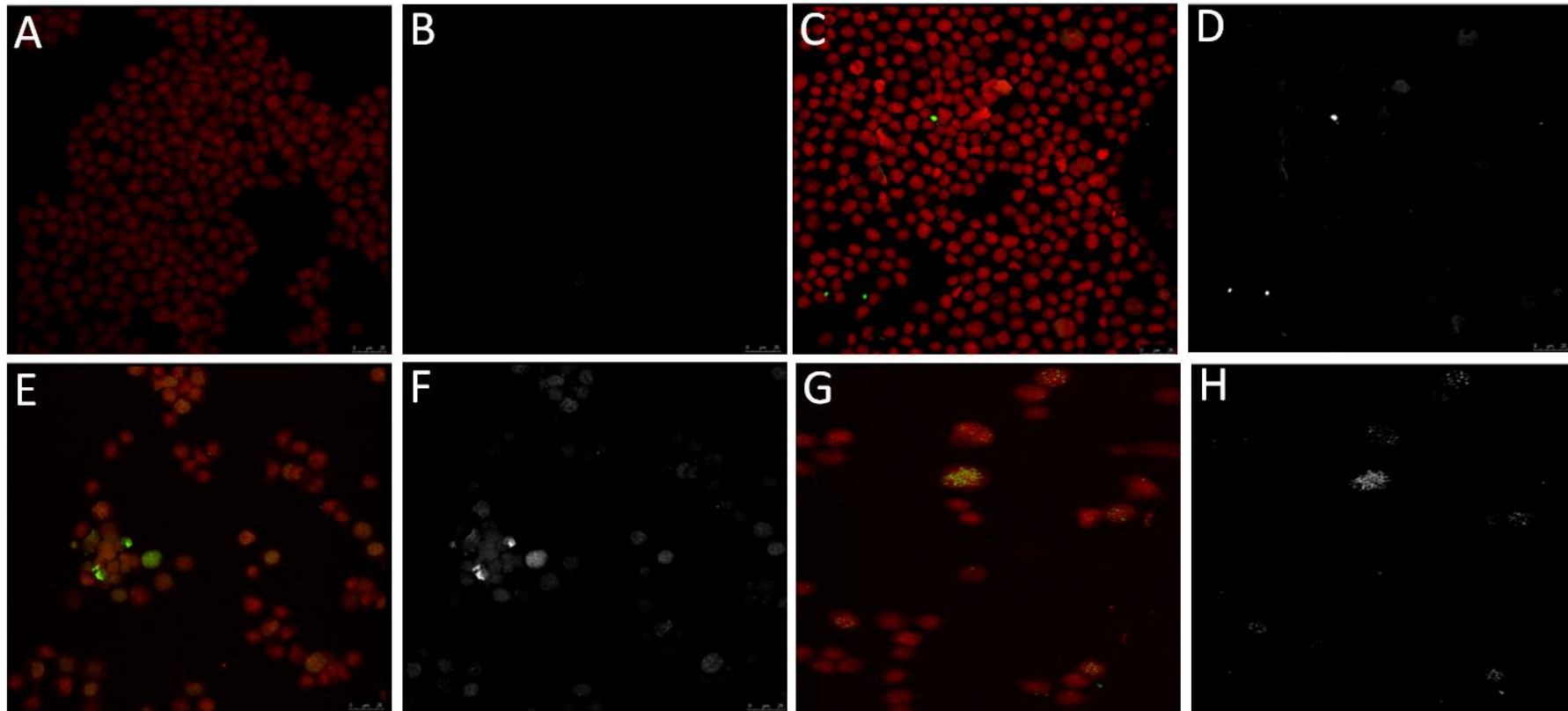


Figure 5.10: Validation of the γ -H2AX signal with fluorescence microscopy using HT-29 cells exposed to oxaliplatin with and without antibody labelling for γ -H2AX.

A and B represent HT-29 cells treated with oxaliplatin without anti-H2AX antibody staining; C and D represent untreated HT-29 cells stained with anti-H2AX; E-H represent HT-29 cells treated with oxaliplatin and stained with anti-H2AX. A, C, E, G show nuclei stain (channel one: red input image) selected for nuclei identification; B, D, F, H show foci stain (channel two: green input image) selected for γ -H2AX foci identification. Slides were analysed with Leica SPE2 confocal microscope and data analysis performed using CellProfiler Software.

5.4.2. Colon cancer cells treated with oxaliplatin or SN-38, run directly on the DEPArray platform using two different exposure times, validated with cytospin and fluorescence microscopy: Discussion and Conclusions

Based on these results, it was demonstrated that the DEPArray system was able to quantify differences in signal intensity as a result of drug induction of γ -H2AX in colon cancer cells. The use of fluorescence microscopy validated the data observed with the DEPArray platform. There were no detectable γ -H2AX cells observed in HT-29 cells treated with SN-38 but without the γ -H2AX antibody or in untreated cells with the γ -H2AX antibody present. In contrast, in SN-38 treated cells with the γ -H2AX antibody present there was a visible increase in γ -H2AX positive cells. Unfortunately during the analysis, most of the treated cells were lost due to the washing and spinning steps involved and the total amount of cells were not sufficient to make accurate and validated comparisons. This was particularly evident in cells treated with oxaliplatin limiting the data available for analysis.

Due to the fact that future development work will be required to be repeated on the CellSearch System to allow optimisation for patient samples, subsequent experiments were carried out on HT-29 cells treated with 1 μ M topotecan hydrochloride for 2 hours, followed by staining for γ -H2AX and analysis on the CellSearch system prior to DEPArray analysis.

5.5. Colon cancer cells treated with topotecan and run with DEPArray platform after CellSearch System using two different exposure times

The aims for this study were to investigate whether scanning of CTCs with the CellSearch System could have affected the intensity of the FITC signal background and signal/background ratio detected by DEPArray process.

Cells that were previously treated with topotecan and used for the validation of the assay employed in this thesis for the detection of γ -H2AX on CTCs using the CellTracks Autoprep System and the CellTracks Analyzer II (Section 2.8) were utilised. In brief, HT-29 cells were thawed and washed in 10mL PBS, pelleted by centrifugation and re-suspended in

10mL PBS. 50 μ L of the appropriate cell suspension (~500 cells) was added to 7.5 mL healthy donor blood. Cells were left untreated or treated with 1 μ m topotecan hydrochloride for 2 hours at 37°C in the presence of 5% CO₂.

5.5.1. Analysis with the CellSearch System

For each run, four samples from one healthy donor and a CellSearch CTC control sample were run using a CellSearch CTC Kit on the CellTracks Autoprep System and the CellTracks Analyzer II. Cells were prepared for the CellTracks Autoprep System and split into two samples of 750 cells each. Anti-phospho-Histone H2AX (ser139), clone JBW301, FITC conjugated antibody (Millipore) was used and the exposure time for the fourth channel was set at 3 seconds on the CellSearch Analyser II. Spiked and unspiked samples were prepared for analysis (Section 2.7.1), run on the CellTracks Autoprep System and on the CellTracks Analyzer II along with a control sample. γ -H2AX-FITC was diluted as specified in the protocol and used on the spiked samples.

Acceptance criteria for detection of γ -H2AX, as set by the NCI [289], state that untreated cells must be \leq 3% positive for γ -H2AX and treated cells must be \geq 10% positive for γ -H2AX. All three validation runs met these pre-specified criteria. Based on these results, HT-29 cells treated with topotecan were used for these experiments as they were previously confirmed to be \geq 10% positive for γ H2AX (Table 5.4; Figure 5.11).

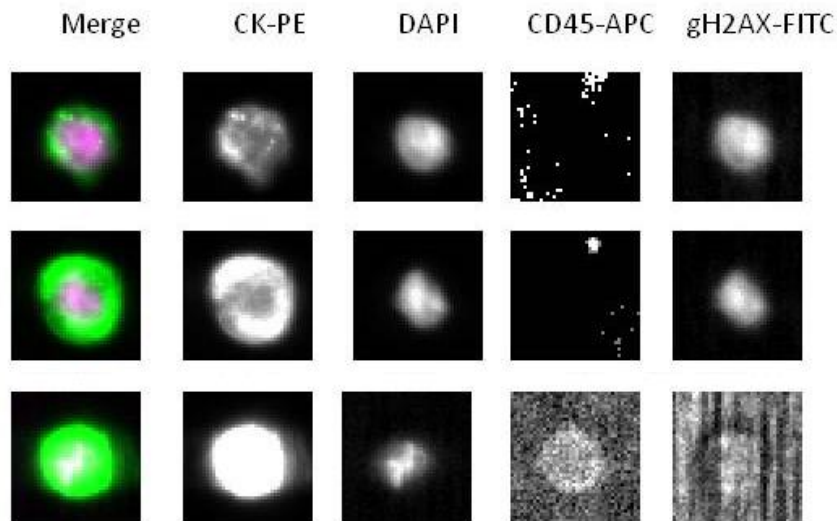


Figure 5.11. HT-29 cells treated with topotecan hydrochloride run on the CellTracks Autoprep System and on the CellTracks Analyzer II. Example of CTCs positive (top two panels) and negative (bottom panel) for γ -H2AX. Merge represents cells stained with CK-PE with the cell nuclei (DAPI) overlaid; CK-PE represents cells stained only with CK-PE (intracellular cytokeratins 8, 18, and/or 19); DAPI represents cell nuclei; CD45-APC represents cells stained for CD45-APC (haematopoietic origin). γ -H2AX represents cells positive (top panels) or negative (bottom panel) for γ -H2AX.

Two identical samples of HT-29 cells were run on the CellSearch machine but only one cartridge was scanned before running both cartridges in the DEPArray platform to establish what impact the CellSearch had on subsequent detection by DEPArray. This experiment was repeated in triplicate. The presence of CTCs was identified as described in Section 2.8.2. One cartridge containing stained CTCs was removed and inserted into the CellTracks Analyzer II for scanning and the second cartridge was left unscanned; both cartridges were then processed with the DEPArray System (Section 2.9) to compare the signal strength. The CellSearch analysis determined that in the scanned sample, approximately 45% of the topotecan treated cells were positive for γ -H2AX (FITC) staining; this experiment is referred to as the first validation.

5.5.2. Analysis with DEPArray platform

For Sample Preparation and Buffer Compatibility see Section 2.8.3 and 2.9. The DEPArray execution system was selected according to the protocol. Cells were sorted based on fluorescence intensity and morphological trait and recovered for downstream analysis. FITCI and FITCII scans were performed on both samples on the DEPArray and the raw data were analysed (Table 5.10 and Figure 5.12).

Table 5.10. DEPArray analysis of HT-29 cells treated with topotecan from the CellSearch cartridge stained with the H2AX-FITC antibody in the fourth channel and scanned using CellTracks system or unscanned (**first validation**). Data analysis was performed with unpaired T-Test on mean intensity minus background for FITCI and FITCII. The scanned group showed a statistically significant increase of FITC staining intensity compared with the unscanned group for both FITC I (*P* value: 0.0035) and for FITC II (*P* value: 0.0049).

	Scanned FITCI	Unscanned FITCI
Mean	24.27	16.28
Standard deviation	16.51	18.58
Standard error	1.72	2.12
N. cell	92	77
	Scanned FITCII	Unscanned FITCII
Mean	613.60	473.79
Standard deviation	313.22	321.95
Standard error	32.66	36.69
N. cell	92	77
Scanned FITCI		Unscanned FITCI
<i>P</i> value		0.0035
Confidence interval		The mean of scanned FITCI minus unscanned FITCI = 7.99 95% confidence interval of this difference: from 2.66 to 13.32
Scanned FITC2		Unscanned FITCII
<i>P</i> value		0.0049
Confidence interval		The mean of scanned FITCII minus unscanned FITCII = 139.81 95% confidence interval of this difference: from 43.07 to 236.54

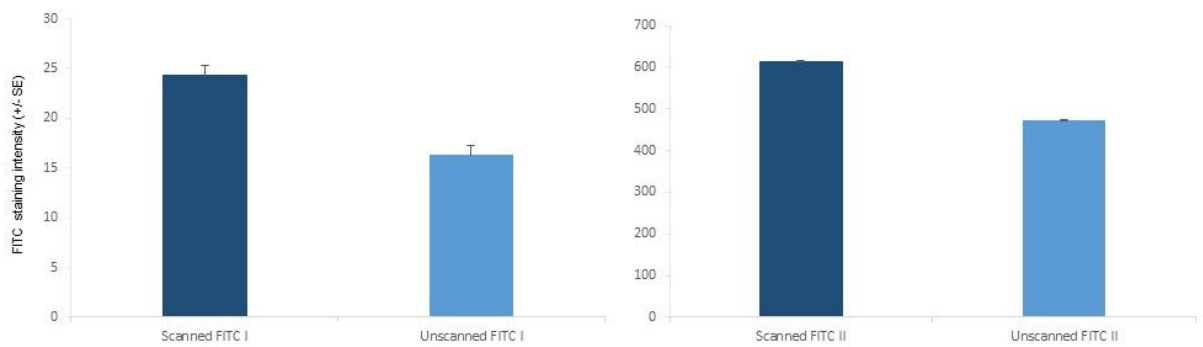


Figure 5.12. DEPArray analysis of HT-29 cells treated with topotecan from the CellSearch cartridge stained with the H2AX-FITC antibody in the fourth channel and scanned using CellTracks system (Sample 1) or unscanned (Sample 2) (first validation). A statistically significant increase of intensity was showed in the scanned samples for FITC I ($P=0.0035$) and FITCII ($P=0.0049$).

Out of 1500 cells that were initially run on the CellSearch, 750 cells were recovered, split into two samples of 375 cells each and one sample was loaded into the DEPArray and scanned. 77 and 92 PE CK positive and APC (CD45) negative cells were found in the unscanned and in the scanned samples, respectively. Raw data were analysed using an unpaired T-test on mean intensity minus background for FITC I and FITC II. The scanned group showed a statistically significant increase of FITC staining intensity compared with the unscanned group for both FITC I (P value: 0.0035) and for FITC II (P value: 0.0049). The data were further analysed by Silicon Biosystems; in the scanned sample (Sample 1) out of 967 particles detected, only 83 PE+/DAPI+/APC- cells were identified, three of which had comparable FITC II signal and background levels (Figure 5.13).

- 83 PE+/DAPI+/APC- cells identified out of 967 particles detected.
- Most of the PE+/DAPI+/APC- cells didn't show a clear positivity in the FITC channel.
- DEPArray™ analysis allowed the identification of only 3 cells in which FITC II signal and background levels are at least comparable.

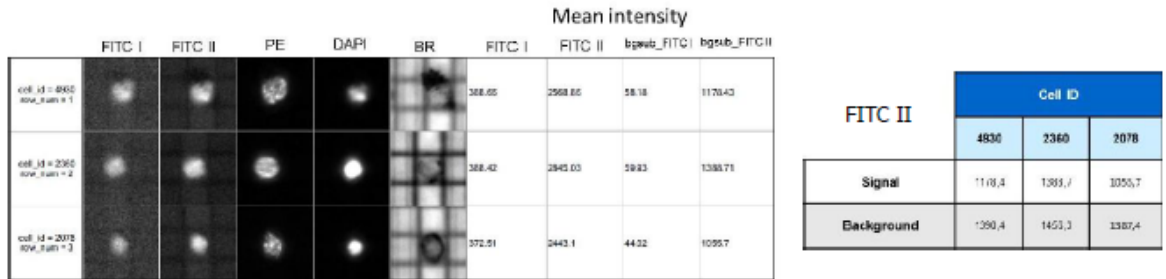


Figure 5.13: Screenshot from the Silicon Biosystems DEPArray system analysis of Sample 1 (scanned) showing three cells with FITC II signal and background level comparable.

In the first and second column from left, the signal in the cells appears faint; in the third column the nuclei look picnotic as in apoptosis.

In the unscanned sample (Sample 2), out of 1237 particles detected, 65 were PE+/DAPI+/APC- and most of these cells did not show a clear positivity in the FITC channel. In this case, DEPArray analysis identified four cells in which the FITC II signal and background level were at least comparable (Figure 5.14). A summary of the first validation run is shown in Table 5.11.

- 65 PE+/DAPI+/APC- cells identified out of 1237 particles detected.
- Most of the PE+/DAPI+/APC- cells didn't show a clear positivity in the FITC channel.
- DEPArray™ analysis allowed the identification of only 4 cells in which FITC II signal and background levels are at least comparable.

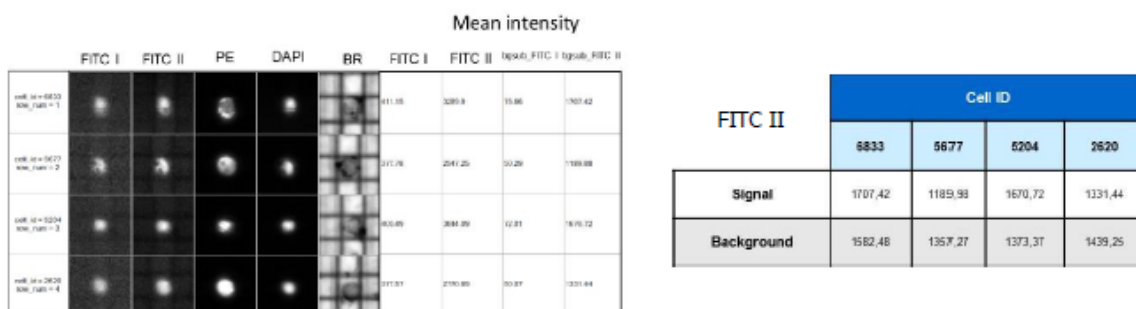


Figure 5.14: Screenshot from the Silicon Biosystems analysis of Sample 2 (unscanned) showing four cells with FITC II signal and background level comparable

Table 5.11. Validation of the DEPArray analysis by Silicon Biosystems

	Sample 1 (scanned)	Sample 2 (unscanned)
No. particles detected	967	1237
No. particles PE+/DAPI+/APC-	83	65
No. cells with comparable FITC II signal/background levels	3	4

5.5.3. Additional validation of CTC Analysis and Enumeration of HT-29 cells and their γ -H2AX (FITC) expression when treated with topotecan (second and third validation)

Additional validation experiments were repeated using cells that were similarly treated with topotecan at the same concentration and for the same period of time and processed on CellTracks Autoprep system along with CTC Control Sample (CellSearch CTC Control Kit) as previously described (Section 2.8).

For the two additional validation experiments, 5078 and 4026 cells were run using the CellSearch platform. The γ -H2AX antibody was diluted as per protocol and loaded in the CellSearch machine. For each additional validation, two identical samples were processed with CellSearch, but on the CellTracks Analyzer II only one cartridge along with the control was scanned, displaying tumour cells positive for CK and DAPI. The other cartridge was left unscanned and they were both processed with the DEPArray afterwards to compare the signal strength (Figures 5.15–5.18). The presence of CTCs in the CellSearch System (Janssen Diagnostic) was identified as previously described. CTCs positive for γ -H2AX (FITC) staining were 1431 (28.2%) and 902 (22.4%) for the two additional validations, respectively. The cartridges containing stained CTCs were then removed and inserted into the CellTracks Analyzer II for scanning.

Sample ID: Topotecan 1		Cartridge ID: 01376915			Patient ID:	
Event	Frame	DAPI/CK-PE	CK-PE	DAPI	CD45-APC	γ H2AX
70	13					
188	32					
1546	131					
1720	128					
1751	156					
1796	161					
1843	168					
1861	170					
1851	169					
1858	170					
1859	170					

Figure 5.15. A screenshot from the CellTracks Analyser demonstrating the Criteria for CTC Analysis. Topotecan treated HT-29 cells for the second validation: CTC candidate images and interpreter detection.

DAPI/CK-PE represents cells stained with CK-PE with the cell nuclei (DAPI) overlaid; CK-PE represents cells stained only with CK-PE; DAPI represents cell nuclei; CD45-APC represents haematopoietic origin; γ -H2AX represents staining for γ -H2AX molecular characterisation. Images with an orange box are positive for nuclear FITC staining.

Sample ID: Untreated		Cartridge ID: 0129025B			Patient ID: gH2AX	
Event	Frame	DAPI/CK-PE	CK-PE	DAPI	CD45-APC	gH2AX
3	3					
4	3					
6	3					
14	4					
20	4					
28	4					
29	4					
43	4					
60	4					

Figure 5.16. A screenshot from the CellTracks Analyser demonstrating the Criteria for CTC Analysis. Untreated HT-29 cells from second validation: CTC candidate images and interpreter detection.

DAPI/CK-PE represents cells stained with CK-PE with the cell nuclei (DAPI) overlaid; CK-PE represents cells stained only with CK-PE; DAPI represents cell nuclei; CD45-APC represents haematopoietic origin; γ -H2AX represents staining for γ -H2AX molecular characterisation. Images with an orange box are positive for nuclear FITC staining.

Sample ID: Topotecan 1		Cartridge ID: 01376915			Patient ID:	
Event	Frame	DAPI/CK-PE	CK-PE	DAPI	CD45-APC	γH2AX
70	13					
188	32					
1546	131					
1720	128					
1751	156					
1796	161					
1843	168					
1861	170					
1851	169					
1858	170					
1859	170					

Figure 5.17. A screenshot from the CellTracks Analyser demonstrating the Criteria for CTC Analysis. Topotecan treated HT-29 cells for the third validation: CTC candidate images and interpreter detection.

DAPI/CK-PE represents cells stained with CK-PE with the cell nuclei (DAPI) overlaid; CK-PE represents cells stained only with CK-PE; DAPI represents cell nuclei; CD45-APC represents haematopoietic origin; γ -H2AX represents staining for γ -H2AX molecular characterisation. Images with an orange box are positive for nuclear FITC staining.

Sample ID: Untreated		Cartridge ID: 01298725			Patient ID:	
Event	Frame	DAPI/CK-PE	CK-PE	DAPI	CD45-APC	gH2AX
46	20					
116	51					
203	80					
250	88					
11	11					
49	21					
131	55					
223	85					

Figure 5.18. A screenshot from the CellTracks Analyser demonstrating the Criteria for CTC Analysis. Untreated HT-29 cells for the third validation: CTC candidate images and interpreter detection.

DAPI/CK-PE represents cells stained with CK-PE with the cell nuclei (DAPI) overlaid; CK-PE represents cells stained only with CK-PE; DAPI represents cell nuclei; CD45-APC represents haematopoietic origin; γ -H2AX represents staining for γ -H2AX molecular characterisation. Images with an orange box are positive for nuclear FITC staining.

5.5.4. Analysis of γ -H2AX (FITC) expression with the DEPArray platform of HT-29 cells treated with topotecan that were scanned and unscanned with the CellTracks Analyzer II system

The DEPArray set-up execution system was selected according to the protocol, HT-29 samples treated with topotecan were loaded, and cell sorting and recovery were performed using the CellSearch system. FITC I and II scans were performed with the DEPArray platform on the two additional validation samples for each experiment (Section 5.2.3). The total number of cells recovered from the CellTracks Analyzer II scanned cartridges were 937 and 773, and the cells recovered from the unscanned cartridge after CellSearch analysis were 949 and 1011, for the two additional validations respectively.

The raw data were downloaded after each experiment and analysed using an unpaired T-test on mean intensity minus background for FITCI and FITCII (Tables 5.12–5.13; Figures 5.19–5.20).

Table 5.12. DEPArray analysis of HT-29 cells treated with topotecan from the CellSearch cartridge stained with the H2AX-FITC antibody in the fourth channel and scanned using CellTracks system or unscanned (second validation). The data were analysed using unpaired T-test on mean intensity minus background for FITCI and FITCII.

	Scanned FITCI	Unscanned FITCI
Mean	26.82	48.93
Standard deviation	14.99	396.08
Standard error	0.49	12.86
N. cell	937	949
	Scanned FITCII	Unscanned FITCII
Mean	732.46	807.32
Standard deviation	233.59	385.27
Standard error	7.53	12.51
N. cell	937	949
Scanned FITCI		Unscanned FITCI
<i>P</i> value		0.088
Confidence interval		The mean of scanned FITCI minus unscanned FITCI = -22.10 95% confidence interval of this difference: from -47.54 to 3.34
Scanned FITCII		Unscanned FITCII
<i>P</i> value		0.0001
Confidence interval		The mean of scanned FITCII minus unscanned FITCII = -74.66 95% confidence interval of this difference: from -103.43 to -45.89

Table 5.13. DEPArray analysis of HT-29 cells treated with topotecan from the CellSearch cartridge stained with the H2AX-FITC antibody in the fourth channel and scanned using CellTracks system or unscanned (third validation). Data analysis was performed with unpaired T-test on mean intensity minus background for FITCI and FITCII.

	Scanned FITCI	Unscanned FITCI
Mean	29.76	47.29
Standard deviation	19.66	20.13
Standard error	0.71	0.63
N. cell	773	1011
	Scanned FITCII	Unscanned FITCII
Mean	817.43	1257.23
Standard deviation	466.52	599.99
Standard error	16.78	18.87
N. cell	773	1011
Scanned FITCI		Unscanned FITCI
<i>P</i> value	0.0001	
Confidence interval	The mean of scanned FITCI minus unscanned FITCI = -17.54 95% confidence interval of this difference: from -19.41 to -15.67	
Scanned FITCII		Unscanned FITCII
<i>P</i> value	0.0001	
Confidence interval	The mean of scanned FITCII minus unscanned FITCII = -439.79 95% confidence interval of this difference: from -491.07 to -388.53	

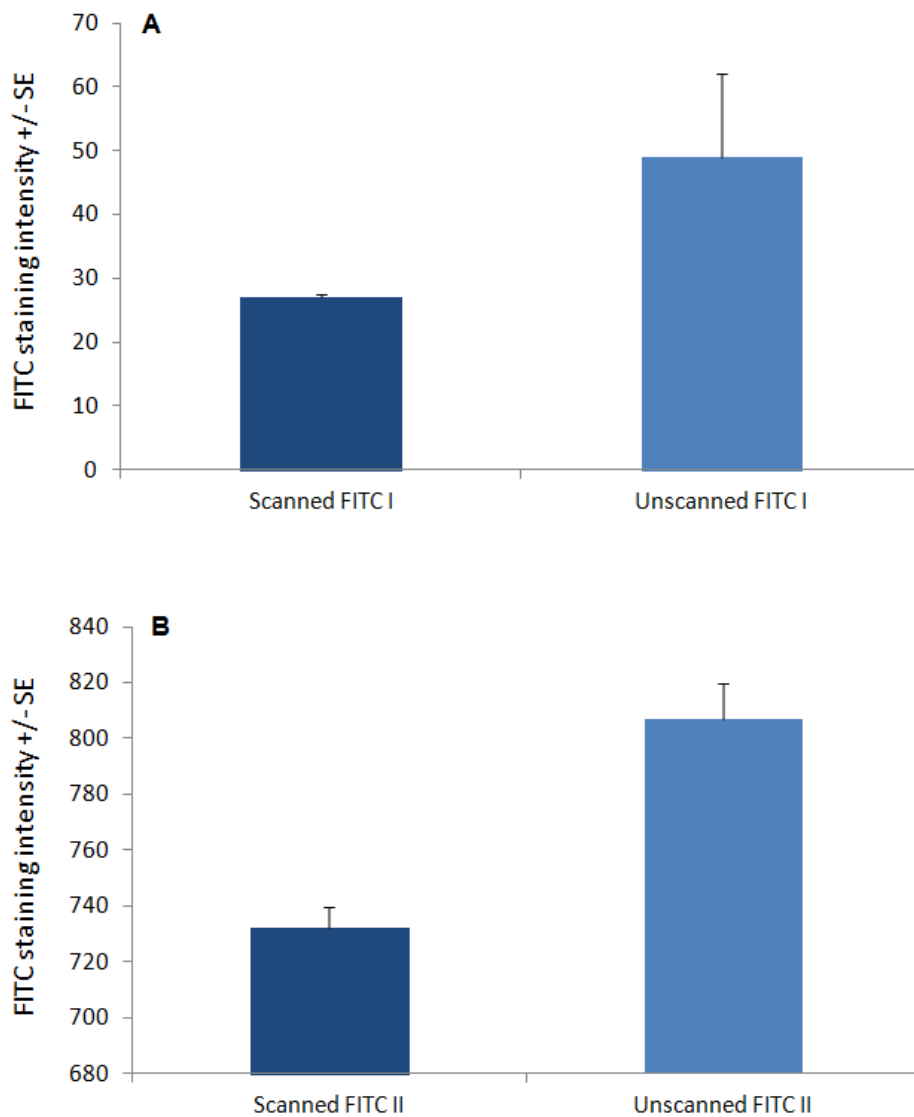


Figure 5.19. DEPArray analysis of HT-29 cells treated with topotecan from the CellSearch cartridge stained with the H2AX-FITC antibody in the fourth channel and scanned using CellTracks system or unscanned (second validation). A. FITC I scanned/unscanned and B. FITC II scanned/unscanned. A statistically significant increase of intensity was showed in the unscanned samples for FITC II ($P=0.0001$), but not for FITC I ($P=0.0881$)

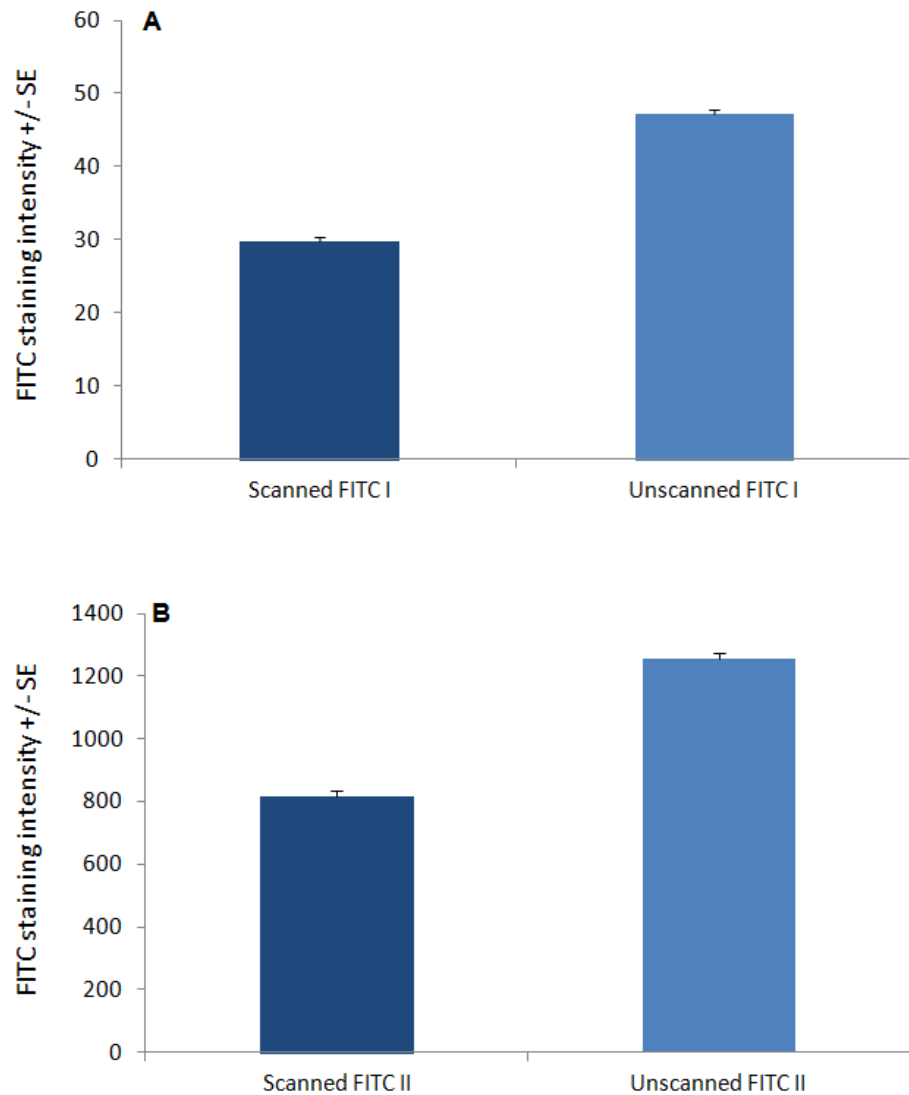


Figure 5.20. DEPArray analysis of HT-29 cells treated with topotecan from the CellSearch cartridge stained with the H2AX-FITC antibody in the fourth channel and scanned using CellTracks system (Sample 1) or unscanned (Sample 2) (third validation). A. FITC I scanned/unscanned and B. FITC II scanned/unscanned. A statistically significant increase of intensity was shown in the unscanned samples for both FITC I and FITC II ($P=0.0001$).

The results showed a statistically significant increase of intensity in the unscanned samples for FITCII ($P=0.0001$) in the second validation, and for both FITCI and FITCII in the third ($P=0.0001$) validation. FITCI in the second validation was not statistically significant ($P=0.09$). Unfortunately, as in the previous experiments, most of the PE+/DAPI+/APC- cells did not show a clear positivity in the FITC channels. DEPAArray analysis allowed the identification of only four cells in which FITCII and background intensity level were at least comparable. Fluorescent staining of γ -H2AX was very faint and needed to be set up for a clear detection.

5.5.5. Further statistical analyses of the second and third validation runs using mean intensity only on FITCII data

Additional analyses of raw data for the second and third validation runs were analysed using an unpaired T-test on mean intensity for FITCII, rather than mean intensity minus the background. The results confirmed a statistically significant increase in intensity in the unscanned samples for FITCII in both the second ($P=0.03$) and third ($P=0.0001$) validations. Analyses were also performed grouping data for low and high intensity FITCII signal. A statistically significant increased intensity ($P=0.02$) was confirmed in the second validation of the unscanned sample for high intensity value (Figure 5.21 and Table 5.14), while in the third validation the FITCII intensity between the scanned versus unscanned samples was statistically significant for both low and high value intensities (Figure 5.22 and Table 5.15).

The distribution of the FITCII intensity for these analyses of the second and third DEPAArray validation experiments of CellTracks Analyser II scanned and unscanned cells was also assessed. These data demonstrate that the distribution and therefore γ -H2AX staining of the CellTracks Analyser II unscanned samples appeared to be more specific than the scanned samples for both validation runs (Figure 5.23).

Table 5.14. DEPArray analysis of HT-29 cells treated with topotecan from the CellSearch cartridge stained with the H2AX-FITC antibody in the fourth channel and scanned using CellTracks system or unscanned (second validation). Data analysis was performed with unpaired T-test on mean intensity for FITCII and on data grouped for low (LV) and high values (HV).

	Scanned FITCII	Unscanned FITCII
Mean	2277	2325
Standard deviation	349.2	600.8
Standard error	11.41	19.50
N. cell	937	949
<i>P</i> value	0.0344	
	Scanned FITCII LV	Unscanned FITCII LV
Mean	2060	2064
Standard deviation	91.26	125
Standard error	4.22	5.77
N. cell	467	473
<i>P</i> value	0.6198	
	Scanned FITCII HV	Unscanned FITCII HV
Mean	2493	2585
Standard deviation	376	754
Standard error	17.4	34.6
N. cell	470	476
<i>P</i> value	0.0179	

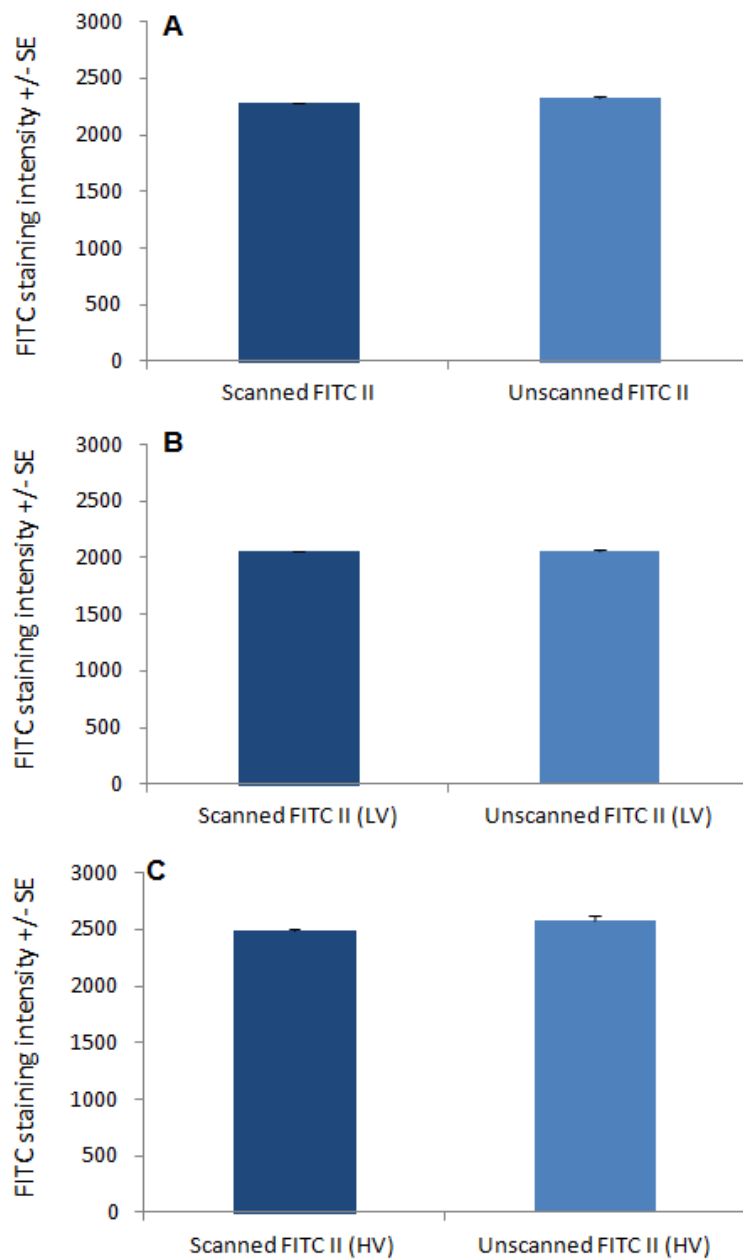


Figure 5.21. DEPArray analysis of HT-29 cells treated with topotecan from the CellSearch cartridge stained with the H2AX-FITC antibody in the fourth channel and scanned using CellTracks system or unscanned (second validation). A. Data were analysed for FITC II using mean intensity. B. The results confirmed a statistically significant increase in intensity in the unscanned samples for FITCII for low intensity value (LV) ($P=0.03$). C. A statistically significant increased intensity was confirmed in the second validation of the unscanned sample for high intensity value (HV) ($P=0.02$)

Table 5.15. DEPArray analysis of HT-29 cells treated with topotecan from the CellSearch cartridge stained with the H2AX-FITC antibody in the fourth channel and scanned using CellTracks system or unscanned (third validation). Data analysis was performed with unpaired T-test on mean intensity for FITCII and on data grouped for low (LV) and high values (HV).

	Scanned FITCII	Unscanned FITCII
Mean	2330.11	2815.49
Standard deviation	479.33	650.98
Standard error	17.24	20.48
N. cell	773	1011
<i>P</i> value	0.0001	
	Scanned FITCII LV	Unscanned FITCII LV
Mean	1969.93	2388.177
Standard deviation	140.82	199.46
Standard error	7.17	8.88
N. cell	385	505
<i>P</i> value	0.0001	
	Scanned FITCII HV	Unscanned FITCII HV
Mean	2687.49	3241.97
Standard deviation	426.06	665.58
Standard error	21.74	29.71
N. cell	388	506
<i>P</i> value	0.0001	

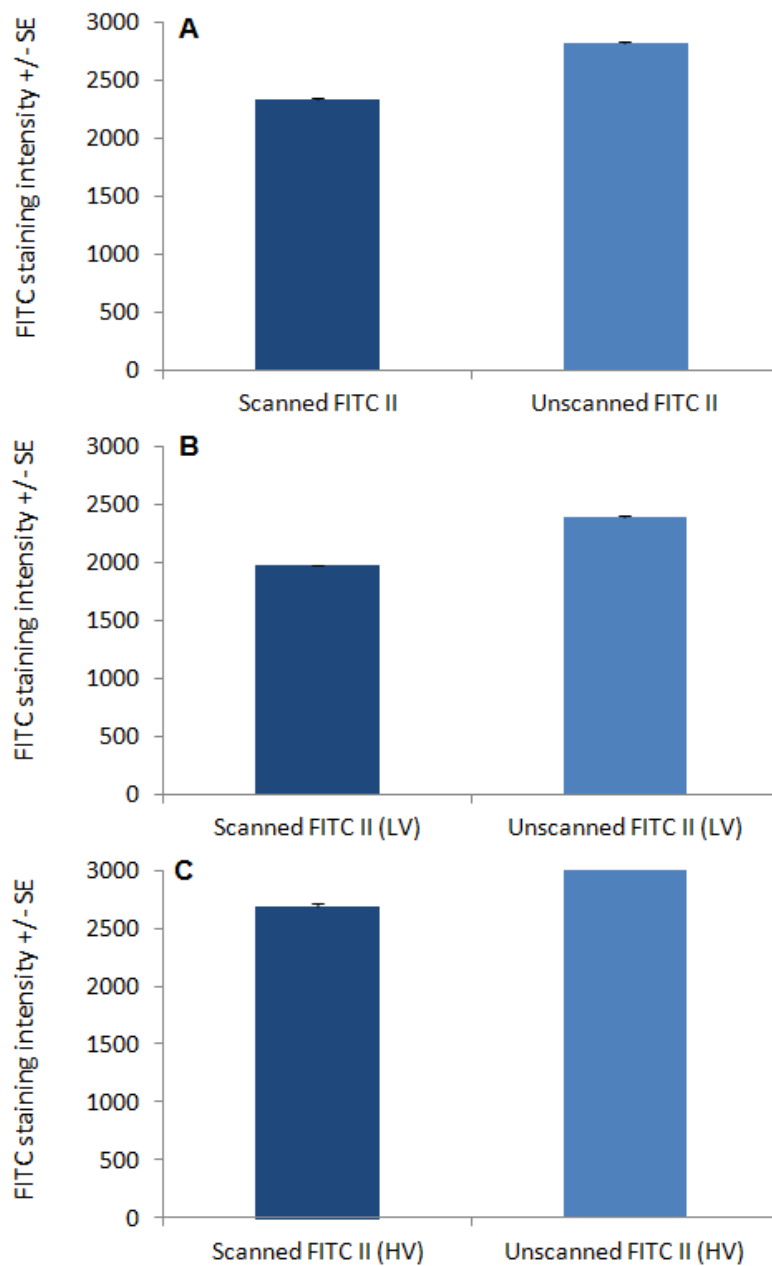


Figure 5.22. DEPArray analysis of HT-29 cells treated with topotecan from the CellSearch cartridge stained with the H2AX-FITC antibody in the fourth channel and scanned using CellTracks system or unscanned (third validation). A. Data were analysed for FITC II using mean intensity. The results were statistically significant for FITCII intensity between the scanned versus unscanned samples and for both low (LV; B) and high value (HV; C) intensities (P= 0.0001).

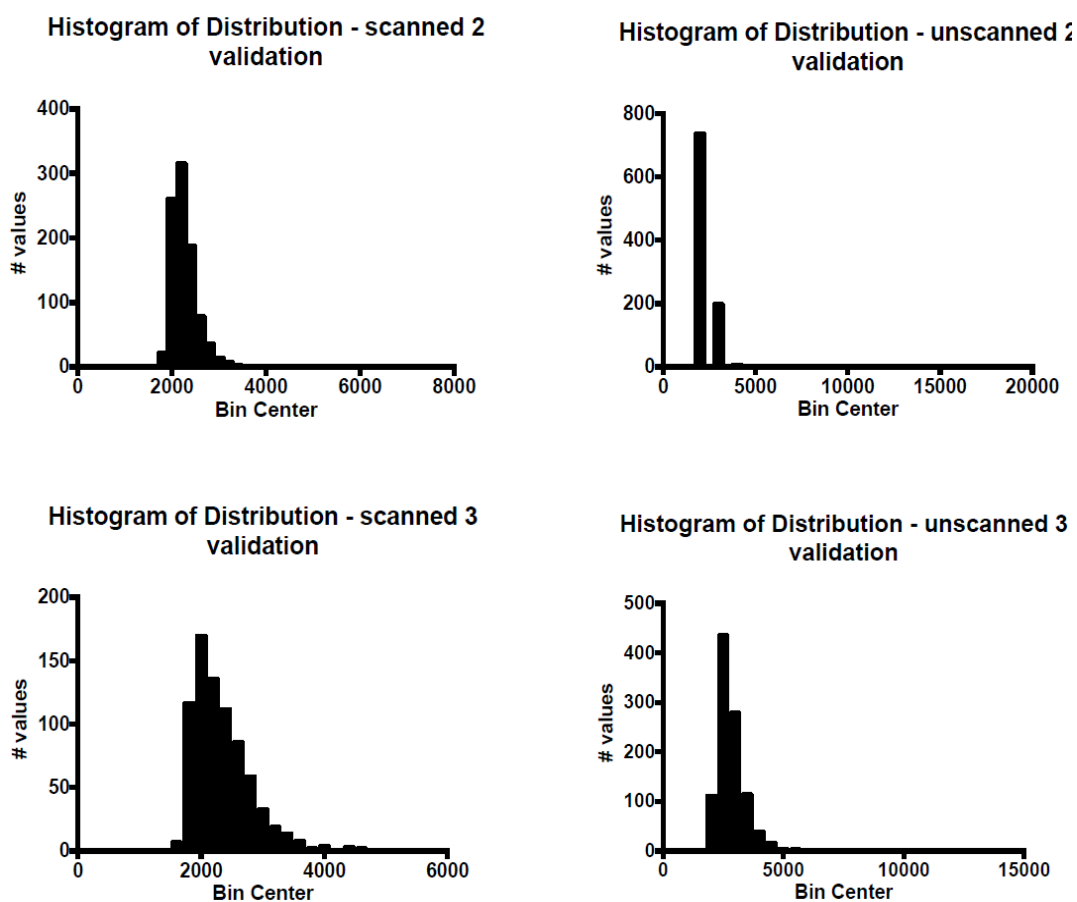


Figure 5.23. Distribution of the FITCII intensity observed following DEPArray analyses for the second and third validation experiments of CellTracks Analyser II scanned and unscanned cells. These data demonstrate that the distribution and therefore γ -H2AX staining of the CellTracks Analyser II unscanned samples appeared to be more specific than the scanned samples for both validation runs.

5.5.6. Discussion and conclusions of the validation experiments for the colon cancer cells drug treated and run with the DEPArray platform after the CellSearch System

Data from these validation experiments were reviewed by myself and by the Silicon Biosystems team.

In the first experiment (Section 5.3) the samples were treated with oxaliplatin and SN-38 and run with the DEPArray after CellSearch system. This initial experiment was performed to verify the workflow on the DEPArray system. The analysis was performed based on mean intensity with the background subtracted to provide an estimation of the ratio of the signal to background.

FITCI is usually used for DEPArray analysis. In this case, the background intensity should be less than 500 gray, while the exposure time for FITCII for DEPArray analysis corresponded to an exposure time of 3 seconds with the CellSearch platform.

With the initial standard set up for the identification of FITC background signal (FITC I: 100 ms and gain 1X) the analysis of the SN-38 treated sample run using the DEPArray platform did not show a clear positivity in the FITC channel for most of the PE+/DAPI+/APC- cells. The untreated control was further analysed with FITC I (100 ms and gain 1X) and FITC II (800 ms and gain 4X), that was added to the analysis in order to maintain the CellSearch System set up to 3 seconds but we could not discriminate between cells expressing or not expressing γ -H2AX, probably due to a possible bleaching of the cells as a consequence of the cartridge scanning (Section 2.9.2.2). As a result, no difference in signal intensity between the treated and untreated cells could be found. The long exposure time and gain required increased the level of the background resulting in a low signal/background ratio. The CellSearch System allows detection of the FITC stain in the nuclei of the cells if they were γ -H2AX positive, but the distinct foci were not visible due to the low magnification limitation of the CellSearch System platform (20x). In this validation experiment where samples were treated with oxaliplatin and SN-38 and run with the DEPArray after CellSearch system the Alexa Fluor 488-detected in the FITC channel was used which is more stable than the FITC antibody used with the CellSearch platform that can bleach

more easily. In the same experiment, PI was used instead of DAPI, and this could have created a steric hindrance for the binding of the antibody. Furthermore, the images showed that the PE signal was saturated which could have contributed to a shift, in part, of the signal to the FITC channel, as well as to mixed results. The possibility that the scanning caused an excitement of the fluorochrome on the γ -H2AX antibody resulting in an increased intensity of the FITC signal with the DEPArray analysis is unlikely, due to the time interval (one week) between the CellSearch scan and DEPArray run.

In the second experiment (Section 5.4) the cells were run directly in the DEPArray system (and not scanned on the CellSearch/CellTracks Analyzer II system). Based on these results, it was demonstrated that the DEPArray system was able to quantify differences in signal intensity as a result of drug induction of γ -H2AX in colon cancer cells.

Unfortunately during the analysis, most of the treated cells were lost due to the washing and spinning steps involved and the total amount of cells were not sufficient to make accurate and validated comparisons.

The third experiment (Section 5.5) was therefore planned due to the fact that future development work will be required to be repeated on the CellSearch System to allow optimisation for patient samples.

Three validations were carried out on HT-29 cells treated with 1 μ M topotecan hydrochloride for 2 hours, followed by staining for γ -H2AX and analysis on the CellSearch system prior to DEPArray analysis.

1st validation: Table 5.10.

Two different exposure times were used, FITCI (100 ms and gain 1X) and FITCII (800 ms and gain 4X). The results showed a statistically significant increase in intensity of the FITCI and FITCII signal in the sample that was previously scanned in the CellSearch platform. However, the 750 cells that were initially retrieved from the CellSearch system were further split into two samples and only one sample was run due to an operator mistake, therefore data were not available for comparison and to confirm the findings of the experiment. It would have been preferable to have had both sets of data to allow for a more accurate

statistical comparison compared with the data available from one sample (92 cells from the scanned cartridge and 77 cells from the unscanned cartridge). Furthermore, several cells appeared to be apoptotic and because of the typical changes occurring during this process, the fluorescent staining of cytokeratin and γ -H2AX could have been negatively affected.

As a result of the inconclusive nature of the first experiment run, additional validation runs were performed.

2nd and 3rd validation: Tables 5.12., 5.13.

In these validations, the number of cells recovered was increased and the intensity of the other channels in the DEPArray machine was adjusted to avoid saturation. The results showed a statistically significant increase of intensity in the CellSearch/CellTracks Analyzer II unscanned samples when compared with the scanned samples for FITCII ($P=0.0001$) in the second validation, and for both FITCI and FITCII in the third validation ($P=0.0001$). FITCI in the second validation was not statistically significant ($P=0.09$) and therefore a difference in signal intensity between the CellSearch/CellTracks Analyzer II scanned and unscanned sample was not confirmed. Unfortunately, as in the previous experiments, most of the PE+/DAPI+/APC- cells did not show a clear positivity in the FITC channels. DEPArray analysis allowed the identification of only four cells in which FITCII and background intensity level were at least comparable (Figure 5.14). Fluorescent staining of γ -H2AX was also very faint. In these experiments the FITCI signal was very low (below 50) compared to the cut off value of approximately 1000 (Table 5.10, 5.12, 5.13). In fact, the signal and the background should not be similar and should differ in gray levels.

Moreover the magnitude used by the DEPArray system is 20x; this parameter cannot be modified and may not be powerful enough to detect a γ -H2AX signal in the cell nuclei.

As results of the very low FITCI signal intensity, the data for the second and third validations of the third experiment were re-evaluated taking into consideration only the mean intensity values of FITCII, rather than the mean intensity with the background

subtracted. Although it can be useful to formulate an idea of the ratio between the actual γ -H2AX signal and the background, this could be misleading since it derives from a mathematical interpolation of the raw data. As already noted, the mean intensity parameter is the mean of all gray levels measured within the ROI. It has been suggested to be used for diffused cell staining in the nucleus, cytoplasm or on the cell plasma membrane. This is differentiated from the maximum intensity parameter which represents the maximum of all gray levels measured within the ROI and is usually used to define cell staining in the nucleus, cytoplasm or on the cell plasma membrane.

After having analysed the selected cells, it was noted that they fell within a wide range of signal intensities with two groups of CTCs being distinguished: the first group had a high mean intensity value and a second group had low mean intensity values. Statistical analyses were performed on the two separate groups to determine if it was appropriate to separate the groups for further analyses. The results from these additional analyses confirmed a statistically significant increase in intensity in the unscanned samples for FITCII in both the second ($P=0.03$) and third ($P=0.0001$) validations when compared with the scanned samples. In addition, when the distribution of the FITCII intensity for these analyses was evaluated the distribution and therefore γ -H2AX staining of the CellTracks Analyser II unscanned samples appeared to be more specific than the scanned samples for both validation runs (Figure 5.24).

In conclusion, the studies reported here appear to show that when cells are identified using the CellSearch system and scanned with the CellTracks Analyser II prior to DEPArray analysis for γ -H2AX intensity, the signal for γ -H2AX is lost when compared to cells that are not scanned with the CellTracks Analyser II. Therefore, future validation of these methods should exclude analysis of isolated cells with the CellTracks Analyser II, instead moving straight to analysis with the DEPArray system.

The combination of CellSearch enrichment and DEPArray sorting have been already shown to deliver 100% pure cells appropriate for reproducible downstream next-generation sequencing analysis.

Future development in this field could be focused to integrate CellSearch and DEPArray to develop companion diagnostics through the enumeration, isolation, and molecular characterization of CTCs, allowing to isolate rare-cell and genetic analyses accelerating the validation of personalized therapies for those patients more likely to respond to targeted drug treatments, monitoring a patient's status by showing if their prognosis is favorable.

CHAPTER 6: Clinical Application and Characterisation of CTCs

6.1. Introduction

As previously discussed, CTC counts could suggest on-going metastasis [243] and they have been correlated with PFS and OS in several tumour types [217]. Using the CellSearch platform, several cut-offs (≥ 5 CTCs at baseline in breast and prostate cancer and >3 in colorectal cancer) [219] have been identified to be associated with shorter median PFS and OS [166, 217]. Furthermore, pre- and post-treatment CTC counts are currently used as prognostic and predictive biomarkers of response to treatment and persistent elevated levels of CTCs after treatment were associated with an adverse outcome [290].

New molecular methods such as the detection of circulating γ -H2AX expression as a marker of response to treatment in CTCs from patients after chemotherapy could potentially be utilised as a predictive biomarker of early response to treatment [290].

The detection of γ -H2AX in CTCs has been validated and the protocol developed by the National Institute of Health (NIH) was tested in the GCLP laboratory at UCL using the CellSearch platform. Unfortunately, the quantification of the signal intensity of DBS in CTCs was not possible with this platform due to limitations of the magnitude of the signal amplification. Therefore, in the current study a system was developed to demonstrate the feasibility of γ -H2AX signal quantification as a predictive biomarker of response in CTCs in colorectal cancer. The aims of this study were to:

1. Investigate the relationship between γ -H2AX expression in CTCs and the γ -H2AX response to treatment
2. Quantify γ -H2AX expression in CTCs using a combined modality approach using the CellSearch and DEPArray platforms
3. Evaluate γ -H2AX in CTCs as a predictive biomarker (i.e. investigate its utility in predicting early response to treatment)

6.2. Patient Recruitment, demographics and baseline characteristics

Between May 2014 and March 2015, 16 patients with colorectal cancer starting chemotherapy with FOLFOX or FOLFIRI were consented into the study to investigate γ -H2AX expression in CTCs (National Research Ethics Service Committee, NRES, London, Bloomsbury, 12/LO/1654). Patient demographics and baseline characteristics are shown in Table 6.1. Patients information was not available for three patients and two patients were incorrectly enrolled as not having sites of metastases and had not received any prior lines of chemotherapy. For the remaining 11 patients, 64% were male, median (range) age was 68 (32–74), the most common histology type was adenocarcinoma of the colon (55% of patients), the most common site of metastases was the liver (91% of patients), median (range) prior lines of chemotherapy was 2 (1–6), and the most common last chemotherapy was FOLFIRI in combination with bevacizumab (Avastin; 45% of patients).

Table 6.1. Patient demographics and baseline characteristics

Sample number	Sex	Age	Histology	Site(s) of metastases	Lines of prior chemotherapy	Last chemotherapy
001	NA					
002	F	64	Adc colon	Liver	1	Folfox
003	M	64	Adc rectum	Nodal	3	Folfiri + avastin
004	M	32	Adc colon	Liver, peritoneum	1	Folfox + avastin
005	F	74	Adc colon	Liver, lung, omental, peritoneal	6	Folfiri
006	M	68	Adc cecal, ascending Colon	No metastases	0	Folfox
007	F	74	Adc colon	Liver, peritoneum	2	Folfiri + avastin
008	M	73	Adc colon	Liver, lung	1	Folfiri + avastin
009	M	72	Adc rectum	Liver, pelvis, LN	2	Folfiri + avastin
010	F	65	Adc colon	No metastases	0	Adjuvant folfox
011	M	68	Adc colo-rectum	Liver, lung, bone, brain	2	Folfiri + avastin
012	NA					
013	F	60	Adc rectum	Liver, portal vein, LN	1	Folfox + avastin
014	M	58	Adc colo-rectum	Liver, LN	1	Folfox + avastin
015	M	73	Adc colon	Liver	2	Folfiri
016	NA					

Adc, adenocarcinoma; F, female; M, male; LN, lymph node; NA, patient information not available

6.3 Patient Laboratory Measurements Results

The majority of patients did not have any CTCs in the samples collected pre- or post-infusion. Only one of 16 patients (011) had both a pre-chemotherapy CTC that was negative for γ -H2AX and a CTC following chemotherapy that was positive for γ -H2AX. Two samples contained CTCs that were positive for γ -H2AX in both the pre- and post-chemotherapy samples (001, 015), three had CTCs positive for γ -H2AX only in the pre-chemotherapy samples (003, 004, 014) and in sample 008 we found only one CTC positive for γ -H2AX in the sample post-chemotherapy but no CTC samples were obtained from the pre-infusion blood (Table 6.2).

Table 6.2. CTC collection and γ -H2AX analysis of patient samples pre- and post-chemotherapy with FOLFOX or FOLFIRI using the CellSearch platform and Analyzer II

Sample number	CTCs obtained pre-chemotherapy	Pre-chemotherapy CTCs positive for γ -H2AX	CTCs obtained post-chemotherapy	Post-chemotherapy CTCs positive for γ -H2AX
001	1	1	1	1
002	0	0	0	0
003	1	1	1	0
004	1	1	1	0
005	2	0	0	0
006	0	0	0	0
007	0	0	0	0
008	0	0	1	1
009	0	0	0	0
010	0	0	0	0
011	1	0	1	1
012	0	0	0	0
013	0	0	0	0
014	2	2	0	0
015	21	5	17	4
016	0	Sample could not be scanned due to ferrofluid aggregates in the cartridge	0	0

6.4. Discussion and Conclusions

The aim of this study was to determine if the CellSearch platform and the CellSearch Analyzer II were suitable tools to isolate CTCs and determine γ -H2AX expression in CTCs from peripheral blood samples from patients with CRC prior to, and following treatment with FOLFOX or FOLFIRI, followed by the use of the DEPArray machine. If both the number of CTCs could be identified and γ -H2AX expression levels determined before and after treatment with chemotherapy it may be possible to determine if the patient is responding to their chemotherapy treatment. As described earlier, CTC counts correlate

with clinical outcome in several cancers including breast, prostate, colorectal and lung cancer [290]. In addition, pre- and post-treatment CTC counts can be used as prognostic and predictive biomarkers of response to treatment [290]. Many anticancer treatments, including chemotherapy, act by damaging DNA and hindering cell function and proliferation. γ -H2AX accumulates in cells as an early response to DNA double-strand breaks, which is the most deleterious lesion as a result of anticancer therapy and therefore γ -H2AX is generally considered as a surrogate marker of DNA damage [291]. γ -H2AX could therefore be used as a predictive biomarker of early response to treatment and may help aid a more personalised treatment approach to patients receiving chemotherapy.

In the current study, it was demonstrated that we were able to isolate CTCs from peripheral blood samples from patients with CRC using the CellSearch platform and we were able to demonstrate the presence of CTCs that expressed γ -H2AX. However, in all but one sample (015), the numbers of CTCs were lower than would be expected as CTCs have been reported to be found in frequencies in the order of 1–10 CTCs per ml of peripheral blood in patients with metastatic disease [178, 291]. Up to 15 ml of peripheral blood was used in the current experiment and therefore we would have expected over 15 CTCs per sample if patients had metastatic disease. It is unknown as to why low numbers of CTCs were observed. As one sample contained a relatively high number of CTCs, it is unlikely that methodological reasons are due to the low number of CTCs observed. Reasons could be due to patients having a small tumour burden, or the low number of patients enrolled in this study compared with those previously reported, which may have contributed to the non-conclusive results obtained. Unfortunately, due to time constraints it was not possible to collect additional samples.

Similarly, the data from the CTCs that expressed γ -H2AX were also inconclusive, with only one patient having a pre-chemotherapy CTC that was negative for γ -H2AX and a CTC following chemotherapy that was positive for γ -H2AX. There were a number of patients who had CTCs that were positive for γ -H2AX prior to chemotherapy, this could be due to several reasons including CTCs undergoing apoptosis prior to their chemotherapy,

possibly as a carryover from previous treatment lines as patients who had received previous treatments were allowed to enter the study.

CHAPTER 7: Overall Discussion and Conclusions

Colorectal cancer is the third most common cancer in males and females and the fourth overall in the UK, accounting for 13% of all new cases [1]. There are currently no predictive biomarkers available to assess the response to chemotherapy for a patient with CRC. γ -H2AX foci represent double strand DNA breaks and therefore DNA damage. γ -H2AX induction has been studied in cancer cells treated with different chemotherapy agents and in CTCs from patient blood samples processed using the CellSearch system in conjunction with γ -H2AX-AF488 antibody staining. γ -H2AX signal was detected as a percentage of γ -H2AX-positive CTCs per total CTCs recovered following chemotherapy [214]. However, at present this is still an unmet need since the current methods available for the detection of DNA damage in patient samples have showed a limited applicability in the clinic to monitor tumour response to chemotherapy. Compared with other approaches, the combination of CTC enrichment with nuclear γ -H2AX detection is a distinctive and innovative technique that could provide valuable information on a patients' response to treatment and their prognosis. The development of a high throughput γ -H2AX foci-counting system for clinical utilisation to allow a faster analysis and automated microscopic examination may provide this [214, 244, 288]. It is still unknown whether detecting γ -H2AX in CTCs will correlate with clinical efficacy and clinical trials are currently investigating the correlation between drug effects on disease progression with γ -H2AX-positive CTCs. Examples of such studies include NCT00576654 and NCT01386385 which are evaluating the effect of veliparib in combination with chemotherapies in advanced solid tumours or advanced non-small cell lung cancer, respectively.

The studies presented here were performed to address the lack of a method allowing the quantification of the γ -H2AX induction in CTCs; the study aimed to develop a method to quantify changes in γ -H2AX (as a marker of DNA damage and therefore response to treatment) in CTCs from mCRC patients undergoing treatment with FOLFOX or FOLFIRI, using the DEPArray System as a new approach.

The initial feasibility experiments investigated the induction of γ -H2AX foci on human adenocarcinoma colorectal cells (HT-29 cells) by performing dose response experiments

with increasing concentrations of oxaliplatin and SN-38, and to select doses of these drugs that induce a peak of γ -H2AX foci for use in future experiments. An increase in the number of γ -H2AX foci were observed after treatment with oxaliplatin and SN-38 (Figures 3.2 and 3.4), in agreement with previous studies that showed that H2AX was phosphorylated in response to DNA DSBs induced by DNA topo I cleavage complexes [276] and oxaliplatin [266]. In colorectal cancer cells, treatment with 1, 5, and 10 μ M oxaliplatin for 2 hours generated more γ -H2AX foci than in untreated cells, and more foci formed with increasing drug concentrations (Figure 3.2). Using the same doses and time of drug exposure as that used for oxaliplatin, following SN-38 treatment more foci per cell were detected likely due to the occurrence of continual DNA DSBs. It is possible that the different responses observed between the same concentrations of oxaliplatin and SN-38 in HT-29 cells is because the IC₅₀ of oxaliplatin is greater than that of SN-38 (22.17 vs 1.93, respectively [278]). When HT-29 cells were incubated with lower concentrations of SN-38 foci were detected after 1 hour of drug exposure at the 0.01 and 0.05 μ M SN-38 doses (Figure 3.4). Based on these results, the final concentrations that were selected for the time course experiments (Chapter 4) were 5 μ M and 0.01 μ M for oxaliplatin and SN-38, respectively. Following the feasibility experiments, a time course study was performed to determine any changes in the levels of, and temporal differences including the time of γ -H2AX foci peak in human adenocarcinoma colorectal cells following treatment with oxaliplatin and SN-38. The tumour suppressor p53 protein is a transcription factor inducing cell cycle arrest, senescence, and apoptosis under cellular stress. Dysregulation of *TP53* tumour suppressor gene is one of the most frequent events contributing to the transformation of CRC, as well as the aggressive and metastatic features of CRC. Different types of *TP53* mutations play a pivotal role in determining the biologic behaviour of CRC, such as invasive depth, metastatic site and even the prognosis of patients [279]. The HT-29 cell type has been reported to express a mutated *p53* gene whereas the HCT-116 cell line does not [280]. As the *TP53* gene mutation in HT-29 cells may affect the response to treatment the time course experiments assessed both cell types. The aim of these time course experiments was to determine the optimum time for CTC collection from patients

post infusion of FOLFOX or FOLFIRI and to provide data for the γ -H2AX quantification using the CellSearch and DEPArray platform. These studies demonstrated a sustained increase in the number of γ -H2AX foci formations following treatment of the HT-29 and HCT-116 cells with oxaliplatin and SN-38 (Figures 4.1–4.8) in agreement with previous studies [283]. The rise of foci was observed between 2–6 hours post-treatment, after which they gradually decreased returning close to the baseline distribution at 26 hours due to DNA repair. Minor differences were observed between the two CRC cell lines in response to treatment with oxaliplatin or SN-38; in both cells, there was a rapid peak to a mean of ~10 foci/group in the first hour post-treatment which plateaued at a steady rate until 18 hours post-dose where the mean γ -H2AX foci/group declined to ~10 (7.32-11.73), and 6-8 foci/group by 26 hours post dose (6.22-8.57). The minor differences that were nevertheless observed with the different treatments and cell lines used could be explained by the different mode of action of the drugs as well as intrinsic differences in the cell lines. As noted above, the genetic status of the different cell lines may contribute to differences observed between the two cell lines used; the presence of *TP53* gene mutations (as well as *BRAF* mutations) in HT-29 cells may result in the cells responding to treatment differently [280]. Oxaliplatin and SN-38 are pharmacologically distinct and have different mechanisms of action. Various mechanisms of action are ascribed to oxaliplatin however like other platinum-based compounds, oxaliplatin exerts its cytotoxic effect mostly through DNA damage by causing DNA lesions (crosslinks), arresting DNA synthesis and through the inhibition of messenger RNA synthesis [274]. The active form of SN-38, irinotecan, inhibits the action of topoisomerase I, preventing relegation of the DNA strand by binding to the topoisomerase I-DNA complex. The formation of a cleavable drug-Topoisomerase I-DNA complex results in lethal double-strand DNA breakage and cell death [284]. These differences in the mode of action of the drugs resulting in DNA damage, as well as genetic differences of the cell lines used, may contribute to the different temporal effects in the formation of γ -H2AX foci that were observed. Based on these results, the optimal time for CTC collection from patients was determined to be 2 hours post infusion of FOLFOX or FOLFIRI. This time point was chosen as: 1. γ -H2AX induction was observed with both cell lines and

treatments at this time point; 2. 2 hours post-infusion would avoid patients having to undergo a prolonged stay in the hospital following completion of their treatment.

Next, a protocol for the quantification of γ -H2AX intensity using the CellSearch System and the DEPArray System was developed which aimed to evaluate the γ -H2AX signal using both systems with *in vitro* validation using human adenocarcinoma colorectal cells treated with oxaliplatin, SN-38 or topotecan which could be used for future clinical applications as an early indicator of response to treatment. The CellSearch System (CellSearch Circulating Tumour Cell Kit; CellTracks Autoprep System; CellTracks Analyzer II) was previously validated to detect γ -H2AX induction in topotecan treated or X-ray irradiated and untreated HT-29 CRC cells spiked into peripheral blood from healthy donors (Section 5.2). The CellTracks Analyzer II provides data on the overall number of CTCs present within the sample as well as the number and percentage of CTCs which are positive for γ -H2AX. The results from these validation experiments demonstrated that the CellSearch Circulating Tumour Cell Kit and the CellSearch CellTracks Autoprep System, using the Anti-phospho-Histone H2A.X (ser139), clone JBW301, FITC conjugated γ -H2AX antibody (57 μ g/mL), with the CellTracks Analyzer II (with exposure for the fourth channel [FITC] set at 3 seconds) can identify the overall number of CTCs consistent with those that were included in the spiked samples (Tables 5.1–5.4) and can detect γ -H2AX in the cells. In blood that was spiked with HT-29 cells X-ray irradiated or treated with topotecan had CTCs positive for γ -H2AX above the pre-defined NCI acceptance threshold of $\geq 10\%$ positive for γ -H2AX whereas untreated HT-29 spiked samples had low numbers of CTCs positive for γ -H2AX were detected, all of which were below the pre-defined threshold of $\leq 3\%$ positive for γ -H2AX.

I evaluated the CellSearch System combined with the DEPArray platform using HT-29 cells treated with oxaliplatin or SN-38 spiked into peripheral blood from healthy volunteers. The samples were processed on the CellTracks Autoprep system using a different γ -H2AX antibody (Mouse anti-H2AX monoclonal primary antibody and Goat anti-mouse Alexa Fluor 488 IgG secondary antibody) than previously used. This method was shown to be effective for determining CTCs based on cell morphology, positivity for CK-PE and DAPI

and negativity for CD45-APC however the rate of γ -H2AX induction in oxaliplatin and SN-38 treated cells was low following CellSearch analysis with many of the positive cells having a faint signal for γ -H2AX; 177 cells out of the 1158 (15.28%) cells treated with oxaliplatin and 217 cells out of 1181 (18.37%) cells treated with SN-38 were detected as being γ -H2AX positive compared with 5.10% for the untreated controls (Figure 5.2). This could be explained by 1. the use of different treatment protocols for the fixation and staining of the cells, and 2. the different antibodies used as described above. The CellSearch System allows detection of the FITC stain in the nuclei of the cells if they were γ -H2AX positive, but the distinct foci were not visible due to the low magnification limitation of the CellSearch System platform (20x). The cells used in these experiments were then evaluated on the DEPArray platform. Following several DEPArray set-up modifications (Section 5.3.4) which were required for the identification of the DEPArray FITC signal after the CellSearch scan of the cell samples, a clear discrimination between cells expressing or not expressing γ -H2AX was not observed due to a possible bleaching of the cells because of the CellSearch cartridge scanning. Thus, no difference in signal intensity between the treated and untreated cells could be found; the long exposure time and gain required increased the level of the background resulting in a low signal/background ratio. As γ -H2AX positive cells could not be identified using the DEPArray System after the CellSearch System, we evaluated the DEPArray platform without using the CellSearch methods beforehand. HT-29 cells were either untreated or treated with oxaliplatin or SN-38 with and without antibody labelling for γ -H2AX, the cells were then evaluated using the DEPArray system with two different exposure times for FITC. The results from these experiments showed a significantly increased intensity of FITC staining for SN-38 treated cells compared with the untreated control group for both FITC I ($P < 0.0001$) and FITC II ($P < 0.004$; Tables 5.8–5.9; Figure 5.8) demonstrating that the DEPArray system was able to quantify differences in signal intensity as a result of drug induction of γ -H2AX in colon cancer cells. The use of fluorescence microscopy validated the data observed with the DEPArray platform. There were no detectable γ -H2AX cells observed in HT-29 cells treated with SN-38 but without the γ -H2AX antibody or in untreated cells with the γ -H2AX

antibody present. In contrast, in SN-38 treated cells with the γ -H2AX antibody present there was a visible increase in γ -H2AX positive cells. Unfortunately during the analysis, most of the treated cells were lost due to the washing and spinning steps involved and the total amount of cells were not sufficient to make accurate and validated comparisons. This was particularly evident in cells treated with oxaliplatin.

As any future development methods will require analysis on the CellSearch System to allow optimisation for patient samples, subsequent experiments were carried out on HT-29 cells treated with topotecan spiked into peripheral blood from healthy volunteers followed by staining for γ -H2AX and analysis on the CellSearch system prior to DEPArray analysis to investigate whether scanning of CTCs with the CellSearch System could have affected the intensity of the FITC signal background and signal/background ratio detected by DEPArray process. These experiments were performed using treated cells that were used for the validation of the detection of γ -H2AX on CTCs using the CellSearch CellTracks Autoprep System with and without prior scanning with the CellTracks Analyzer II. In the first experiment the results showed a statistically significant increase in intensity of the FITC I and FITC II signal in the sample that was previously scanned in the CellSearch platform and then assessed on the DEPArray platform. However, due to an experimental error, the results of the first experiment could not be further evaluated and confirmed and therefore two additional experiments were performed. The results showed a statistically significant increase of intensity in the CellSearch/CellTracks Analyzer II unscanned samples when compared with the scanned samples for FITC II ($P=0.0001$) in the second validation, and for both FITC I and FITC II in the third validation ($P=0.0001$). FITC I in the second validation was not statistically significant ($P=0.09$) and therefore a difference in signal intensity between the CellSearch/CellTracks Analyzer II scanned and unscanned sample was not confirmed. Unfortunately, as in the previous experiments, most of the PE+/DAPI+/APC- cells did not show a clear positivity in the FITC channels. DEPArray analysis allowed the identification of only four cells in which FITC II and background intensity level were at least comparable (Figure 5.14). Due to low FITC I signal

intensity, the data for the second and third validations were re-evaluated taking into consideration only the mean intensity values of FITC II, rather than the mean intensity with the background subtracted. Following the analysis of selected cells, it was noted that they fell within a wide range of signal intensities with two groups of CTCs being distinguished: the first group had a high mean intensity value and a second group had low mean intensity values. Statistical analyses were performed on the two separate groups to determine if it was appropriate to separate the groups for further analyses. The results from these additional analyses confirmed a statistically significant increase in intensity in the unscanned samples for FITCII in both the second ($P=0.03$) and third ($P=0.0001$) validations when compared with the scanned samples. In addition, when the distribution of the FITCII intensity for these analyses was evaluated the distribution and therefore γ -H2AX staining of the CellTracks Analyser II unscanned samples appeared to be more specific than the scanned samples for both validation runs (Figure 5.23). These studies appear to show that when cells are identified using the CellSearch system and scanned with the CellTracks Analyser II prior to DEPArray analysis for γ -H2AX intensity, the signal for γ -H2AX is lost when compared to cells that are not scanned with the CellTracks Analyser II. Therefore, future validation of these methods should exclude analysis of isolated cells with the CellTracks Analyser II, instead moving straight to analysis with the DEPArray system.

Once a protocol had been developed for the identification of γ -H2AX foci on isolated CTCs, it was utilized to demonstrate the feasibility of γ -H2AX signal quantification as a predictive radiological biomarker of response (i.e. investigate its utility in predicting early response to treatment) in CTCs from patients with CRC. These experiments aimed to determine if the CellSearch platform and the CellSearch Analyzer II were suitable tools to isolate CTCs and determine γ -H2AX expression in CTCs from peripheral blood samples from patients with CRC prior to, and following treatment with FOLFOX or FOLFIRI, followed by the DEPArray platform. If both the number of CTCs could be identified and γ -H2AX expression levels determined before and after treatment with chemotherapy it may be possible to determine if the patient is responding to their chemotherapy treatment. As described

earlier, CTC counts correlate with clinical outcome in several cancers including breast, prostate, colorectal and lung cancer [290]. Due to the mechanism of action of most anticancer treatments, γ -H2AX accumulates in cells as an early response to DNA double-strand breaks, therefore γ -H2AX is generally considered as a surrogate marker of DNA damage [291]. γ -H2AX could be used as a predictive biomarker of early response to treatment and may help aid a more personalised treatment approach to patients receiving chemotherapy [290]. In the study performed here, we were able to isolate CTCs from peripheral blood samples from patients with CRC using the CellSearch platform and we were able to demonstrate the presence of CTCs that expressed γ -H2AX. However, in all but one sample the numbers of CTCs were lower than would be expected and the reasons for this are unknown; CTCs have been reported to be found in frequencies in the order of 1–10 CTCs per ml of peripheral blood in patients with metastatic disease [178, 291]. As one sample contained a relatively high number of CTCs, it is unlikely that methodological reasons have caused the low number of CTCs observed. Potential explanations include patients having a small tumour burden, or the low number of patients enrolled in this study compared with those previously reported, which may have contributed to the non-conclusive results obtained. Unfortunately, due to time constraints it was not possible to collect additional samples. Similarly, the data from the CTCs that expressed γ -H2AX were also inconclusive, with only one patient having a pre-chemotherapy CTC that was negative for γ -H2AX and a CTC following chemotherapy that was positive for γ -H2AX. There were a number of patients who had CTCs that were positive for γ -H2AX prior to chemotherapy, this could be due to several reasons including CTCs undergoing apoptosis prior to their chemotherapy, possibly as a carryover from previous treatment lines as patients who had received previous treatments were allowed to enter the study.

Additional aims of this study which were not undertaken due to time constraints were to quantify γ -H2AX expression in CTCs using a combined modality approach using the CellSearch and DEPArray platforms and to evaluate γ -H2AX in CTCs as a predictive biomarker (i.e. investigate its utility in predicting early response to treatment). Further research is required to determine if the CellSearch and DEPArray platforms could be

utilised together to determine if both CTC counts and the expression of γ -H2AX in CTCs from peripheral blood samples of patients with CRC could be used to predict early patient outcomes to chemotherapy treatment.

References

1. Siegel, R., C. Desantis, and A. Jemal, *Colorectal cancer statistics, 2014*. CA Cancer J Clin, 2014. 64(2): p. 104-17.
2. Siegel, R.L., K.D. Miller, and A. Jemal, *Cancer statistics, 2016*. CA Cancer J Clin, 2016. 66(1): p. 7-30.
3. Doubeni, C.A., et al., *Socioeconomic status and the risk of colorectal cancer: an analysis of more than a half million adults in the National Institutes of Health-AARP Diet and Health Study*. Cancer, 2012. 118(14): p. 3636-44.
4. Jemal, A., et al., *Global cancer statistics*. CA Cancer J Clin, 2011. 61(2): p. 69-90.
5. Willett, W.C., *Diet and cancer: an evolving picture*. JAMA, 2005. 293(2): p. 233-4.
6. Doubeni, C.A., et al., *Contribution of behavioral risk factors and obesity to socioeconomic differences in colorectal cancer incidence*. J Natl Cancer Inst, 2012. 104(18): p. 1353-62.
7. Center, M.M., A. Jemal, and E. Ward, *International trends in colorectal cancer incidence rates*. Cancer Epidemiol Biomarkers Prev, 2009. 18(6): p. 1688-94.
8. Davis, D.M., et al., *Is it time to lower the recommended screening age for colorectal cancer?* J Am Coll Surg, 2011. 213(3): p. 352-61.
9. Singh, K.E., et al., *Colorectal Cancer Incidence Among Young Adults in California*. J Adolesc Young Adult Oncol, 2014. 3(4): p. 176-184.
10. Tawadros, P.S., et al., *Adenocarcinoma of the rectum in patients under age 40 is increasing: impact of signet-ring cell histology*. Dis Colon Rectum, 2015. 58(5): p. 474-8.
11. Ryerson, A.B., et al., *Annual Report to the Nation on the Status of Cancer, 1975-2012, featuring the increasing incidence of liver cancer*. Cancer, 2016. 122(9): p. 1312-37.
12. Center, M.M., et al., *Worldwide variations in colorectal cancer*. CA Cancer J Clin, 2009. 59(6): p. 366-78.
13. Eddy, D.M., *Screening for colorectal cancer*. Ann Intern Med, 1990. 113(5): p. 373-84.
14. Burt, R.W., J.A. DiSario, and L. Cannon-Albright, *Genetics of colon cancer: impact of inheritance on colon cancer risk*. Annu Rev Med, 1995. 46: p. 371-9.
15. Lynch, H.T., et al., *Genetics, natural history, tumor spectrum, and pathology of hereditary nonpolyposis colorectal cancer: an updated review*. Gastroenterology, 1993. 104(5): p. 1535-49.
16. Ponz de Leon, M., et al., *Identification of hereditary nonpolyposis colorectal cancer in the general population. The 6-year experience of a population-based registry*. Cancer, 1993. 71(11): p. 3493-501.

17. Troisi, R.J., A.N. Freedman, and S.S. Devesa, *Incidence of colorectal carcinoma in the U.S.: an update of trends by gender, race, age, subsite, and stage, 1975-1994*. *Cancer*, 1999. 85(8): p. 1670-6.
18. Jessup, J.M., et al., *The National Cancer Data Base. Report on colon cancer*. *Cancer*, 1996. 78(4): p. 918-26.
19. Vasen, H.F., et al., *Familial colorectal cancer risk: ESMO clinical recommendations*. *Ann Oncol*, 2009. 20 Suppl 4: p. 51-3.
20. Jasperson, K.W., et al., *Hereditary and familial colon cancer*. *Gastroenterology*, 2010. 138(6): p. 2044-58.
21. Samadder, N.J., K. Jasperson, and R.W. Burt, *Hereditary and common familial colorectal cancer: evidence for colorectal screening*. *Dig Dis Sci*, 2015. 60(3): p. 734-47.
22. Fearnhead, N.S., M.P. Britton, and W.F. Bodmer, *The ABC of APC*. *Hum Mol Genet*, 2001. 10(7): p. 721-33.
23. Palomaki, G.E., et al., *EGAPP supplementary evidence review: DNA testing strategies aimed at reducing morbidity and mortality from Lynch syndrome*. *Genet Med*, 2009. 11(1): p. 42-65.
24. Ekbohm, A., et al., *Ulcerative colitis and colorectal cancer. A population-based study*. *N Engl J Med*, 1990. 323(18): p. 1228-33.
25. Farraye, F.A., et al., *AGA technical review on the diagnosis and management of colorectal neoplasia in inflammatory bowel disease*. *Gastroenterology*, 2010. 138(2): p. 746-74, 774 e1-4; quiz e12-3.
26. Farraye, F.A., et al., *AGA medical position statement on the diagnosis and management of colorectal neoplasia in inflammatory bowel disease*. *Gastroenterology*, 2010. 138(2): p. 738-45.
27. Stewart, R.J., et al., *Sex differences in subsite incidence of large-bowel cancer*. *Dis Colon Rectum*, 1983. 26(10): p. 658-60.
28. Schub, R. and F.U. Steinheber, *Rightward shift of colon cancer. A feature of the aging gut*. *J Clin Gastroenterol*, 1986. 8(6): p. 630-4.
29. Mamazza, J. and P.H. Gordon, *The changing distribution of large intestinal cancer*. *Dis Colon Rectum*, 1982. 25(6): p. 558-62.
30. Vukasin, A.P., et al., *Increasing incidence of cecal and sigmoid carcinoma. Data from the Connecticut Tumor Registry*. *Cancer*, 1990. 66(11): p. 2442-9.
31. Garden, O.J., et al., *Guidelines for resection of colorectal cancer liver metastases*. *Gut*, 2006. 55 Suppl 3: p. iii1-8.
32. Ajithkumar, T.V., *Oxford desk reference. Oncology*. Oxford desk reference. 2011, Oxford ; New York: Oxford University Press. xxi, 714 p.

33. Ireland, T.A.o.C.o.G.B.a., *Guidelines for the Management of Colorectal Cancer*. 2007.
34. Polat, E., et al., *Diagnostic value of preoperative serum carcinoembryonic antigen and carbohydrate antigen 19-9 in colorectal cancer*. *Curr Oncol*, 2014. 21(1): p. e1-7.
35. Edge, S., et al., *AJCC Cancer Staging Manual*. 7 ed. 2010: Springer-Verlag New York. XV, 648.
36. Wiggers, T., J.W. Arends, and A. Volovics, *Regression analysis of prognostic factors in colorectal cancer after curative resections*. *Dis Colon Rectum*, 1988. 31(1): p. 33-41.
37. Chapuis, P.H., et al., *A multivariate analysis of clinical and pathological variables in prognosis after resection of large bowel cancer*. *Br J Surg*, 1985. 72(9): p. 698-702.
38. Tominaga, T., et al., *Prognostic factors for patients with colon or rectal carcinoma treated with resection only. Five-year follow-up report*. *Cancer*, 1996. 78(3): p. 403-8.
39. Shepherd, N.A., K.J. Baxter, and S.B. Love, *The prognostic importance of peritoneal involvement in colonic cancer: a prospective evaluation*. *Gastroenterology*, 1997. 112(4): p. 1096-102.
40. Wolmark, N., B. Fisher, and H.S. Wieand, *The prognostic value of the modifications of the Dukes' C class of colorectal cancer. An analysis of the NSABP clinical trials*. *Ann Surg*, 1986. 203(2): p. 115-22.
41. Chen, S.L. and A.J. Bilchik, *More extensive nodal dissection improves survival for stages I to III of colon cancer: a population-based study*. *Ann Surg*, 2006. 244(4): p. 602-10.
42. Tepper, J.E., et al., *Impact of number of nodes retrieved on outcome in patients with rectal cancer*. *J Clin Oncol*, 2001. 19(1): p. 157-63.
43. Baxter, N.N., et al., *An evaluation of the relationship between lymph node number and staging in pT3 colon cancer using population-based data*. *Dis Colon Rectum*, 2010. 53(1): p. 65-70.
44. Chang, G.J., et al., *Lymph node evaluation and survival after curative resection of colon cancer: systematic review*. *J Natl Cancer Inst*, 2007. 99(6): p. 433-41.
45. Berger, A.C., et al., *Colon cancer survival is associated with decreasing ratio of metastatic to examined lymph nodes*. *J Clin Oncol*, 2005. 23(34): p. 8706-12.
46. Ceelen, W., Y. Van Nieuwenhove, and P. Pattyn, *Prognostic value of the lymph node ratio in stage III colorectal cancer: a systematic review*. *Ann Surg Oncol*, 2010. 17(11): p. 2847-55.

47. Moore, J., et al., *Staging error does not explain the relationship between the number of lymph nodes in a colon cancer specimen and survival*. *Surgery*, 2010. 147(3): p. 358-65.
48. Parsons, H.M., et al., *Association between lymph node evaluation for colon cancer and node positivity over the past 20 years*. *JAMA*, 2011. 306(10): p. 1089-97.
49. Compton, C., et al., *American Joint Committee on Cancer Prognostic Factors Consensus Conference: Colorectal Working Group*. *Cancer*, 2000. 88(7): p. 1739-57.
50. Willett, C.G., et al., *Does postoperative irradiation play a role in the adjuvant therapy of stage T4 colon cancer?* *Cancer J Sci Am*, 1999. 5(4): p. 242-7.
51. Wittekind, C., et al., *TNM residual tumor classification revisited*. *Cancer*, 2002. 94(9): p. 2511-6.
52. Betge, J., et al., *Intramural and extramural vascular invasion in colorectal cancer: prognostic significance and quality of pathology reporting*. *Cancer*, 2012. 118(3): p. 628-38.
53. Sternberg, A., et al., *Validation of a new classification system for curatively resected colorectal adenocarcinoma*. *Cancer*, 1999. 86(5): p. 782-92.
54. Takahashi, Y., et al., *Vessel counts and expression of vascular endothelial growth factor as prognostic factors in node-negative colon cancer*. *Arch Surg*, 1997. 132(5): p. 541-6.
55. Quah, H.M., et al., *Identification of patients with high-risk stage II colon cancer for adjuvant therapy*. *Dis Colon Rectum*, 2008. 51(5): p. 503-7.
56. Wolmark, N., et al., *The prognostic significance of preoperative carcinoembryonic antigen levels in colorectal cancer. Results from NSABP (National Surgical Adjuvant Breast and Bowel Project) clinical trials*. *Ann Surg*, 1984. 199(4): p. 375-82.
57. Thirunavukarasu, P., et al., *C-stage in colon cancer: implications of carcinoembryonic antigen biomarker in staging, prognosis, and management*. *J Natl Cancer Inst*, 2011. 103(8): p. 689-97.
58. Locker, G.Y., et al., *ASCO 2006 update of recommendations for the use of tumor markers in gastrointestinal cancer*. *J Clin Oncol*, 2006. 24(33): p. 5313-27.
59. Hamilton, S.R. and L.A. Aaltonen, *World Health Organization Classification of Tumours of the Digestive System*. International Agency for Research on Cancer (IARC), 2000.
60. Fleming, M., et al., *Colorectal carcinoma: Pathologic aspects*. *J Gastrointest Oncol*, 2012. 3(3): p. 153-73.
61. Green, J.B., et al., *Mucinous carcinoma--just another colon cancer?* *Dis Colon Rectum*, 1993. 36(1): p. 49-54.

62. Secco, G.B., et al., *Primary mucinous adenocarcinomas and signet-ring cell carcinomas of colon and rectum*. *Oncology*, 1994. 51(1): p. 30-4.
63. Consorti, F., et al., *Prognostic significance of mucinous carcinoma of colon and rectum: a prospective case-control study*. *J Surg Oncol*, 2000. 73(2): p. 70-4.
64. Nitsche, U., et al., *Mucinous and signet-ring cell colorectal cancers differ from classical adenocarcinomas in tumor biology and prognosis*. *Ann Surg*, 2013. 258(5): p. 775-82; discussion 782-3.
65. Shin, U.S., et al., *Mucinous rectal cancer: effectiveness of preoperative chemoradiotherapy and prognosis*. *Ann Surg Oncol*, 2011. 18(8): p. 2232-9.
66. Lee, D.W., et al., *Prognostic implication of mucinous histology in colorectal cancer patients treated with adjuvant FOLFOX chemotherapy*. *Br J Cancer*, 2013. 108(10): p. 1978-84.
67. Nissan, A., et al., *Signet-ring cell carcinoma of the colon and rectum: a matched control study*. *Dis Colon Rectum*, 1999. 42(9): p. 1176-80.
68. Psathakis, D., et al., *Ordinary colorectal adenocarcinoma vs. primary colorectal signet-ring cell carcinoma: study matched for age, gender, grade, and stage*. *Dis Colon Rectum*, 1999. 42(12): p. 1618-25.
69. Frizelle, F.A., et al., *Adenosquamous and squamous carcinoma of the colon and upper rectum: a clinical and histopathologic study*. *Dis Colon Rectum*, 2001. 44(3): p. 341-6.
70. Masoomi, H., et al., *Population-based evaluation of adenosquamous carcinoma of the colon and rectum*. *Dis Colon Rectum*, 2012. 55(5): p. 509-14.
71. Petrelli, N.J., et al., *Adenosquamous carcinoma of the colon and rectum*. *Dis Colon Rectum*, 1996. 39(11): p. 1265-8.
72. Compton, C.C., et al., *Prognostic factors in colorectal cancer. College of American Pathologists Consensus Statement 1999*. *Arch Pathol Lab Med*, 2000. 124(7): p. 979-94.
73. Sauer, R., et al., *Preoperative versus postoperative chemoradiotherapy for rectal cancer*. *N Engl J Med*, 2004. 351(17): p. 1731-40.
74. Joye, I. and K. Haustermans, *Clinical target volume delineation for rectal cancer radiation therapy: time for updated guidelines?* *Int J Radiat Oncol Biol Phys*, 2015. 91(4): p. 690-1.
75. Hernando-Requejo, O., et al., *Complete pathological responses in locally advanced rectal cancer after preoperative IMRT and integrated-boost chemoradiation*. *Strahlenther Onkol*, 2014. 190(6): p. 515-20.
76. Sastre, J., et al., *Risk-adapted adjuvant chemotherapy after concomitant fluoropyrimidine-radiotherapy neoadjuvant treatment for patients with resectable cT3-4 or N+ rectal cancer*. *Anticancer Drugs*, 2011. 22(2): p. 185-90.

77. Rodel, C., et al., *Preoperative chemoradiotherapy and postoperative chemotherapy with fluorouracil and oxaliplatin versus fluorouracil alone in locally advanced rectal cancer: initial results of the German CAO/ARO/AIO-04 randomised phase 3 trial.* *Lancet Oncol*, 2012. 13(7): p. 679-87.
78. Schmoll, H.J., et al., *Preoperative chemoradiotherapy and postoperative chemotherapy with capecitabine and oxaliplatin versus capecitabine alone in locally advanced rectal cancer: Disease-free survival results at interim analysis.* *J Clin Oncol*, 2014. 32(5s): p. abstr 3501.
79. Allegra, C., et al., *Neoadjuvant therapy for rectal cancer: Mature results from NSABP protocol R-04.* *J Clin Oncol*, 2014. 32(Suppl 3): p. abstr 390.
80. Bonjer, H.J., et al., *Laparoscopically assisted vs open colectomy for colon cancer: a meta-analysis.* *Arch Surg*, 2007. 142(3): p. 298-303.
81. Johnston, P.G., *Stage II colorectal cancer: to treat or not to treat.* *Oncologist*, 2005. 10(5): p. 332-4.
82. Sinicrope, F.A., *DNA mismatch repair and adjuvant chemotherapy in sporadic colon cancer.* *Nat Rev Clin Oncol*, 2010. 7(3): p. 174-7.
83. Andre, T., et al., *Adjuvant Fluorouracil, Leucovorin, and Oxaliplatin in Stage II to III Colon Cancer: Updated 10-Year Survival and Outcomes According to BRAF Mutation and Mismatch Repair Status of the MOSAIC Study.* *J Clin Oncol*, 2015. 33(35): p. 4176-87.
84. Goodwin, R.A. and T.R. Asmis, *Overview of systemic therapy for colorectal cancer.* *Clin Colon Rectal Surg*, 2009. 22(4): p. 251-6.
85. Cheeseman, S.L., et al., *A 'modified de Gramont' regimen of fluorouracil, alone and with oxaliplatin, for advanced colorectal cancer.* *Br J Cancer*, 2002. 87(4): p. 393-9.
86. Hochster, H.S., et al., *Safety and efficacy of oxaliplatin and fluoropyrimidine regimens with or without bevacizumab as first-line treatment of metastatic colorectal cancer: results of the TREE Study.* *J Clin Oncol*, 2008. 26(21): p. 3523-9.
87. de Gramont, A., et al., *Randomized trial comparing monthly low-dose leucovorin and fluorouracil bolus with bimonthly high-dose leucovorin and fluorouracil bolus plus continuous infusion for advanced colorectal cancer: a French intergroup study.* *J Clin Oncol*, 1997. 15(2): p. 808-15.
88. Douillard, J.Y., et al., *Irinotecan combined with fluorouracil compared with fluorouracil alone as first-line treatment for metastatic colorectal cancer: a multicentre randomised trial.* *Lancet*, 2000. 355(9209): p. 1041-7.

89. Saltz, L.B., et al., *Irinotecan plus fluorouracil and leucovorin for metastatic colorectal cancer. Irinotecan Study Group.* N Engl J Med, 2000. 343(13): p. 905-14.
90. de Gramont, A., et al., *Leucovorin and fluorouracil with or without oxaliplatin as first-line treatment in advanced colorectal cancer.* J Clin Oncol, 2000. 18(16): p. 2938-47.
91. Giacchetti, S., et al., *Phase III multicenter randomized trial of oxaliplatin added to chronomodulated fluorouracil-leucovorin as first-line treatment of metastatic colorectal cancer.* J Clin Oncol, 2000. 18(1): p. 136-47.
92. Hurwitz, H.I., et al., *Efficacy and safety of bevacizumab in metastatic colorectal cancer: pooled analysis from seven randomized controlled trials.* Oncologist, 2013. 18(9): p. 1004-12.
93. Sobrero, A.F., et al., *EPIC: phase III trial of cetuximab plus irinotecan after fluoropyrimidine and oxaliplatin failure in patients with metastatic colorectal cancer.* J Clin Oncol, 2008. 26(14): p. 2311-9.
94. Bokemeyer, C., et al., *Efficacy according to biomarker status of cetuximab plus FOLFOX-4 as first-line treatment for metastatic colorectal cancer: the OPUS study.* Ann Oncol, 2011. 22(7): p. 1535-46.
95. Van Cutsem, E., et al., *Open-label phase III trial of panitumumab plus best supportive care compared with best supportive care alone in patients with chemotherapy-refractory metastatic colorectal cancer.* J Clin Oncol, 2007. 25(13): p. 1658-64.
96. O'Neil, B.H. and A.P. Venook, *Trying to Understand Differing Results of FIRE-3 and 80405: Does the First Treatment Matter More Than Others?* J Clin Oncol, 2015. 33(32): p. 3686-8.
97. Cassidy, J., et al., *XELOX (capecitabine plus oxaliplatin): active first-line therapy for patients with metastatic colorectal cancer.* J Clin Oncol, 2004. 22(11): p. 2084-91.
98. Tournigand, C., et al., *FOLFIRI followed by FOLFOX6 or the reverse sequence in advanced colorectal cancer: a randomized GERCOR study.* J Clin Oncol, 2004. 22(2): p. 229-37.
99. Goldberg, R.M., et al., *A randomized controlled trial of fluorouracil plus leucovorin, irinotecan, and oxaliplatin combinations in patients with previously untreated metastatic colorectal cancer.* J Clin Oncol, 2004. 22(1): p. 23-30.
100. Maindrault-Goebel, F., et al., *High-dose intensity oxaliplatin added to the simplified bimonthly leucovorin and 5-fluorouracil regimen as second-line therapy for metastatic colorectal cancer (FOLFOX 7).* Eur J Cancer, 2001. 37(8): p. 1000-5.

101. Chibaudel, B., et al., *Can chemotherapy be discontinued in unresectable metastatic colorectal cancer? The GERCOR OPTIMOX2 Study*. J Clin Oncol, 2009. 27(34): p. 5727-33.
102. Grothey, A., et al., *Intermittent oxaliplatin (oxali) administration and time-to-treatment-failure (TTF) in metastatic colorectal cancer (mCRC): Final results of the phase III CONcePT trial*. J Clin Oncol, 2008. 26(15S): p. Abst 4010.
103. Falcone, A., et al., *Phase III trial of infusional fluorouracil, leucovorin, oxaliplatin, and irinotecan (FOLFOXIRI) compared with infusional fluorouracil, leucovorin, and irinotecan (FOLFIRI) as first-line treatment for metastatic colorectal cancer: the Gruppo Oncologico Nord Ovest*. J Clin Oncol, 2007. 25(13): p. 1670-6.
104. Masi, G., et al., *Randomized trial of two induction chemotherapy regimens in metastatic colorectal cancer: an updated analysis*. J Natl Cancer Inst, 2011. 103(1): p. 21-30.
105. Heinemann, V., et al., *FOLFIRI plus cetuximab versus FOLFIRI plus bevacizumab as first-line treatment for patients with metastatic colorectal cancer (FIRE-3): a randomised, open-label, phase 3 trial*. Lancet Oncol, 2014. 15(10): p. 1065-75.
106. Wang, C.C. and J. Li, *An update on chemotherapy of colorectal liver metastases*. World J Gastroenterol, 2012. 18(1): p. 25-33.
107. Bupathi, M., D.H. Ahn, and T. Bekaii-Saab, *Spotlight on bevacizumab in metastatic colorectal cancer: patient selection and perspectives*. Gastrointest Cancer, 2016. 6: p. 21-30.
108. Chau, I. and D. Cunningham, *Treatment in advanced colorectal cancer: what, when and how?* Br J Cancer, 2009. 100(11): p. 1704-19.
109. Tournigand, C., et al., *OPTIMOX1: a randomized study of FOLFOX4 or FOLFOX7 with oxaliplatin in a stop-and-go fashion in advanced colorectal cancer--a GERCOR study*. J Clin Oncol, 2006. 24(3): p. 394-400.
110. Adams, R.A., et al., *Intermittent versus continuous oxaliplatin and fluoropyrimidine combination chemotherapy for first-line treatment of advanced colorectal cancer: results of the randomised phase 3 MRC COIN trial*. Lancet Oncol, 2011. 12(7): p. 642-53.
111. Hochster, H.S., et al., *Improved time to treatment failure with an intermittent oxaliplatin strategy: results of CONcePT*. Ann Oncol, 2014. 25(6): p. 1172-8.
112. Cunningham, D., et al., *Bevacizumab plus capecitabine versus capecitabine alone in elderly patients with previously untreated metastatic colorectal cancer (AVEX): an open-label, randomised phase 3 trial*. Lancet Oncol, 2013. 14(11): p. 1077-85.
113. Hocking, C.M. and T.J. Price, *Panitumumab in the management of patients with KRAS wild-type metastatic colorectal cancer*. Therap Adv Gastroenterol, 2014. 7(1): p. 20-37.

114. De Stefano, A. and C. Carlomagno, *Beyond KRAS: Predictive factors of the efficacy of anti-EGFR monoclonal antibodies in the treatment of metastatic colorectal cancer*. World J Gastroenterol, 2014. 20(29): p. 9732-43.
115. Fakih, M.G., *Metastatic colorectal cancer: current state and future directions*. J Clin Oncol, 2015. 33(16): p. 1809-24.
116. Stintzing, S., et al., *FOLFIRI plus cetuximab versus FOLFIRI plus bevacizumab as first-line treatment for patients with metastatic colorectal cancer-subgroup analysis of patients with KRAS: mutated tumours in the randomised German AIO study KRK-0306*. Ann Oncol, 2012. 23(7): p. 1693-9.
117. Lenz, H.J., et al., *CALGB/SWOG 80405: Phase III trial of irinotecan/5-FU/Leucovorin (FOLFIRI) or oxaliplatin/5-FU/leucovorin (MFOLFOX6) with bevacizumab (BV) or cetuximab (CET) for patients (PTS) with expanded RAS analyses untreated metastatic adenocarcinoma of the colon or rectum (MCRC)* Ann Oncol, 2014. 25(Suppl 5): p. v1-v41.
118. Schwartzberg, L.S., et al., *PEAK: a randomized, multicenter phase II study of panitumumab plus modified fluorouracil, leucovorin, and oxaliplatin (mFOLFOX6) or bevacizumab plus mFOLFOX6 in patients with previously untreated, unresectable, wild-type KRAS exon 2 metastatic colorectal cancer*. J Clin Oncol, 2014. 32(21): p. 2240-7.
119. Giantonio, B.J., et al., *Bevacizumab in combination with oxaliplatin, fluorouracil, and leucovorin (FOLFOX4) for previously treated metastatic colorectal cancer: results from the Eastern Cooperative Oncology Group Study E3200*. J Clin Oncol, 2007. 25(12): p. 1539-44.
120. Joulain, F., et al., *Mean overall survival gain with aflibercept plus FOLFIRI vs placebo plus FOLFIRI in patients with previously treated metastatic colorectal cancer*. Br J Cancer, 2013. 109(7): p. 1735-43.
121. Peeters, M., et al., *Final results from a randomized phase 3 study of FOLFIRI {+/-} panitumumab for second-line treatment of metastatic colorectal cancer*. Ann Oncol, 2014. 25(1): p. 107-16.
122. Cunningham, D., et al., *Cetuximab monotherapy and cetuximab plus irinotecan in irinotecan-refractory metastatic colorectal cancer*. N Engl J Med, 2004. 351(4): p. 337-45.
123. Grothey, A., et al., *Regorafenib monotherapy for previously treated metastatic colorectal cancer (CORRECT): an international, multicentre, randomised, placebo-controlled, phase 3 trial*. Lancet, 2013. 381(9863): p. 303-12.
124. Mayer, R.J., et al., *Randomized trial of TAS-102 for refractory metastatic colorectal cancer*. N Engl J Med, 2015. 372(20): p. 1909-19.

125. Kuczynski, E.A., et al., *Drug rechallenge and treatment beyond progression--implications for drug resistance*. Nat Rev Clin Oncol, 2013. 10(10): p. 571-87.
126. Grady, W.M. and C.C. Pritchard, *Molecular alterations and biomarkers in colorectal cancer*. Toxicol Pathol, 2014. 42(1): p. 124-39.
127. Allegra, C.J., et al., *American Society of Clinical Oncology provisional clinical opinion: testing for KRAS gene mutations in patients with metastatic colorectal carcinoma to predict response to anti-epidermal growth factor receptor monoclonal antibody therapy*. J Clin Oncol, 2009. 27(12): p. 2091-6.
128. Noffsinger, A.E., *Serrated polyps and colorectal cancer: new pathway to malignancy*. Annu Rev Pathol, 2009. 4: p. 343-64.
129. Kane, M.F., et al., *Methylation of the hMLH1 promoter correlates with lack of expression of hMLH1 in sporadic colon tumors and mismatch repair-defective human tumor cell lines*. Cancer Res, 1997. 57(5): p. 808-11.
130. Domingo, E., et al., *BRAF screening as a low-cost effective strategy for simplifying HNPCC genetic testing*. J Med Genet, 2004. 41(9): p. 664-8.
131. Wang, L., et al., *BRAF mutations in colon cancer are not likely attributable to defective DNA mismatch repair*. Cancer Res, 2003. 63(17): p. 5209-12.
132. Popat, S., R. Hubner, and R.S. Houlston, *Systematic review of microsatellite instability and colorectal cancer prognosis*. J Clin Oncol, 2005. 23(3): p. 609-18.
133. Walther, A., R. Houlston, and I. Tomlinson, *Association between chromosomal instability and prognosis in colorectal cancer: a meta-analysis*. Gut, 2008. 57(7): p. 941-50.
134. Siena, S., et al., *Biomarkers predicting clinical outcome of epidermal growth factor receptor-targeted therapy in metastatic colorectal cancer*. J Natl Cancer Inst, 2009. 101(19): p. 1308-24.
135. Walther, A., et al., *Genetic prognostic and predictive markers in colorectal cancer*. Nat Rev Cancer, 2009. 9(7): p. 489-99.
136. Bardelli, A. and S. Siena, *Molecular mechanisms of resistance to cetuximab and panitumumab in colorectal cancer*. J Clin Oncol, 2010. 28(7): p. 1254-61.
137. Chittenden, T.W., et al., *Functional classification analysis of somatically mutated genes in human breast and colorectal cancers*. Genomics, 2008. 91(6): p. 508-11.
138. Deacu, E., et al., *Activin type II receptor restoration in ACVR2-deficient colon cancer cells induces transforming growth factor-beta response pathway genes*. Cancer Res, 2004. 64(21): p. 7690-6.
139. Eppert, K., et al., *MADR2 maps to 18q21 and encodes a TGFbeta-regulated MAD-related protein that is functionally mutated in colorectal carcinoma*. Cell, 1996. 86(4): p. 543-52.

140. Markowitz, S., et al., *Inactivation of the type II TGF-beta receptor in colon cancer cells with microsatellite instability*. Science, 1995. 268(5215): p. 1336-8.
141. Takaku, K., et al., *Intestinal tumorigenesis in compound mutant mice of both Dpc4 (Smad4) and Apc genes*. Cell, 1998. 92(5): p. 645-56.
142. Tanaka, T., et al., *Loss of Smad4 protein expression and 18qLOH as molecular markers indicating lymph node metastasis in colorectal cancer--a study matched for tumor depth and pathology*. J Surg Oncol, 2008. 97(1): p. 69-73.
143. Artale, S., et al., *Mutations of KRAS and BRAF in primary and matched metastatic sites of colorectal cancer*. J Clin Oncol, 2008. 26(25): p. 4217-9.
144. Zauber, P., et al., *Molecular changes in the Ki-ras and APC genes in primary colorectal carcinoma and synchronous metastases compared with the findings in accompanying adenomas*. Mol Pathol, 2003. 56(3): p. 137-40.
145. Rajagopalan, H., et al., *Tumorigenesis: RAF/RAS oncogenes and mismatch-repair status*. Nature, 2002. 418(6901): p. 934.
146. Fuchs, C., et al., *KRAS mutation, cancer recurrence, and patient survival in stage III colon cancer: Findings from CALGB 89803*. J Clin Oncol, 2009. 27(15s): p. abst 4037.
147. Roth, A.D., et al., *Prognostic role of KRAS and BRAF in stage II and III resected colon cancer: results of the translational study on the PETACC-3, EORTC 40993, SAKK 60-00 trial*. J Clin Oncol, 2010. 28(3): p. 466-74.
148. Amado, R.G., et al., *Wild-type KRAS is required for panitumumab efficacy in patients with metastatic colorectal cancer*. J Clin Oncol, 2008. 26(10): p. 1626-34.
149. Bokemeyer, C., et al., *Fluorouracil, leucovorin, and oxaliplatin with and without cetuximab in the first-line treatment of metastatic colorectal cancer*. J Clin Oncol, 2009. 27(5): p. 663-71.
150. Karapetis, C.S., et al., *K-ras mutations and benefit from cetuximab in advanced colorectal cancer*. N Engl J Med, 2008. 359(17): p. 1757-65.
151. Van Cutsem, E., et al., *Cetuximab and chemotherapy as initial treatment for metastatic colorectal cancer*. N Engl J Med, 2009. 360(14): p. 1408-17.
152. Parsons, D.W., et al., *Colorectal cancer: mutations in a signalling pathway*. Nature, 2005. 436(7052): p. 792.
153. Danielsen, S.A., et al., *Novel mutations of the suppressor gene PTEN in colorectal carcinomas stratified by microsatellite instability- and TP53 mutation- status*. Hum Mutat, 2008. 29(11): p. E252-62.
154. Razis, E., et al., *Potential value of PTEN in predicting cetuximab response in colorectal cancer: an exploratory study*. BMC Cancer, 2008. 8: p. 234.

155. Sartore-Bianchi, A., et al., *Multi-determinants analysis of molecular alterations for predicting clinical benefit to EGFR-targeted monoclonal antibodies in colorectal cancer*. PLoS One, 2009. 4(10): p. e7287.
156. Bittoni, A., et al., *Selecting the best treatment for an individual patient*. Recent Results Cancer Res, 2012. 196: p. 307-18.
157. Aprile, G., et al., *Relevance of BRAF and extended RAS mutational analyses for metastatic colorectal cancer patients*. OA Molecular Oncology, 2013. 1(2): p. 7.
158. Ahlquist, D.A., C.G. Moertel, and D.B. McGill, *Screening for colorectal cancer*. N Engl J Med, 1993. 329(18): p. 1351; author reply 1353-4.
159. Osborn, N.K. and D.A. Ahlquist, *Stool screening for colorectal cancer: molecular approaches*. Gastroenterology, 2005. 128(1): p. 192-206.
160. Ahlquist, D.A., et al., *Stool DNA and occult blood testing for screen detection of colorectal neoplasia*. Ann Intern Med, 2008. 149(7): p. 441-50, W81.
161. Itzkowitz, S., et al., *A simplified, noninvasive stool DNA test for colorectal cancer detection*. Am J Gastroenterol, 2008. 103(11): p. 2862-70.
162. Itzkowitz, S.H., et al., *Improved fecal DNA test for colorectal cancer screening*. Clin Gastroenterol Hepatol, 2007. 5(1): p. 111-7.
163. French, A.J., et al., *Prognostic significance of defective mismatch repair and BRAF V600E in patients with colon cancer*. Clin Cancer Res, 2008. 14(11): p. 3408-15.
164. Ribic, C.M., et al., *Tumor microsatellite-instability status as a predictor of benefit from fluorouracil-based adjuvant chemotherapy for colon cancer*. N Engl J Med, 2003. 349(3): p. 247-57.
165. Boulay, J.L., et al., *SMAD4 is a predictive marker for 5-fluorouracil-based chemotherapy in patients with colorectal cancer*. Br J Cancer, 2002. 87(6): p. 630-4.
166. Watanabe, T., et al., *Molecular predictors of survival after adjuvant chemotherapy for colon cancer*. N Engl J Med, 2001. 344(16): p. 1196-206.
167. Braun, M.S., et al., *Predictive biomarkers of chemotherapy efficacy in colorectal cancer: results from the UK MRC FOCUS trial*. J Clin Oncol, 2008. 26(16): p. 2690-8.
168. Ezzeldin, H.H. and R.B. Diasio, *Predicting fluorouracil toxicity: can we finally do it?* J Clin Oncol, 2008. 26(13): p. 2080-2.
169. Schwab, M., et al., *Role of genetic and nongenetic factors for fluorouracil treatment-related severe toxicity: a prospective clinical trial by the German 5-FU Toxicity Study Group*. J Clin Oncol, 2008. 26(13): p. 2131-8.
170. Hoskins, J.M., et al., *UGT1A1*28 genotype and irinotecan-induced neutropenia: dose matters*. J Natl Cancer Inst, 2007. 99(17): p. 1290-5.

171. Palomaki, G.E., et al., *Can UGT1A1 genotyping reduce morbidity and mortality in patients with metastatic colorectal cancer treated with irinotecan? An evidence-based review.* Genet Med, 2009. 11(1): p. 21-34.
172. Yu, M. and W.M. Grady, *Therapeutic targeting of the phosphatidylinositol 3-kinase signaling pathway: novel targeted therapies and advances in the treatment of colorectal cancer.* Therap Adv Gastroenterol, 2012. 5(5): p. 319-37.
173. Yuan, T.L. and L.C. Cantley, *PI3K pathway alterations in cancer: variations on a theme.* Oncogene, 2008. 27(41): p. 5497-510.
174. Di Nicolantonio, F., et al., *Wild-type BRAF is required for response to panitumumab or cetuximab in metastatic colorectal cancer.* J Clin Oncol, 2008. 26(35): p. 5705-12.
175. Wagle, N., et al., *Dissecting therapeutic resistance to RAF inhibition in melanoma by tumor genomic profiling.* J Clin Oncol, 2011. 29(22): p. 3085-96.
176. Sleijfer, S., et al., *Circulating tumour cell detection on its way to routine diagnostic implementation?* Eur J Cancer, 2007. 43(18): p. 2645-50.
177. Mocellin, S., et al., *Circulating tumor cells: the 'leukemic phase' of solid cancers.* Trends Mol Med, 2006. 12(3): p. 130-9.
178. Miller, M.C., G.V. Doyle, and L.W. Terstappen, *Significance of Circulating Tumor Cells Detected by the CellSearch System in Patients with Metastatic Breast Colorectal and Prostate Cancer.* J Oncol, 2010. 2010: p. 617421.
179. Allard, W.J., et al., *Tumor cells circulate in the peripheral blood of all major carcinomas but not in healthy subjects or patients with nonmalignant diseases.* Clin Cancer Res, 2004. 10(20): p. 6897-904.
180. Lorente, D., J. Mateo, and J.S. de Bono, *Molecular characterization and clinical utility of circulating tumor cells in the treatment of prostate cancer.* Am Soc Clin Oncol Educ Book, 2014: p. e197-203.
181. O'Flaherty, J.D., et al., *Circulating tumour cells, their role in metastasis and their clinical utility in lung cancer.* Lung Cancer, 2012. 76(1): p. 19-25.
182. Lowes, L.E., et al., *Image cytometry analysis of circulating tumor cells.* Methods Cell Biol, 2011. 102: p. 261-90.
183. Hou, J.M., et al., *Clinical significance and molecular characteristics of circulating tumor cells and circulating tumor microemboli in patients with small-cell lung cancer.* J Clin Oncol, 2012. 30(5): p. 525-32.
184. Khan, M.S., et al., *Early Changes in Circulating Tumor Cells Are Associated with Response and Survival Following Treatment of Metastatic Neuroendocrine Neoplasms.* Clin Cancer Res, 2016. 22(1): p. 79-85.
185. Went, P.T., et al., *Frequent EpCam protein expression in human carcinomas.* Hum Pathol, 2004. 35(1): p. 122-8.

186. Ksiazkiewicz, M., A. Markiewicz, and A.J. Zaczek, *Epithelial-mesenchymal transition: a hallmark in metastasis formation linking circulating tumor cells and cancer stem cells*. Pathobiology, 2012. 79(4): p. 195-208.
187. Wicha, M.S. and D.F. Hayes, *Circulating tumor cells: not all detected cells are bad and not all bad cells are detected*. J Clin Oncol, 2011. 29(12): p. 1508-11.
188. Cristofanilli, M., et al., *Circulating tumor cells, disease progression, and survival in metastatic breast cancer*. N Engl J Med, 2004. 351(8): p. 781-91.
189. de Bono, J.S., et al., *Circulating tumor cells predict survival benefit from treatment in metastatic castration-resistant prostate cancer*. Clin Cancer Res, 2008. 14(19): p. 6302-9.
190. Cohen, S.J., et al., *Relationship of circulating tumor cells to tumor response, progression-free survival, and overall survival in patients with metastatic colorectal cancer*. J Clin Oncol, 2008. 26(19): p. 3213-21.
191. Danila, D.C., et al., *Circulating tumor cell number and prognosis in progressive castration-resistant prostate cancer*. Clin Cancer Res, 2007. 13(23): p. 7053-8.
192. Smerage, J.B., et al., *Circulating tumor cells and response to chemotherapy in metastatic breast cancer: SWOG S0500*. J Clin Oncol, 2014. 32(31): p. 3483-9.
193. Rack, B., et al., *Circulating tumor cells predict survival in early average-to-high risk breast cancer patients*. J Natl Cancer Inst, 2014. 106(5).
194. United States National Institutes of Health. *ClinicalTrials.gov*. 2016 [cited 2013 9 September]; Available from: <https://clinicaltrials.gov/>.
195. Cohen, S.J., et al., *Prognostic significance of circulating tumor cells in patients with metastatic colorectal cancer*. Ann Oncol, 2009. 20(7): p. 1223-9.
196. Gazzaniga, P., et al., *Circulating tumor cells in metastatic colorectal cancer: do we need an alternative cutoff?* J Cancer Res Clin Oncol, 2013. 139(8): p. 1411-6.
197. Gorges, T.M., et al., *Improved Detection of Circulating Tumor Cells in Metastatic Colorectal Cancer by the Combination of the CellSearch(R) System and the AdnaTest(R)*. PLoS One, 2016. 11(5): p. e0155126.
198. Chang, Y.T., et al., *A Prospective Study of Comparing Multi-Gene Biomarker Chip and Serum Carcinoembryonic Antigen in the Postoperative Surveillance for Patients with Stage I-III Colorectal Cancer*. PLoS One, 2016. 11(10): p. e0163264.
199. Hinz, S., et al., *Detection of circulating tumor cells with CK20 RT-PCR is an independent negative prognostic marker in colon cancer patients - a prospective study*. BMC Cancer, 2017. 17(1): p. 53.
200. Zhao, R., et al., *Expression and clinical relevance of epithelial and mesenchymal markers in circulating tumor cells from colorectal cancer*. Oncotarget, 2017. 8(6): p. 9293-9302.

201. Koyanagi, K., et al., *Prognostic relevance of occult nodal micrometastases and circulating tumor cells in colorectal cancer in a prospective multicenter trial*. Clin Cancer Res, 2008. 14(22): p. 7391-6.
202. Lankiewicz, S., et al., *Circulating tumour cells as a predictive factor for response to systemic chemotherapy in patients with advanced colorectal cancer*. Mol Oncol, 2008. 2(4): p. 349-55.
203. Yap, T.A., et al., *Envisioning the future of early anticancer drug development*. Nat Rev Cancer, 2010. 10(7): p. 514-23.
204. Attard, G. and J.S. de Bono, *Utilizing circulating tumor cells: challenges and pitfalls*. Curr Opin Genet Dev, 2011. 21(1): p. 50-8.
205. Maheswaran, S., et al., *Detection of mutations in EGFR in circulating lung-cancer cells*. N Engl J Med, 2008. 359(4): p. 366-77.
206. Alemar, J. and E.R. Schuur, *Progress in using circulating tumor cell information to improve metastatic breast cancer therapy*. J Oncol, 2013. 2013: p. 702732.
207. Hayes, D.F., et al., *Monitoring expression of HER-2 on circulating epithelial cells in patients with advanced breast cancer*. Int J Oncol, 2002. 21(5): p. 1111-7.
208. Kummar, S., et al., *Phase I study of PARP inhibitor ABT-888 in combination with topotecan in adults with refractory solid tumors and lymphomas*. Cancer Res, 2011. 71(17): p. 5626-34.
209. Cohen, S.J., et al., *Isolation and characterization of circulating tumor cells in patients with metastatic colorectal cancer*. Clin Colorectal Cancer, 2006. 6(2): p. 125-32.
210. de Bono, J.S., et al., *Potential applications for circulating tumor cells expressing the insulin-like growth factor-I receptor*. Clin Cancer Res, 2007. 13(12): p. 3611-6.
211. Miyamoto, D.T., et al., *Androgen receptor signaling in circulating tumor cells as a marker of hormonally responsive prostate cancer*. Cancer Discov, 2012. 2(11): p. 995-1003.
212. Buim, M.E., et al., *Detection of KRAS mutations in circulating tumor cells from patients with metastatic colorectal cancer*. Cancer Biol Ther, 2015. 16(9): p. 1289-95.
213. Kidess-Sigal, E., et al., *Enumeration and targeted analysis of KRAS, BRAF and PIK3CA mutations in CTCs captured by a label-free platform: Comparison to ctDNA and tissue in metastatic colorectal cancer*. Oncotarget, 2016. 7(51): p. 85349-85364.
214. Wang, L.H., et al., *Monitoring drug-induced gammaH2AX as a pharmacodynamic biomarker in individual circulating tumor cells*. Clin Cancer Res, 2010. 16(3): p. 1073-84.

215. Wang, L., et al., *Assessment of CTC-based pharmacodynamic biomarkers in NCI clinical trials of targeted anticancer therapeutics*. *Cancer Res*, 2013. 73(Suppl 8).
216. Luger, K., et al., *Crystal structure of the nucleosome core particle at 2.8 Å resolution*. *Nature*, 1997. 389(6648): p. 251-60.
217. Redon, C.E., et al., *gamma-H2AX and other histone post-translational modifications in the clinic*. *Biochim Biophys Acta*, 2012. 1819(7): p. 743-56.
218. Noll, M. and R.D. Kornberg, *Action of micrococcal nuclease on chromatin and the location of histone H1*. *J Mol Biol*, 1977. 109(3): p. 393-404.
219. Talbert, P.B. and S. Henikoff, *Histone variants--ancient wrap artists of the epigenome*. *Nat Rev Mol Cell Biol*, 2010. 11(4): p. 264-75.
220. Stryer, L., *Biochemistry (4th edition)*. 1998: W.H.Freeman & Co Ltd.
221. Kinner, A., et al., *Gamma-H2AX in recognition and signaling of DNA double-strand breaks in the context of chromatin*. *Nucleic Acids Res*, 2008. 36(17): p. 5678-94.
222. Fernandez-Capetillo, O., et al., *H2AX: the histone guardian of the genome*. *DNA Repair (Amst)*, 2004. 3(8-9): p. 959-67.
223. Rogakou, E.P., et al., *Megabase chromatin domains involved in DNA double-strand breaks in vivo*. *J Cell Biol*, 1999. 146(5): p. 905-16.
224. Kouzarides, T., *Chromatin modifications and their function*. *Cell*, 2007. 128(4): p. 693-705.
225. Escargueil, A.E., et al., *What histone code for DNA repair?* *Mutat Res*, 2008. 658(3): p. 259-70.
226. Burma, S., et al., *ATM phosphorylates histone H2AX in response to DNA double-strand breaks*. *J Biol Chem*, 2001. 276(45): p. 42462-7.
227. Park, E.J., et al., *DNA-PK is activated by nucleosomes and phosphorylates H2AX within the nucleosomes in an acetylation-dependent manner*. *Nucleic Acids Res*, 2003. 31(23): p. 6819-27.
230. Sulli, G., R. Di Micco, and F. d'Adda di Fagagna, *Crosstalk between chromatin state and DNA damage response in cellular senescence and cancer*. *Nat Rev Cancer*, 2012. 12(10): p. 709-20.
231. Jekimovs, C., et al., *Chemotherapeutic compounds targeting the DNA double-strand break repair pathways: the good, the bad, and the promising*. *Front Oncol*, 2014. 4: p. 86.
232. Kaugars, G.E., et al., *The use of exfoliative cytology for the early diagnosis of oral cancers: is there a role for it in education and private practice?* *J Cancer Educ*, 1998. 13(2): p. 85-9.
233. Van Den Broeck, A., et al., *Loss of histone H4K20 trimethylation occurs in preneoplasia and influences prognosis of non-small cell lung cancer*. *Clin Cancer Res*, 2008. 14(22): p. 7237-45.

234. Piekarz, R.L., et al., *Inhibitor of histone deacetylation, depsipeptide (FR901228), in the treatment of peripheral and cutaneous T-cell lymphoma: a case report.* Blood, 2001. 98(9): p. 2865-8.
235. Skaland, I., et al., *Phosphohistone H3 expression has much stronger prognostic value than classical prognosticators in invasive lymph node-negative breast cancer patients less than 55 years of age.* Mod Pathol, 2007. 20(12): p. 1307-15.
236. Bonner, W.M., et al., *GammaH2AX and cancer.* Nat Rev Cancer, 2008. 8(12): p. 957-67.
237. Hochhauser, D., et al., *Phase I study of sequence-selective minor groove DNA binding agent SJG-136 in patients with advanced solid tumors.* Clin Cancer Res, 2009. 15(6): p. 2140-7.
238. Karp, J.E., et al., *A phase 1 clinical-laboratory study of clofarabine followed by cyclophosphamide for adults with refractory acute leukemias.* Blood, 2007. 110(6): p. 1762-9.
239. Huang, X., et al., *Assessment of histone H2AX phosphorylation induced by DNA topoisomerase I and II inhibitors topotecan and mitoxantrone and by the DNA cross-linking agent cisplatin.* Cytometry A, 2004. 58(2): p. 99-110.
240. Zhao, H., F. Traganos, and Z. Darzynkiewicz, *Kinetics of histone H2AX phosphorylation and Chk2 activation in A549 cells treated with topotecan and mitoxantrone in relation to the cell cycle phase.* Cytometry A, 2008. 73(6): p. 480-9.
241. Sedelnikova, O.A., et al., *Quantitative detection of (125)IdU-induced DNA double-strand breaks with gamma-H2AX antibody.* Radiat Res, 2002. 158(4): p. 486-92.
242. Cai, Z., K.A. Vallis, and R.M. Reilly, *Computational analysis of the number, area and density of gamma-H2AX foci in breast cancer cells exposed to (111)In-DTPA-hEGF or gamma-rays using Image-J software.* Int J Radiat Biol, 2009. 85(3): p. 262-71.
243. Olive, P.L., J.P. Banath, and L.T. Sinnott, *Phosphorylated histone H2AX in spheroids, tumors, and tissues of mice exposed to etoposide and 3-amino-1,2,4-benzotriazine-1,3-dioxide.* Cancer Res, 2004. 64(15): p. 5363-9.
244. Ivashkevich, A., et al., *Use of the gamma-H2AX assay to monitor DNA damage and repair in translational cancer research.* Cancer Lett, 2012. 327(1-2): p. 123-33.
245. Ewald, B., D. Sampath, and W. Plunkett, *Nucleoside analogs: molecular mechanisms signaling cell death.* Oncogene, 2008. 27(50): p. 6522-37.
246. Mazouzi, A., G. Velimezi, and J.I. Loizou, *DNA replication stress: causes, resolution and disease.* Exp Cell Res, 2014. 329(1): p. 85-93.
247. Podhorecka, M., A. Skladanowski, and P. Bozko, *H2AX Phosphorylation: Its Role in DNA Damage Response and Cancer Therapy.* J Nucleic Acids, 2010. 2010.

248. Xu, Y. and C. Her, *Inhibition of Topoisomerase (DNA) I (TOP1): DNA Damage Repair and Anticancer Therapy*. *Biomolecules*, 2015. 5(3): p. 1652-70.
249. Nitiss, J.L., *Targeting DNA topoisomerase II in cancer chemotherapy*. *Nat Rev Cancer*, 2009. 9(5): p. 338-50.
250. Dickey, J.S., et al., *H2AX: functional roles and potential applications*. *Chromosoma*, 2009. 118(6): p. 683-92.
251. Sedelnikova, O.A. and W.M. Bonner, *GammaH2AX in cancer cells: a potential biomarker for cancer diagnostics, prediction and recurrence*. *Cell Cycle*, 2006. 5(24): p. 2909-13.
252. Novik, K.L., et al., *Genetic variation in H2AFX contributes to risk of non-Hodgkin lymphoma*. *Cancer Epidemiol Biomarkers Prev*, 2007. 16(6): p. 1098-106.
253. Srivastava, N., et al., *Copy number alterations of the H2AFX gene in sporadic breast cancer patients*. *Cancer Genet Cytogenet*, 2008. 180(2): p. 121-8.
254. Bartkova, J., et al., *DNA damage response as a candidate anti-cancer barrier in early human tumorigenesis*. *Nature*, 2005. 434(7035): p. 864-70.
255. Duffy, M.J., *Tumor markers in clinical practice: a review focusing on common solid cancers*. *Med Princ Pract*, 2013. 22(1): p. 4-11.
256. Krebs, M.G., et al., *Circulating tumour cells: their utility in cancer management and predicting outcomes*. *Ther Adv Med Oncol*, 2010. 2(6): p. 351-65.
257. Bolke, E., et al., *Gene expression of circulating tumour cells and its correlation with tumour stage in breast cancer patients*. *Eur J Med Res*, 2009. 14(8): p. 359-63.
258. Smirnov, D.A., et al., *Global gene expression profiling of circulating tumor cells*. *Cancer Res*, 2005. 65(12): p. 4993-7.
259. Fong, P.C., et al., *Inhibition of poly(ADP-ribose) polymerase in tumors from BRCA mutation carriers*. *N Engl J Med*, 2009. 361(2): p. 123-34.
260. Yoon, A.J., et al., *Expression of activated checkpoint kinase 2 and histone H2AX in exfoliative oral cells after exposure to ionizing radiation*. *Radiat Res*, 2009. 171(6): p. 771-5.
261. Sarkaria, J.N., et al., *Comparison between pulsed-field gel electrophoresis and the comet assay as predictive assays for radiosensitivity in fibroblasts*. *Radiat Res*, 1998. 150(1): p. 17-22.
262. Huang, X., H.D. Halicka, and Z. Darzynkiewicz, *Detection of histone H2AX phosphorylation on Ser-139 as an indicator of DNA damage (DNA double-strand breaks)*. *Curr Protoc Cytom*, 2004. Chapter 7: p. Unit 7 27.
263. Nakamura, A., et al., *Techniques for gamma-H2AX detection*. *Methods Enzymol*, 2006. 409: p. 236-50.
264. Huang, X., et al., *Cytometric assessment of DNA damage in relation to cell cycle phase and apoptosis*. *Cell Prolif*, 2005. 38(4): p. 223-43.

265. Bracht, K., et al., *5-Fluorouracil response in a large panel of colorectal cancer cell lines is associated with mismatch repair deficiency*. Br J Cancer, 2010. 103(3): p. 340-6.
266. Chiu, S.J., et al., *Oxaliplatin-induced gamma-H2AX activation via both p53-dependent and -independent pathways but is not associated with cell cycle arrest in human colorectal cancer cells*. Chem Biol Interact, 2009. 182(2-3): p. 173-82.
267. Fuchs, A.B., et al., *Electronic sorting and recovery of single live cells from microlitre sized samples*. Lab Chip, 2006. 6(1): p. 121-6.
268. Peeters, D.J., et al., *Semiautomated isolation and molecular characterisation of single or highly purified tumour cells from CellSearch enriched blood samples using dielectrophoretic cell sorting*. Br J Cancer, 2013. 108(6): p. 1358-67.
269. Redon, C.E., et al., *gamma-H2AX as a biomarker of DNA damage induced by ionizing radiation in human peripheral blood lymphocytes and artificial skin*. Adv Space Res, 2009. 43(8): p. 1171-1178.
270. Tsai, W.S., et al., *Circulating Tumor Cell Count Correlates with Colorectal Neoplasm Progression and Is a Prognostic Marker for Distant Metastasis in Non-Metastatic Patients*. Sci Rep, 2016. 6: p. 24517.
271. Mah, L.J., A. El-Osta, and T.C. Karagiannis, *gammaH2AX: a sensitive molecular marker of DNA damage and repair*. Leukemia, 2010. 24(4): p. 679-86.
272. Friesner, J.D., et al., *Ionizing radiation-dependent gamma-H2AX focus formation requires ataxia telangiectasia mutated and ataxia telangiectasia mutated and Rad3-related*. Mol Biol Cell, 2005. 16(5): p. 2566-76.
273. Schmid, T.E., O. Zlobinskaya, and G. Multhoff, *Differences in Phosphorylated Histone H2AX Foci Formation and Removal of Cells Exposed to Low and High Linear Energy Transfer Radiation*. Curr Genomics, 2012. 13(6): p. 418-25.
274. Alcindor, T. and N. Beauger, *Oxaliplatin: a review in the era of molecularly targeted therapy*. Curr Oncol, 2011. 18(1): p. 18-25.
275. Tu, W.Z., et al., *gammaH2AX foci formation in the absence of DNA damage: mitotic H2AX phosphorylation is mediated by the DNA-PKcs/CHK2 pathway*. FEBS Lett, 2013. 587(21): p. 3437-43.
276. Pommier, Y., et al., *Repair of topoisomerase I-mediated DNA damage*. Prog Nucleic Acid Res Mol Biol, 2006. 81: p. 179-229.
277. Benada, J. and L. Macurek, *Targeting the Checkpoint to Kill Cancer Cells*. Biomolecules, 2015. 5(3): p. 1912-37.
278. Mariani, M., et al., *Gender influences the class III and V beta-tubulin ability to predict poor outcome in colorectal cancer*. Clin Cancer Res, 2012. 18(10): p. 2964-75.

279. Li, X.L., et al., *P53 mutations in colorectal cancer - molecular pathogenesis and pharmacological reactivation*. World J Gastroenterol, 2015. 21(1): p. 84-93.
280. Ahmed, D., et al., *Epigenetic and genetic features of 24 colon cancer cell lines*. Oncogenesis, 2013. 2: p. e71.
281. Tanaka, T., et al., *Cytometry of ATM activation and histone H2AX phosphorylation to estimate extent of DNA damage induced by exogenous agents*. Cytometry A, 2007. 71(9): p. 648-61.
282. Furuta, T., et al., *Phosphorylation of histone H2AX and activation of Mre11, Rad50, and Nbs1 in response to replication-dependent DNA double-strand breaks induced by mammalian DNA topoisomerase I cleavage complexes*. J Biol Chem, 2003. 278(22): p. 20303-12.
283. Abu-Sanad, A., et al., *Simultaneous inhibition of ATR and PARP sensitizes colon cancer cell lines to irinotecan*. Front Pharmacol, 2015. 6: p. 147.
284. Xu, Y. and M.A. Villalona-Calero, *Irinotecan: mechanisms of tumor resistance and novel strategies for modulating its activity*. Ann Oncol, 2002. 13(12): p. 1841-51.
285. Sclafani, F., et al., *TP53 mutational status and cetuximab benefit in rectal cancer: 5-year results of the EXPERT-C trial*. J Natl Cancer Inst, 2014. 106(7).
286. Redon, C.E., et al., *Recent developments in the use of gamma-H2AX as a quantitative DNA double-strand break biomarker*. Aging (Albany NY), 2011. 3(2): p. 168-74.
287. Toyooka, T., M. Ishihama, and Y. Ibuki, *Phosphorylation of histone H2AX is a powerful tool for detecting chemical photogenotoxicity*. J Invest Dermatol, 2011. 131(6): p. 1313-21.
288. Matsuzaki, K., et al., *Whole cell-ELISA to measure the gammaH2AX response of six aneuploids and eight DNA-damaging chemicals*. Mutat Res, 2010. 700(1-2): p. 71-9.
289. Kinders, R.J., et al., *Development of a validated immunofluorescence assay for gammaH2AX as a pharmacodynamic marker of topoisomerase I inhibitor activity*. Clin Cancer Res, 2010. 16(22): p. 5447-57.
290. Toss, A., et al., *CTC enumeration and characterization: moving toward personalized medicine*. Ann Transl Med, 2014. 2(11): p. 108.
291. Shah, K., et al., *gammaH2AX expression in cytological specimens as a biomarker of response to radiotherapy in solid malignancies*. Diagn Cytopathol, 2016. 44(2): p. 141-6.